TTI: RF7257-1

DEVELOPMENT OF A RADAR ANALYSIS PROGRAM FOR LAYER THICKNESS DETERMINATIONS

by Emmanuel Fernando

Research Report RF7257-1

Texas Transportation Institute
Texas A&M University
College Station, Texas 77843-3135

Florida Department of Transportation

in cooperation with the
Federal Highway Administration and
the Florida Department of Transportation

Technical Report Documentation Page

1. Report No.	2. Government Accession No.	3. Recipient's Catalog No.
FL-00/RF7257-1		

4. Title and Subtitle	5. Report Date
DEVELOPMENT OF A RADAR ANALYSIS PROGRAM FOR LAYER THICKNESS DETERMINATIONS	February 2000
	6. Performing Organization Code

7. Author(s)	8. Performing Organization Report No.
Emmanuel G. Fernando	Research Report RF7257-1

9. Performing Organization Name and Address	10. Work Unit No. (TRAIS)
Texas Transportation Institute The Texas A&M University System College Station, Texas 77843-3135	11. Contract or Grant No. Project No. 0510706

12. Sponsoring Agency Name and Address	13. Type of Report and Period Covered
Florida Department of Transportation Haydon Burns Building 605 Suwannee Street Tallahassee, Florida 32399-0459	Research: 1996 - 2000
	14. Sponsoring Agency Code

15. Supplementary Notes

Research performed in cooperation with the Florida Department of Transportation and the U.S. Department of Transportation, Federal Highway Administration.
Research Project Title: Automating Radar Pre-Processing for Network Level Surveys

16. Abstract

Ground Penetrating Radar (GPR) provides a safe, nondestructive method of estimating pavement layer thicknesses at highway speed. To address the need for developing a data base of pavement layer thicknesses over the state highway network, the Florida Department of Transportation (FDOT) funded a project with the Texas Transportation Institute that developed a computer program for analyzing GPR data in a production environment. To achieve this, the program incorporates decision criteria for automated detection of layer interfaces. From a sensitivity analysis, the effects of the decision criteria were observed to be logical and consistent with the expected trends in the variation of the detected peaks with changes in the criteria used. Further tests to verify peak tracking capability demonstrated the stability of the method. In particular, results showed that the algorithm is able to handle gradual or sudden changes in the patterns of the interface reflections as well as gaps in the data.

The amplitudes and arrival times of the interface reflections are used to compute layer thicknesses based on a general *n*-layered pavement model. Verification of the thickness predictions against core data from sites surveyed with GPR showed acceptable accuracy for uncalibrated estimates of surface thickness. In particular, the average of the absolute differences between the means of predicted and measured surface thicknesses was found to be 0.30 inches. Because of the absence of measured base thicknesses, it was not possible to verify the base predictions on the sites tested. It is recommended that this be done by FDOT at a future date, perhaps as part of its GPR implementation efforts. Initial implementation should be directed at the inventory of layer thicknesses for the Turnpikes. The relatively small size of this highway subsystem provides a manageable starting point for the planned development of a network level data base of pavement layer thicknesses in the state.

17. Key Words	18. Distribution Statement
Ground Penetrating Radar, Nondestructive Testing, Pavement Layer Thicknesses	No restrictions. This document is available to the public through NTIS: National Technical Information Service 5285 Port Royal Road Springfield, Virginia 22161

19. Security Classif.(of this report)	20. Security Classif.(of this page)	21. No. of Pages	22. Price
Unclassified	Unclassified	100	

DEVELOPMENT OF A RADAR ANALYSIS PROGRAM FOR LAYER THICKNESS DETERMINATIONS

by

Emmanuel G. Fernando
Associate Research Engineer
Texas Transportation Institute

Research Report RF7257-1
Research Project Number 0510706
Research Project Title: Automating Radar Pre-Processing for Network Level Surveys

Sponsored by the
Florida Department of Transportation
In Cooperation with
U. S. Department of Transportation
Federal Highway Administration

February 2000

TEXAS TRANSPORTATION INSTITUTE
The Texas A&M University System
College Station, Texas 77843-3135

DISCLAIMER

The contents of this report reflect the views of the author who is responsible for the facts and the accuracy of the data presented. The contents do not necessarily reflect the official views or policies of the Florida Department of Transportation (FDOT), or the Federal Highway Administration (FHWA). This report does not constitute a standard, specification, or regulation, nor is it intended for construction, bidding, or permit purposes.

ACKNOWLEDGMENTS

The work reported herein was conducted as part of a research project sponsored by the Florida Department of Transportation and the Federal Highway Administration. The objective of the project was to develop a procedure for analyzing radar data to establish a data base of pavement layer thicknesses over the state highway network. The researchers gratefully acknowledge the strong support and guidance of the project manager, Mr. Bruce Dietrich, of the Florida DOT. Our thanks also go to Mr. Jonathan Moxley, of the Bureau of Materials and Research in Gainesville, for providing the GPR data to verify the thickness predictions against core measurements.

TABLE OF CONTENTS

LIST OF FIGURES

FIGURE Page

FIGURE Page

FIGURE Page

LIST OF TABLES

CHAPTER I. INTRODUCTION

Ground Penetrating Radar (GPR) provides a safe, nondestructive method of estimating pavement layer thicknesses at highway speed. Layer thickness profiles of the type shown in Figure 1 can be generated from radar survey data. This type of information is important for pavement management applications. By quantifying the variability in pavement layer thicknesses, more reliable projections of network maintenance and rehabilitation needs can be established, thus resulting in cost-effective use of available funds. This variability in layer thicknesses is difficult to quantify by coring alone, a method that becomes prohibitively expensive to use for network level inventories of layer thicknesses. In this regard, GPR is another tool that highway agencies may use to develop a network level database of pavement layer thicknesses in the most efficient manner possible.

Recognizing GPR's potential, the Florida Department of Transportation (FDOT) initiated a project in the early 1990s to systematically implement this technology within the Department for the purpose of developing and maintaining a network-wide database of layer thicknesses and base material type. This project, conducted by the Texas Transportation Institute (TTI) and INFRASENSE, covered the following phases:

1. Demonstration of GPR technology *(1)*;
2. Evaluation of the use of GPR in a production environment *(2,3)*; and
3. Radar system development and pilot implementation *(4)*.

The last step resulted in the delivery of a GPR system to the Florida DOT and the transfer of technical know-how in the operation and use of GPR hardware and software for estimating pavement layer thicknesses. From initial implementation efforts by the Department, the need to improve the analysis software was recognized. In particular, Department personnel found the pre-processing of radar data to be tedious. This step requires the identification of layer interfaces for the different pavement sections found in the data. At locations where the interface reflections show much variability, the task of picking the layer interfaces became overwhelming. If GPR implementation was to proceed, the analysis procedure had to be improved so that Department personnel can pre-process the radar data

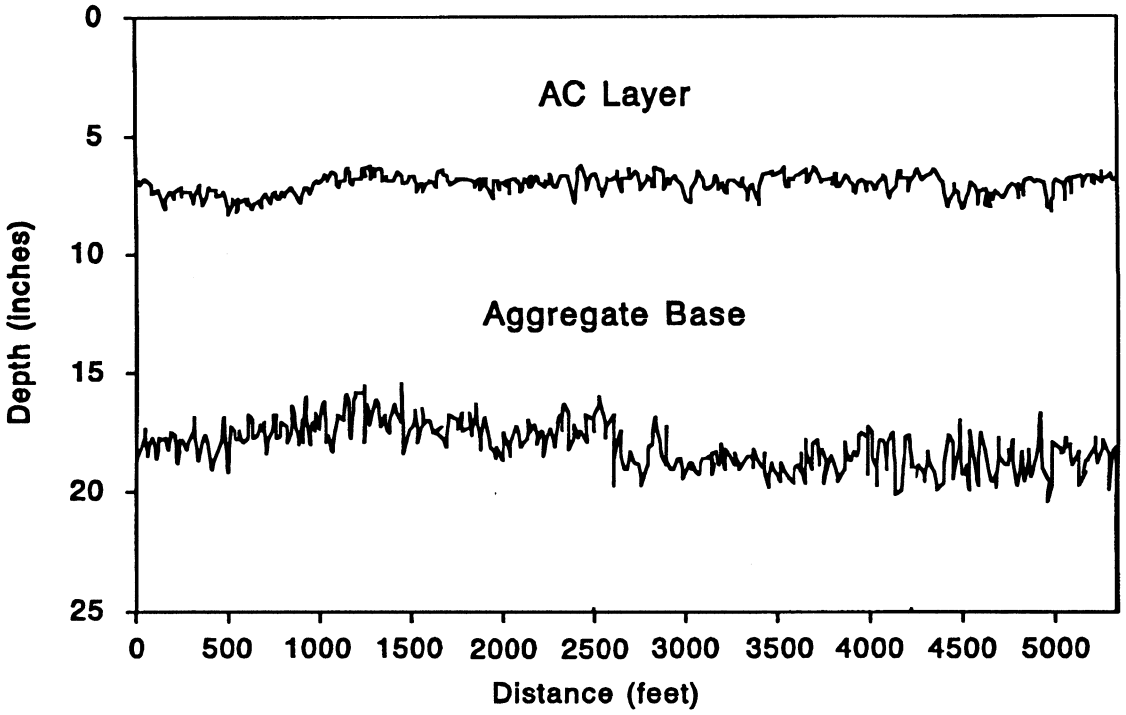

Figure 1. Sample Thickness Profiles From Analysis of GPR Data.

much more expeditiously, consistent with the intended use of GPR for developing a network level pavement layer thickness database. For this reason, the Florida DOT initiated a follow-up study with the Texas Transportation Institute to streamline the pre-processing of radar data. This study led to the development of a new and complete integrated software package for radar data analysis.

RESEARCH OBJECTIVES

FDOT Project 0510706, "Automating Radar Pre-Processing for Network Level Surveys," initially had the objective of automating the pre-processing of radar data. This was to be accomplished by developing an algorithm that automatically identified the relevant layer interface reflections based on user-prescribed criteria presented later in this report. Once these reflections were identified, the data were to be written to a file for input to the PAVLAYER program of INFRASENSE for calculation of pavement layer thicknesses. However, during the course of the development efforts, FDOT communicated the need to

have an integrated package to analyze radar data. Thus, researchers undertook the following additional tasks:

1. Development of a routine to compute layer thicknesses from GPR data for a general *n*-layered pavement;
2. Development of an automated procedure for categorizing predicted thicknesses into surface and base layers;
3. Verification of predicted thicknesses on Florida pavements using coring information obtained from those pavements;
4. Development of a routine to view radar data and to delineate segments within the data;
5. Revision of the ROADSEG program *(5)* developed by TTI; and
6. Integration of all analysis routines into a Windows compatible computer program called TERRA.

The acronym **TERRA** stands for **T**hickness **E**valuation of **R**oads by **RA**dar. A user's guide to this analysis program is presented in a companion report for this study *(6)*. The present report documents the development of the TERRA program to estimate pavement layer thicknesses from GPR measurements.

SCOPE OF RESEARCH REPORT

Chapter I of this report provides a background to this study, a statement of its objectives, and an outline of what the report covers. To provide a basic understanding of the application of radar for estimating pavement layer thicknesses, Chapter II reviews the basic principles of GPR data analysis and provides an example that illustrates the procedure for analyzing radar traces to predict layer thicknesses. Subsequently, Chapter III presents the automated procedure to identify layer interfaces in the radar data, along with the decision criteria by which this is accomplished. This chapter also presents a sensitivity analysis to evaluate the influence of the established criteria on the detection of layer interfaces. In addition, an investigation was made to verify the capability of the method to track layer interfaces that exhibit changes in arrival times or gaps in the data.

In line with the expanded scope of the research project, researchers developed a routine for estimating layer thicknesses for a general *n*-layered pavement and coupled this to

the automated procedure for identifying layer interfaces to develop the initial computer program for analysis of radar data. This computer program is verified in Chapter IV using data taken from a number of Florida pavements. Specifically, radar data taken with the Department's GPR van on these sections were used with the computer program to estimate pavement layer thicknesses which were subsequently compared with measured core thicknesses. The results from these comparisons are presented in Chapter IV. Finally, Chapter V summarizes the development efforts and presents recommendations for implementing the TERRA program within the Florida DOT.

As noted previously, the original objective of this study was to automate the pre-processing of radar data which involved subdividing the data into segments and identifying the layer interfaces for each segment. Thus, initial efforts were spent at evaluating procedures for automatically establishing homogeneous segments within the data using either the detected layer interfaces or the raw radar traces. However, since the scope of work was later expanded to cover the development of a complete program for radar data analysis, further evaluation of procedures to subdivide radar data in the pre-processing stage was discontinued. It was established that this work was no longer necessary after development of the procedure for automated detection of pavement layer interfaces that is presented in Chapter III. The same delineation may be accomplished after estimating the layer thicknesses using the ROADSEG program developed by TTI in the previous radar project. However, for completeness, the appendix of this report documents the efforts made by researchers to evaluate procedures for automatic segment delineation during the pre-processing stage.

It is noted that research efforts included the integration of the procedures developed into the Windows compatible computer program called TERRA. This required the development of a program to view GPR data taken with FDOT's Pulse radar system to delineate segments found in the data. Previously, this was accomplished using one of the modules in the DOS-based data acquisition software of Pulse Radar Incorporated. While this software could have been used, it could not be seamlessly integrated into the TERRA program. Thus, a new Windows compatible routine for viewing and delineating segments in the radar data was developed by researchers and incorporated into TERRA. In addition, software development included the creation of graphical user interfaces for program input and output, and the integration of the ROADSEG program into the analysis package. ROADSEG

is used to delineate homogeneous segments based on the predicted layer thicknesses. The program was developed by TTI in the previous radar project sponsored by the Department. At that time, ROADSEG was intended to be used after radar data have been processed using the PAVLAYER program of INFRASENSE. Since computer code for layer thickness predictions have been incorporated into TERRA, it was logical to integrate routines from ROADSEG into the new program for analyzing radar data. The application of the TERRA program is described in detail in the user's guide *(6)* that accompanies this report. The subsequent chapters document the research efforts made to develop this integrated radar analysis software.

CHAPTER II. ANALYSIS OF GPR DATA

The analysis of radar data to estimate pavement layer thicknesses is based on principles of electromagnetic theory. Ground penetrating radar operates by transmitting short pulses of electromagnetic energy into the pavement using an antenna attached to a survey vehicle (Figure 2). In a multimedia system, such as a pavement layer system, where there is a dielectric discontinuity at the interface of two distinct layers (e.g., asphalt/granular base), a fraction of the electromagnetic (EM) wave will be reflected back to the antenna, and the remaining portion transmitted into the succeeding layer. The amplitude of the reflection from this interface of dielectric discontinuity is a function of the relative dielectric constants of the respective pavement materials, typical values of which are given in Table 1.

As illustrated in Figure 3, the reflections from the different layer interfaces are seen as peaks in the recorded waveform. For example, the reflection from the pavement surface is seen as a peak with amplitude, A_1. This reflection arises due to the dielectric discontinuity between air and the surface material. Similarly, the reflections from the top of the base and the top of the subgrade are seen as peaks with amplitudes, A_2, and A_3, respectively.

It is observed that the amplitudes of the reflections diminish with depth into the pavement, with the largest amplitude being associated with the surface reflection. Compared with the low frequency antennas that are used for seismic testing, the high frequency (e.g., 1 GHz) radar antennas currently used for pavement thickness surveys have a much shallower depth of penetration. However, these antennas do provide a much better resolution of the pavement layers than their low frequency counterparts, and thus better thickness estimates.

As illustrated in Figure 3, the radar trace also shows the arrival time, in nanoseconds, associated with each peak, where one nanosecond is equal to one billionth of a second. Thus, the time interval between two successive peaks can be determined from the radar trace. In Figure 3, for example, the time interval between reflections from the surface to the top of the base is denoted as Δt_1. This time interval represents the time it took the EM wave to travel from the surface to the top of the base, and back (i.e., twice the surface thickness). The travel time of the EM wave within a pavement layer is dependent on the relative dielectric constant

Figure 2. The Florida DOT Radar Van.

Table 1. Typical Dielectrics of Highway Materials.

Material	Relative Dielectric Constant
Air	1
Water	81
Asphalt	3 - 6
Concrete	6 - 11
Limestone	4 - 8
Clays	5 - 40
Dry Sand	3 - 5
Saturated Sand	20 - 30

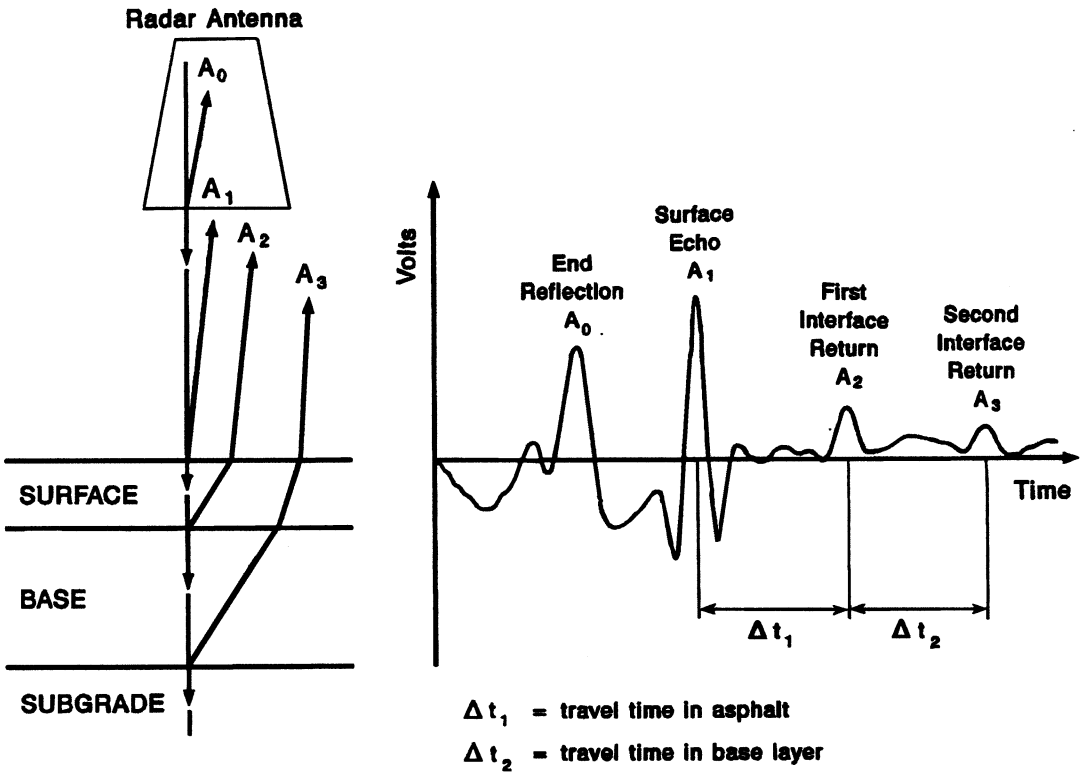

Figure 3. Illustration of Radar Trace Showing Layer Interface Reflections.

of the given layer. The higher the dielectric constant, the longer the travel time of the EM wave within the layer.

By knowing the time it took for the EM wave to travel through a given layer, and its velocity of propagation, the thickness of a given layer can be estimated, very simply, as:

$$thickness = velocity \times \frac{time}{2} \quad (1)$$

Since the measured time between peaks represents the round trip travel time of the EM wave, the thickness computation is based on time divided by two. The velocity of propagation is determined from the relative dielectric constant, ε, of the given layer, using the following equation derived from electromagnetic theory:

$$velocity = \frac{11.8}{\sqrt{\varepsilon}} \quad \text{(inches/nanosecond)} \tag{2}$$

where 11.8 is the radar velocity in free space in inches/nanosecond. Combining Eqs. (1) and (2), the following equation for determining layer thickness is obtained:

$$thickness = \frac{5.9 \times \Delta t}{\sqrt{\varepsilon}} \quad \text{(inches)} \tag{3}$$

where the time interval, Δt, is measured in nanoseconds from the radar trace.
Computation of the surface layer dielectric constant can be made by measuring the ratio of the amplitude of the surface reflection to the amplitude of the incident wave on the pavement surface. This ratio, called the reflection coefficient, ρ, is given by the formula:

$$\rho = \frac{\sqrt{\varepsilon_0} - \sqrt{\varepsilon_1}}{\sqrt{\varepsilon_0} + \sqrt{\varepsilon_1}} \tag{4}$$

where the subscripts 0 and 1 refer to air and pavement surface material respectively. The incident amplitude on the pavement can be estimated by measuring the reflection from a metal plate on the pavement surface. This is why a metal plate reflection test is conducted as part of a radar survey. By rearranging Eq.(4), and noting from Table 1 that the relative dielectric constant of air is 1, the following equation for estimating the surface layer dielectric constant, ε_1, is obtained:

$$\varepsilon_1 = \left[\frac{1 + A_1/A_p}{1 - A_1/A_p}\right]^2 \tag{5}$$

where A_1 = amplitude of reflection from asphalt surface
A_p = amplitude of reflection from metal plate
(= negative of incident amplitude)

A similar analysis can be used to compute the dielectric constant, ε_2, of the base material. The resulting relationship is *(7)*:

$$\varepsilon_2 = \varepsilon_1 \left[\frac{F - R_2}{F + R_2} \right]^2 \qquad (6)$$

where:

$$F = \frac{4\sqrt{\varepsilon_1}}{(1 - \varepsilon_1)}$$

R_2 = ratio of reflected amplitude from the top of the base layer (A_2 in Figure 3), to the reflected amplitude, A_1, from surface

The above equations are used to compute surface and base layer thicknesses from the radar data. To illustrate the application of the above equations, consider the radar trace shown in Figure 4. As noted in Figure 4 as well as in Figure 3, the very first reflection in the recorded waveform is that from the bottom of the antenna, which is a point of dielectric discontinuity, where the EM wave first encounters the air. The reflected signal, which is called the end reflection, has an amplitude, A_0, and includes the noise that is inherent to the system. To facilitate the interpretation of the radar data, the end reflection may be removed from the recorded waveform to eliminate the noise in the radar signal. This requires identification of the end reflection which is accomplished with an end reflection test conducted as part of the radar survey. This test involves pointing the antenna vertically toward the sky to isolate and identify the reflection from the bottom of the antenna and the inherent noise of the radar system. An example of a trace from an end reflection test is shown in Figure 5. By aligning and subtracting this trace from the recorded waveform shown in Figure 4, the processed radar trace shown in Figure 6 is obtained.

The processed radar signal shown in Figure 6 has two peaks associated with the reflections from the surface and the top of the base. These reflections have amplitudes of 3.67 and 0.64 volts, respectively, with a time interval between reflections of 6.60 nanoseconds (ns). The amplitudes of the reflections are used in the analysis to determine the dielectric constants of the surface and base layers from Eqs. (5) and (6). By knowing the dielectric constant of a given layer, and the travel time of the EM wave within the layer from the radar signal, the layer thickness can be estimated using Eq. (3).

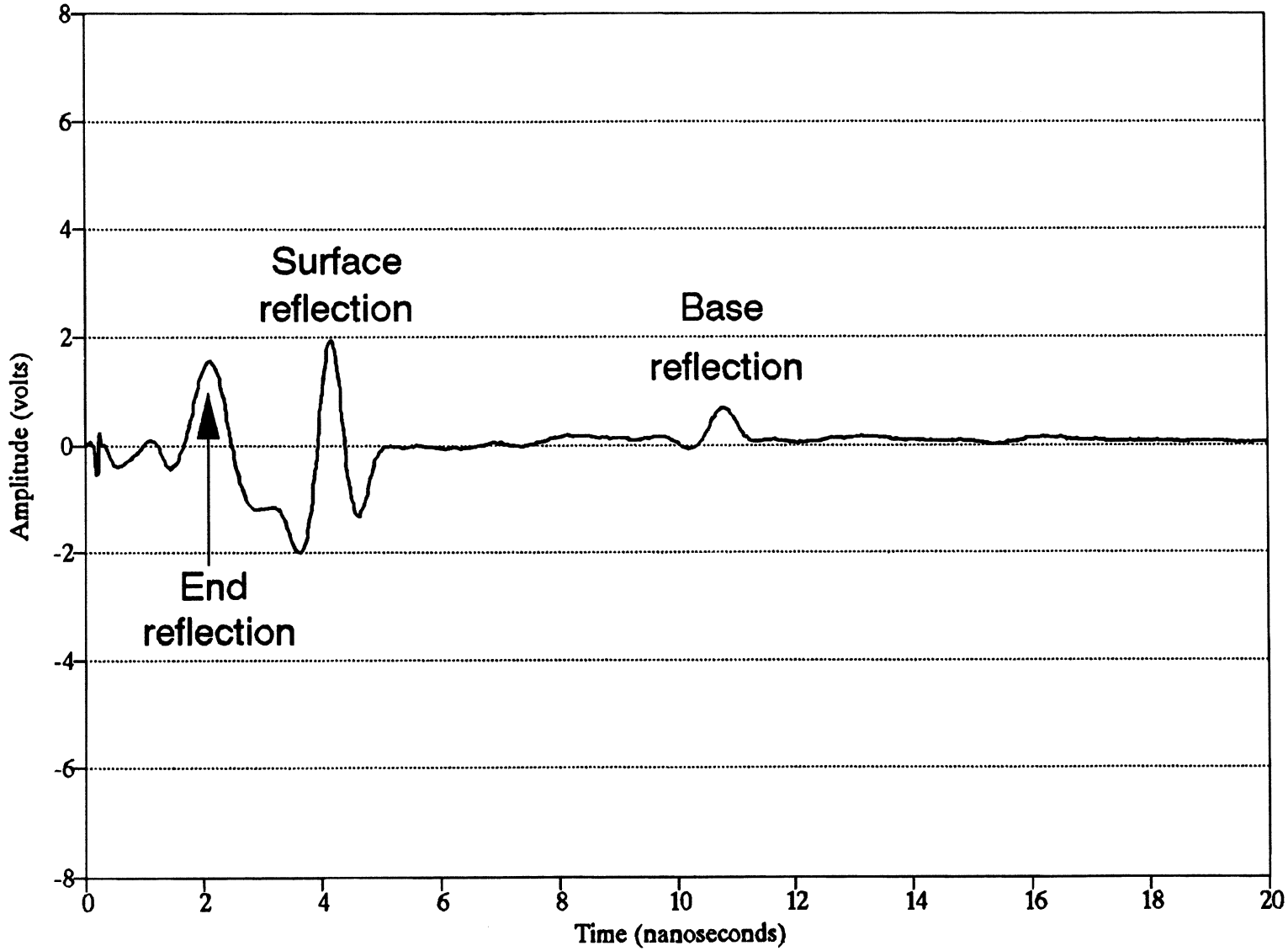

Figure 4. Illustration of a Radar Trace From a Pavement Section.

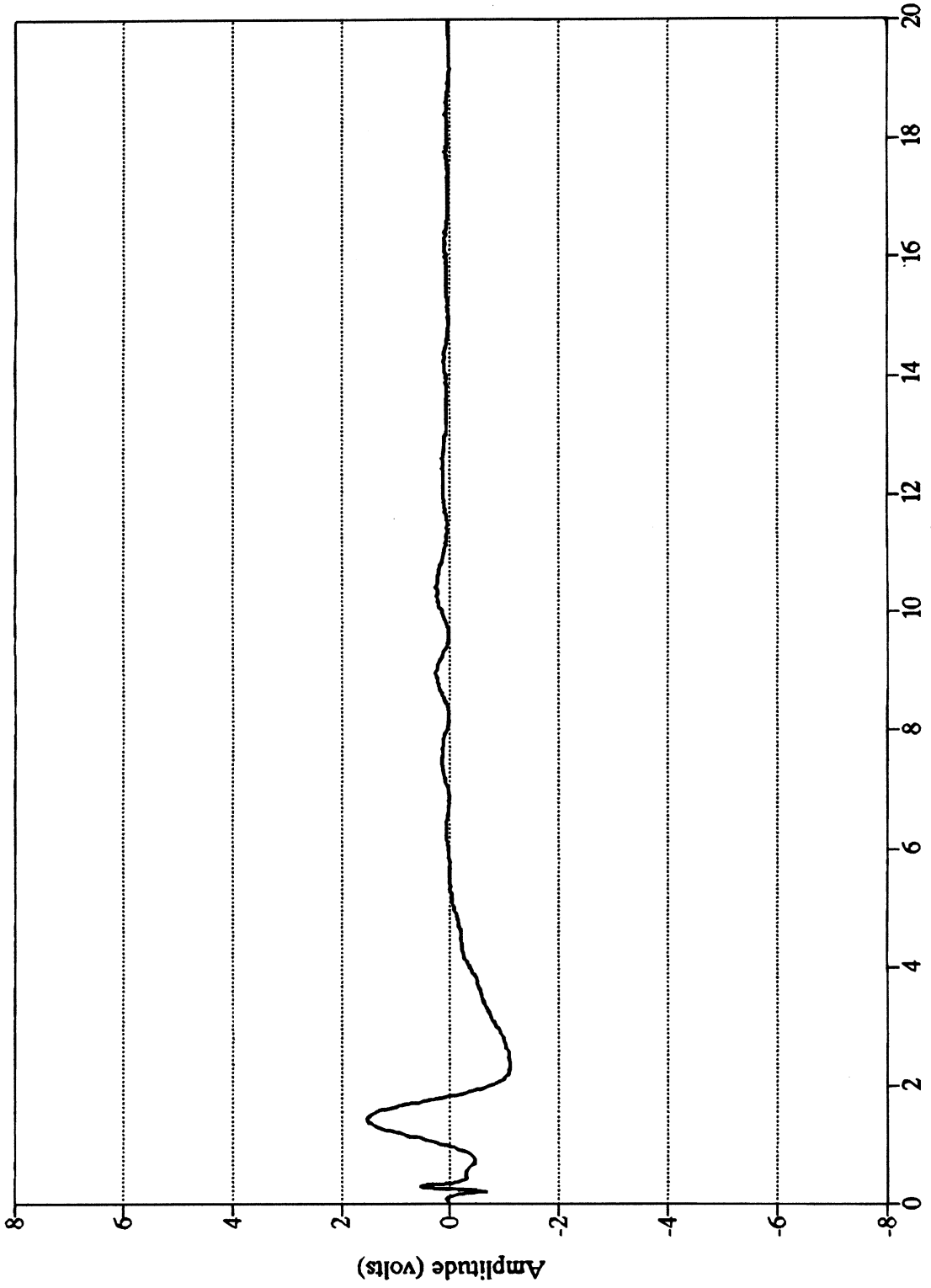

Figure 5. Sample Trace From an End Reflection Test.

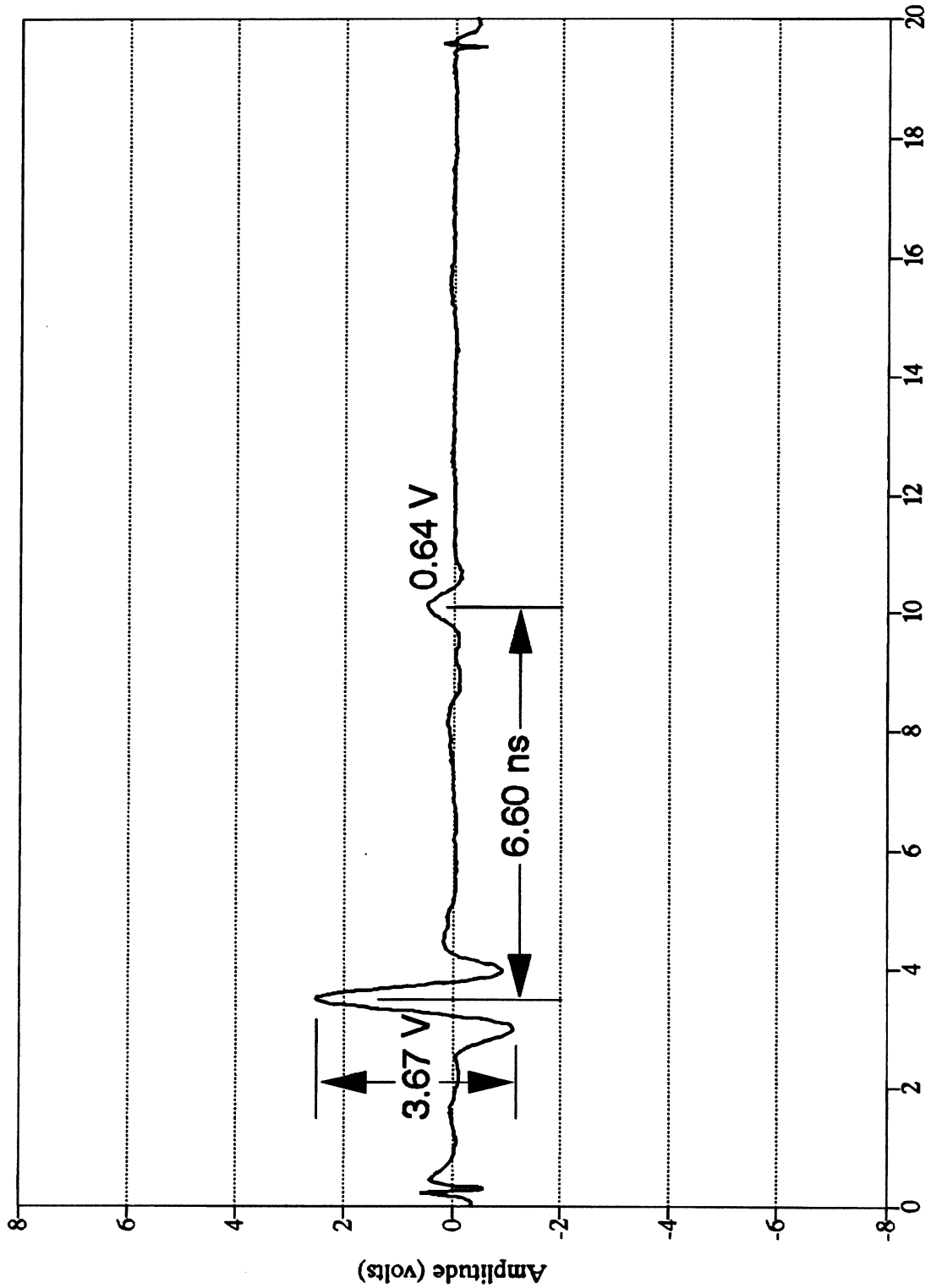

Figure 6. Radar Trace After Removal of End Reflection.

From Eqs. (5) and (6), the amplitude of the incident wave on the pavement surface, as estimated by the reflection from a metal plate, is also required to determine the dielectric constants of the surface and base layers. Thus, a metal plate reflection test is normally conducted as part of the radar survey. A typical trace from this test is shown in Figure 7, where the end reflection has already been removed. From the figure, the amplitude of the incident wave on the pavement surface is estimated to be 10.45 volts.

Using Eqs. (5) and (6), the dielectric constants of the surface and base layers are now calculated as follows:

$$\varepsilon_1 = \left[\frac{1 + 3.67/10.45}{1 - 3.67/10.45}\right]^2 = 4.34$$

$$F = \frac{4\sqrt{4.34}}{(1 - 4.34)} = -2.49$$

and

$$\varepsilon_2 = 4.34\left[\frac{-2.49 - 0.64/3.67}{-2.49 + 0.64/3.67}\right]^2 = 5.75$$

The surface layer thickness, d_1, may now be predicted from Eq. (3) knowing the dielectric constant of the layer (i.e., 4.34) and the travel time of the EM wave within this layer (6.60 ns from Figure 6). Thus:

$$d_1 = \frac{5.9 \times 6.60}{\sqrt{4.34}} = 18.7 \ inches$$

With respect to the base thickness, note that no reflection from the bottom of the base is found from the trace shown in Figure 6. Thus, the base thickness cannot be estimated from

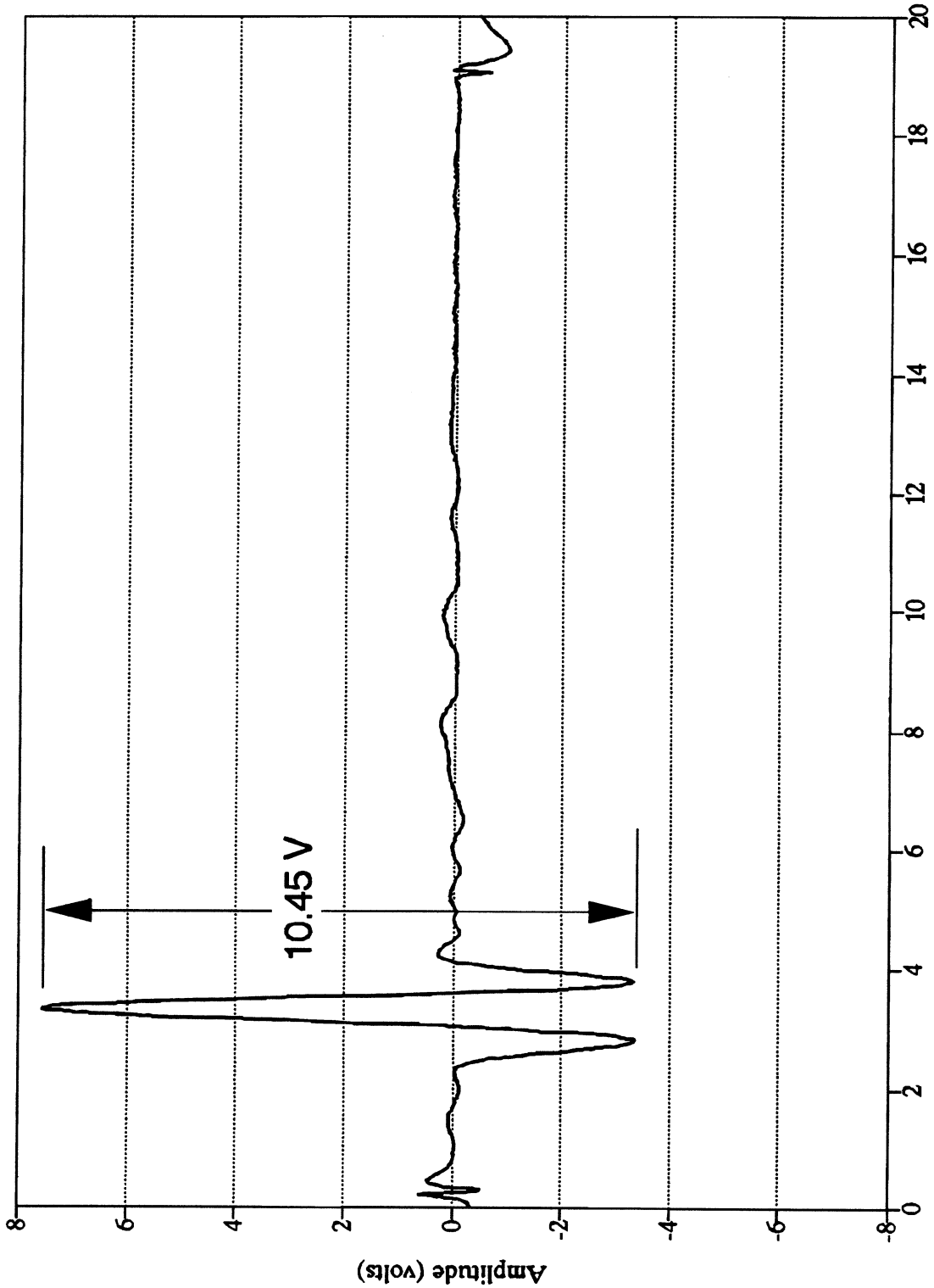

Figure 7. Sample Trace From a Metal Plate Test.

the data given in the example since the travel time of the EM wave within the base is unknown. In practice, the reflection from the interface of two materials that are dielectrically similar will be weak and may not be discernible from the radar data. Example cases include a granular base overlying a sand subgrade; an asphalt concrete surface underlain by an asphalt treated base; and a Portland cement concrete slab overlying a cement treated base. For these cases and in the absence of other data, core measurements will be necessary to determine the thicknesses of layers that cannot be estimated from the radar signals. In these instances, the radar data may be used to establish coring requirements for layer thickness determinations, in particular, to establish where cores should be taken.

The same basic process illustrated in this chapter is used to estimate layer thicknesses from radar data in the TERRA program. However, the identification of layer interface reflections or peaks is accomplished via software based on decision criteria that are presented in the next chapter. Since pavements generally consist of multiple layers and a given layer (such as the surface), may consist of multiple lifts, a procedure for estimating dielectric constants for a general *n*-layered pavement is incorporated in TERRA. In addition, a procedure to correct for antenna bounce during a survey is included in the analysis program.

CHAPTER III.
AUTOMATED PROCEDURE FOR DETECTING LAYER INTERFACES

DECISION CRITERIA FOR LAYER INTERFACE DETECTION

As illustrated in Chapter II, the prediction of layer thicknesses requires information on the amplitudes and arrival times of the interface reflections found in the radar data. Thus, to estimate layer thicknesses, one must first examine the radar signals, and identify the layer interfaces. Once this is done, it becomes relatively simple to write a computer program to determine the arrival times and amplitudes of the interface reflections, and compute the layer thicknesses accordingly. Developing an automated procedure for layer interface detection is relatively more difficult. Radar data from pavements will ordinarily exhibit changes in the number, and the magnitudes and signs of the interface reflections as well as in their arrival times. This arises from changes in pavement structure along the route surveyed. While these changes may be readily obvious to the person viewing the data, a computer cannot function similarly without a set of instructions which it can follow to recognize the features in the data. The set of instructions must be sufficiently robust yet simple enough to be useful in practice.

In developing a procedure to automatically detect layer interfaces, researchers attempted to simulate the thought process a person goes through when analyzing radar data. In this process, one would typically consider the amplitudes of the reflections and the consistency with which a given reflection appears in the data to establish the pavement layer interfaces. Consequently, the procedure for identifying the interface reflections in the TERRA program is based on the following decision criteria:

1. Minimum peak amplitude;
2. Minimum time interval between peaks;
3. Minimum amplitude ratio of successive, closely-spaced peaks that are opposite in sign; and
4. The coherence of the detected peaks from one radar trace to the next.

The minimum required peak amplitude allows the user to specify a cut-off value below which a given reflection is considered too small to be of significance. This minimum is

specified as a percentage of the metal plate reflection since this measures the voltage of the radar wave transmitted to the pavement. A small return amplitude indicates that the radar detects minimal difference in the dielectric properties of layers adjoining a given interface, i.e., the layers appear similar or the same to the radar. The lower the minimum required peak amplitude, the more peaks that will be identified by the computer program. However, the likelihood of getting peaks that are not physically significant also increases with a lower criterion. A suitable guideline would be to use a criterion no smaller than the noise-to-signal ratio of the radar system as determined according to the FDOT radar specifications. This is 1.69 percent from the initial acceptance tests done on FDOT's RODAR IV system by TTI *(4)*. Researchers recommend using as a minimum twice the value of the noise-to-signal ratio.

The minimum required time interval between peaks is used to differentiate a reflection from its adjacent troughs (Figure 8), and to detect closely-spaced successive reflections that are opposite in sign (Figure 9). In the program, if two successive peaks are separated by less than the minimum required time interval, the peak with the larger magnitude is selected if the two peaks are of the same sign. If the peaks are of opposite sign, the amplitude ratio of the peaks is first evaluated. This is simply the ratio of the magnitudes of the smaller to the larger peak. If this ratio is at least equal to the minimum specified by the user, both peaks are selected. The ratio specified can range from above zero to unity. If the amplitude ratio is less than the specified minimum, then only the peak with the larger amplitude is selected.

The coherence of detected peaks is also evaluated to discriminate between radar features that are localized versus those that are more dominant and appear regularly and consistently in the radar data. This is done by specifying the minimum required number of detected peaks as a percentage of the number of radar traces in a given segment. It ranges from above zero to 100 percent. Thus, the number of peaks falling within a given time interval must at least equal the minimum required number for the peaks to be regarded as coherent. Otherwise, the peaks are considered to be localized features and are disregarded. Only peaks appearing after the surface echo are considered in the coherence evaluation.

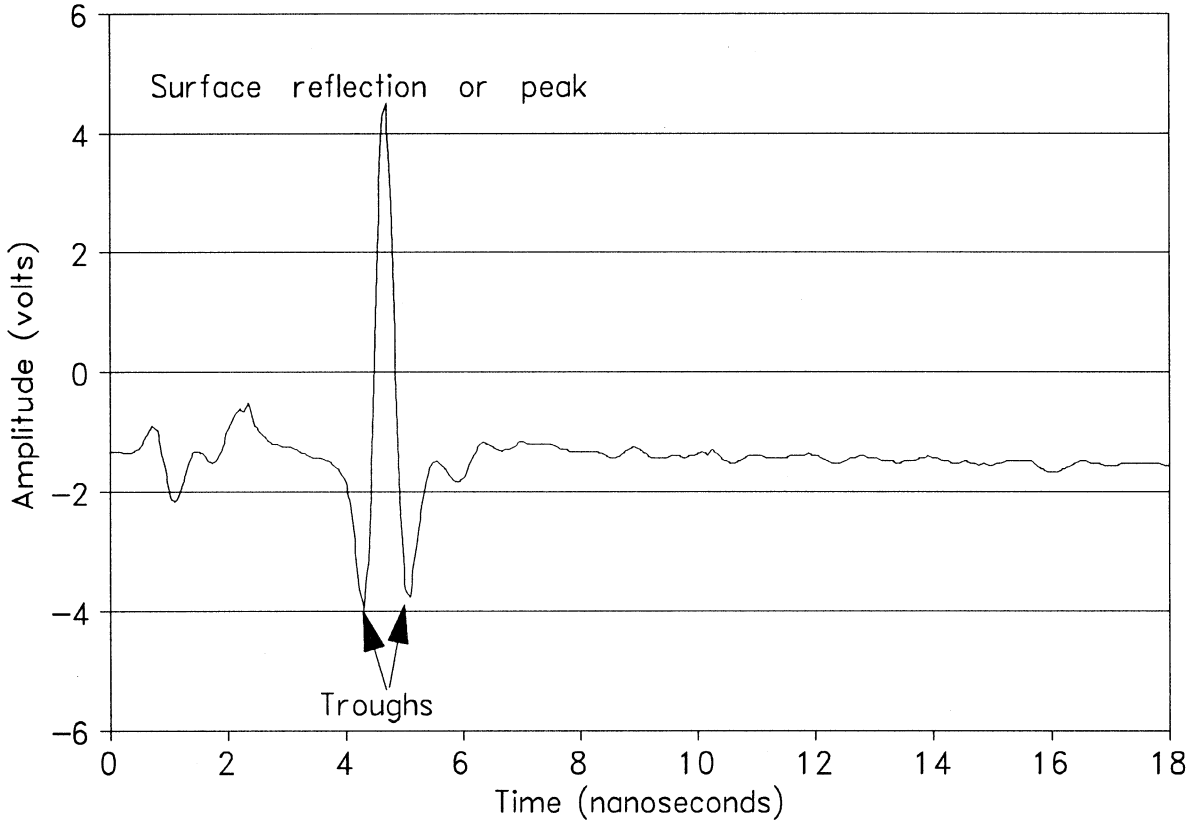

Figure 8. Illustration of the Troughs of a Given Reflection.

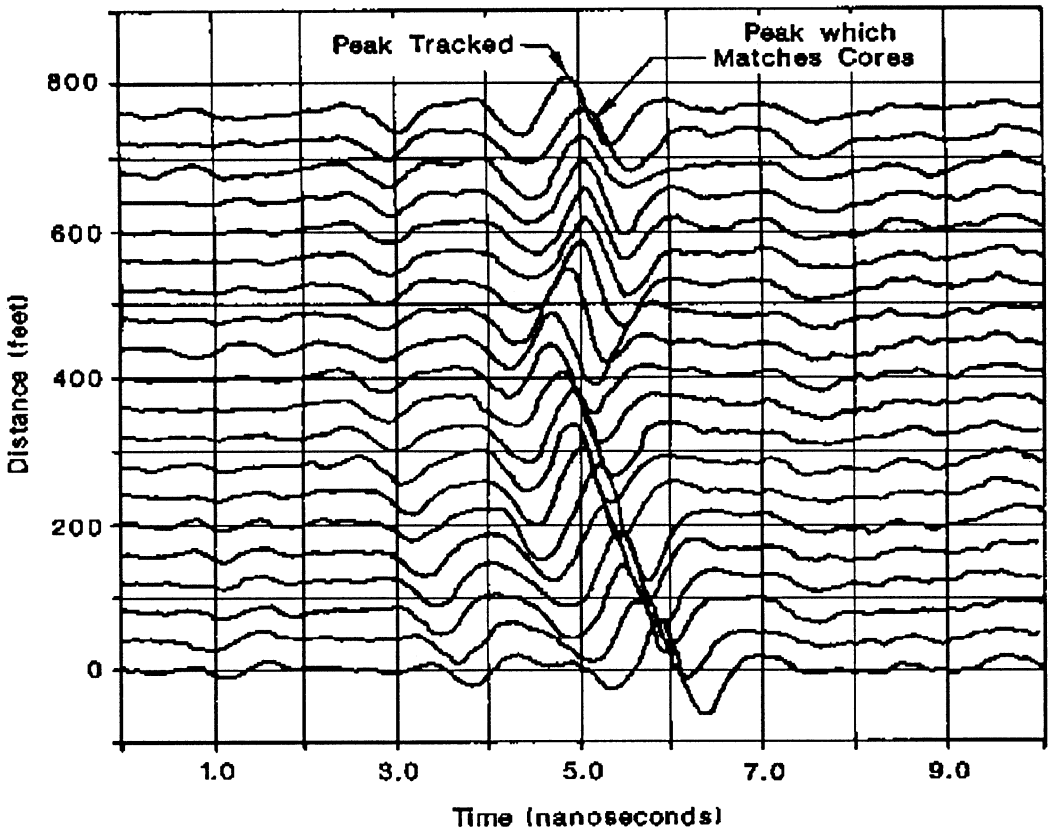

Figure 9. GPR Data With Positive and Negative Reflections Closely Following Each Other.

SENSITIVITY ANALYSIS

Researchers conducted a sensitivity analysis to evaluate the influence of the above criteria on the detection of layer interfaces. This was accomplished by varying each criterion one at a time while holding the other criteria at the base levels. Table 2 shows the different levels established for this investigation. The influence of each criterion was then evaluated based on the changes in the distributions of peak arrival times and amplitudes brought about by varying the levels of the different criteria. The results obtained are summarized in this section.

Table 2. Levels of Decision Criteria Used in the Sensitivity Analysis.

Decision Criterion	Levels[1]
Minimum required peak amplitude as a percentage of the metal plate reflection	3, **5**, 7 percent
Minimum required time interval between reflections	0.5, **1.0**, 1.5 ns
Minimum amplitude ratio of successive closely-spaced peaks that are opposite in sign	0.75, **1.0**
Minimum required number of detected peaks in a given time interval as a percentage of the block size	1, 5, **10**, 20 percent
Block size	**500** traces per block

[1] Bold numbers denote base levels selected.

Figure 10 illustrates the effect of the minimum required peak amplitude, V_m. In the figure, the distributions of the arrival times of detected peaks are plotted for varying levels of V_m. The labels on the abscissa correspond to the upper limits of the arrival time intervals. For example, the label 9 represents arrival times greater than 8 and less than or equal to 9 ns. The ordinate shows the number of peaks falling within a given arrival time interval. It is observed from Figure 10 that the number of detected peaks decreases with increase in the minimum required peak amplitude. Further, this effect is more pronounced at larger arrival times. This result is to be expected because of the attenuation of the radar signal with depth into the pavement.

Figure 11 illustrates the effect of the minimum time interval, T_m, between successive peaks. The distributions of the peak amplitudes with different levels of T_m are plotted in the figure. The labels on the abscissa correspond to the upper limits of the amplitude intervals. For example, the label 0 represents peak amplitudes between -1 and 0 volts. As expected, the number of detected peaks decreases with increase in the minimum required time interval between successive reflections. It was observed in the sensitivity analysis that the lowest time interval of 0.5 ns resulted in troughs being erroneously identified as peaks. From experience, it is recommended that a minimum required time interval of at least 0.9 ns be specified in the analysis.

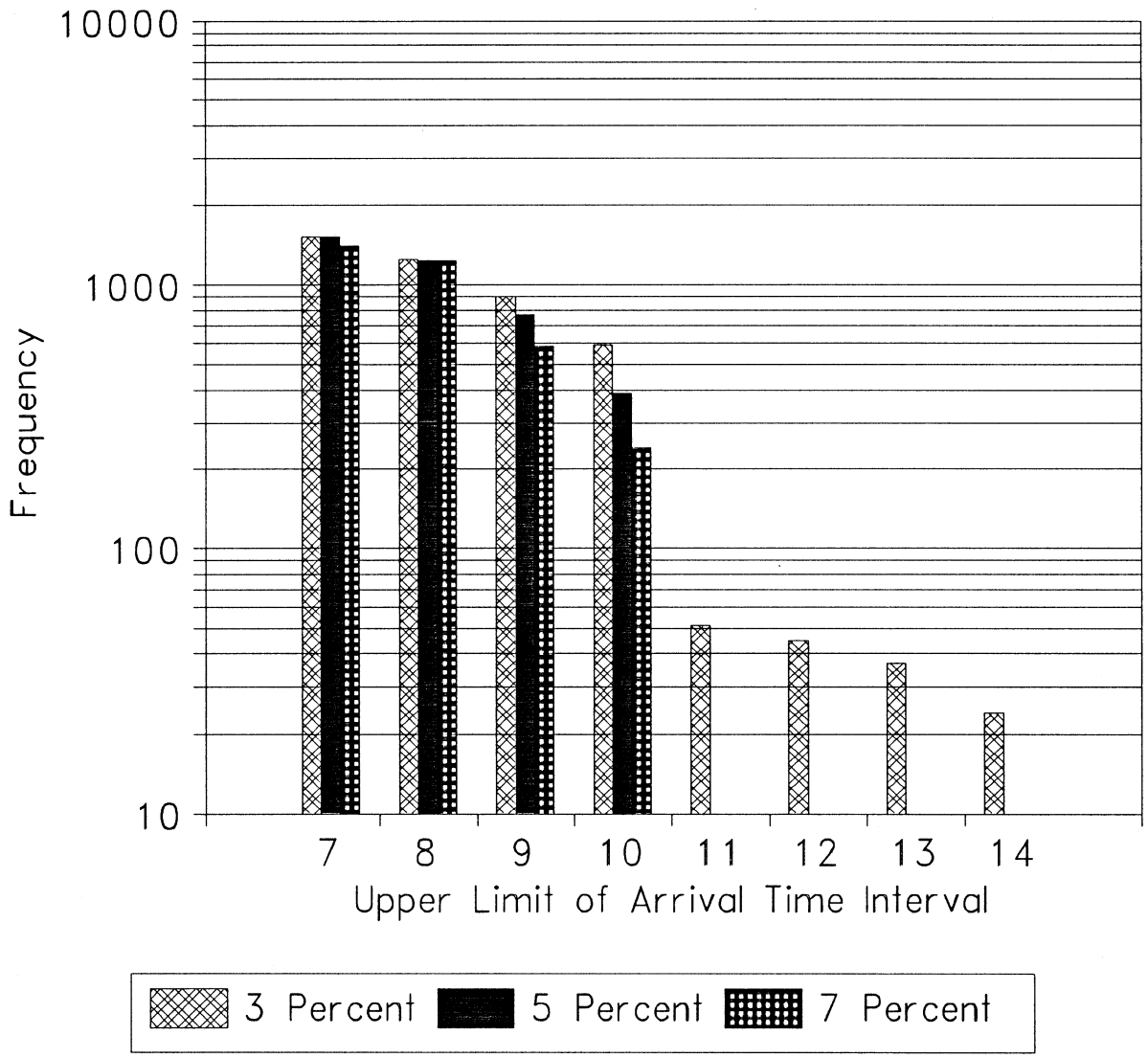

Figure 10. Effect of the Minimum Required Peak Amplitude, V_m.

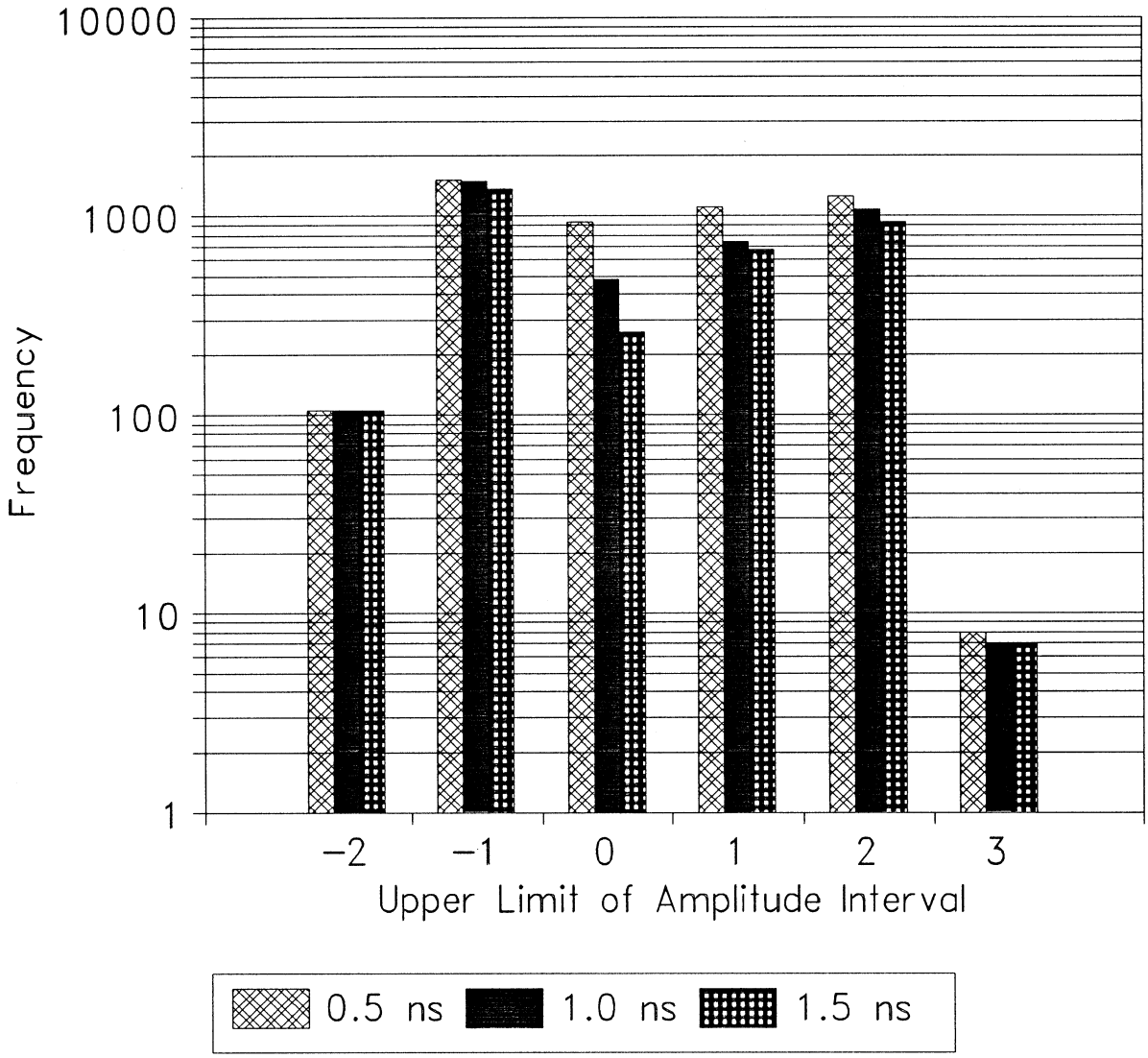

Figure 11. Effect of the Minimum Required Time Interval Between Peaks.

The effect of the minimum required amplitude ratio, R_m, between closely-spaced successive peaks that are opposite in sign is illustrated in Figure 12. In this analysis, the minimum required time interval between successive reflections was set at the base level of 1 ns. Thus, the likelihood of erroneously identifying troughs as peaks in the analysis was eliminated. As observed in Figure 12, the number of detected peaks decreases when the minimum required amplitude ratio, R_m, increases. For the data evaluated, Figure 12 indicates that closely-spaced successive reflections generally occurred between 6 and 8 ns. There is very little difference in the number of selected peaks corresponding to R_m values of 0.75 and 1, for arrival times greater than 8 ns, leading one to suspect that the features of interest were not detected at the larger arrival times. This observation was confirmed by visual examination of the radar data.

Figure 13 shows the effect of the minimum required number of peaks, N_p, in a given time interval. As expected, the number of selected peaks decreases with increase in N_p. The potential for identifying localized features in the radar data was demonstrated when N_p was set at one percent of the prescribed block size in the sensitivity analysis. This is reflected in Figure 13 which shows that a relatively small number of peaks were selected, with arrival times greater than 10 ns, when N_p was set a one percent of the prescribed block size. A number of these peaks corresponded to a localized thickening in the asphalt bound pavement layer which was verified from pavement cores. This localized thickening in the radar data is shown in Figure 14 where the data have been shifted to the left so that the surface reflections are aligned at 1 ns. For project-level investigations, the need for identifying localized features, such as that illustrated in Figure 14, may be justified. However, for network-level application of radar to estimate pavement layer thicknesses, this level of detail is generally unnecessary. Consequently, a larger value of N_p, such as 10 percent of the prescribed block size, may be more appropriate.

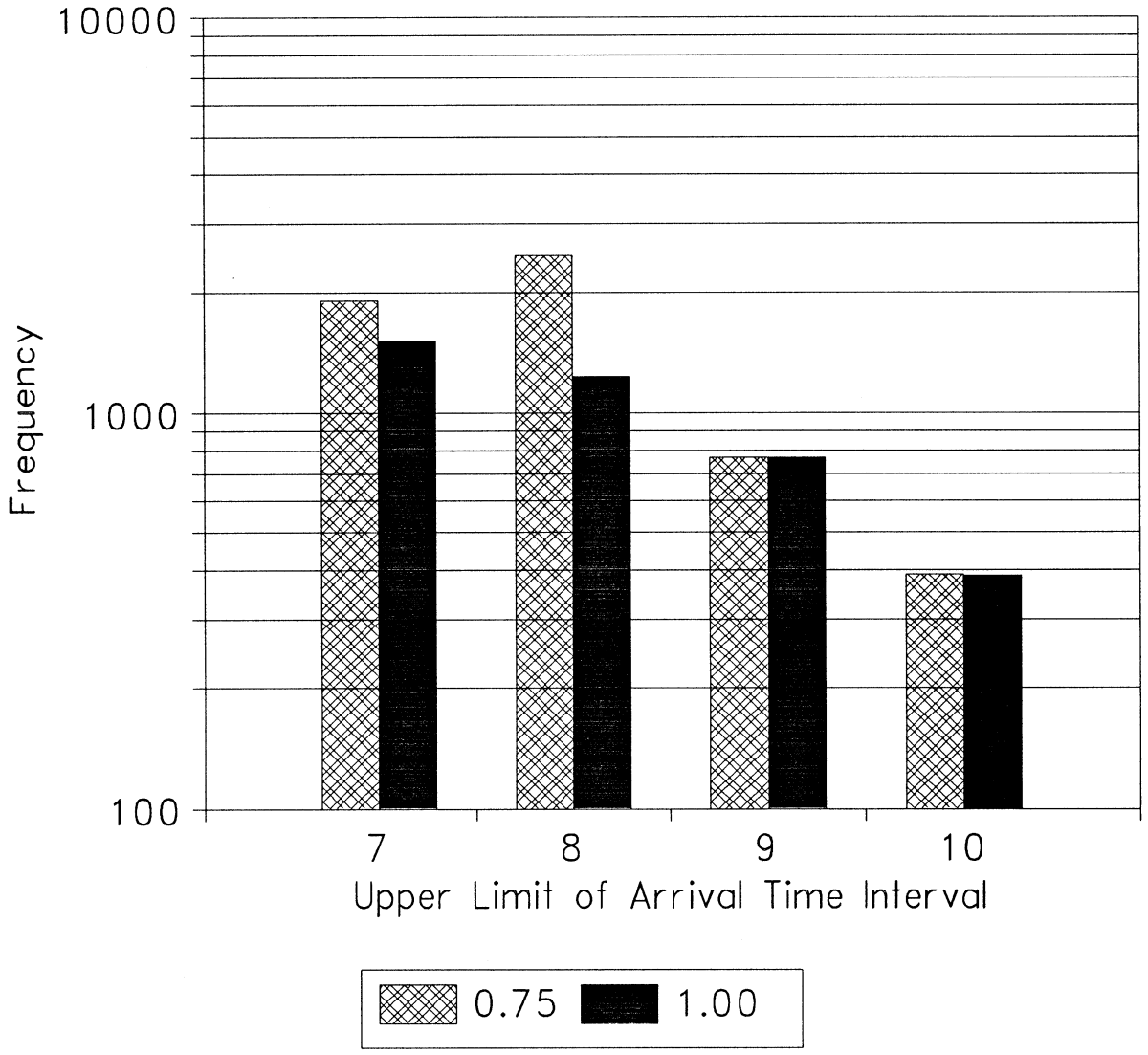

Figure 12. Effect of the Minimum Required Amplitude Ratio Between Closely Spaced Peaks That Are Opposite in Sign.

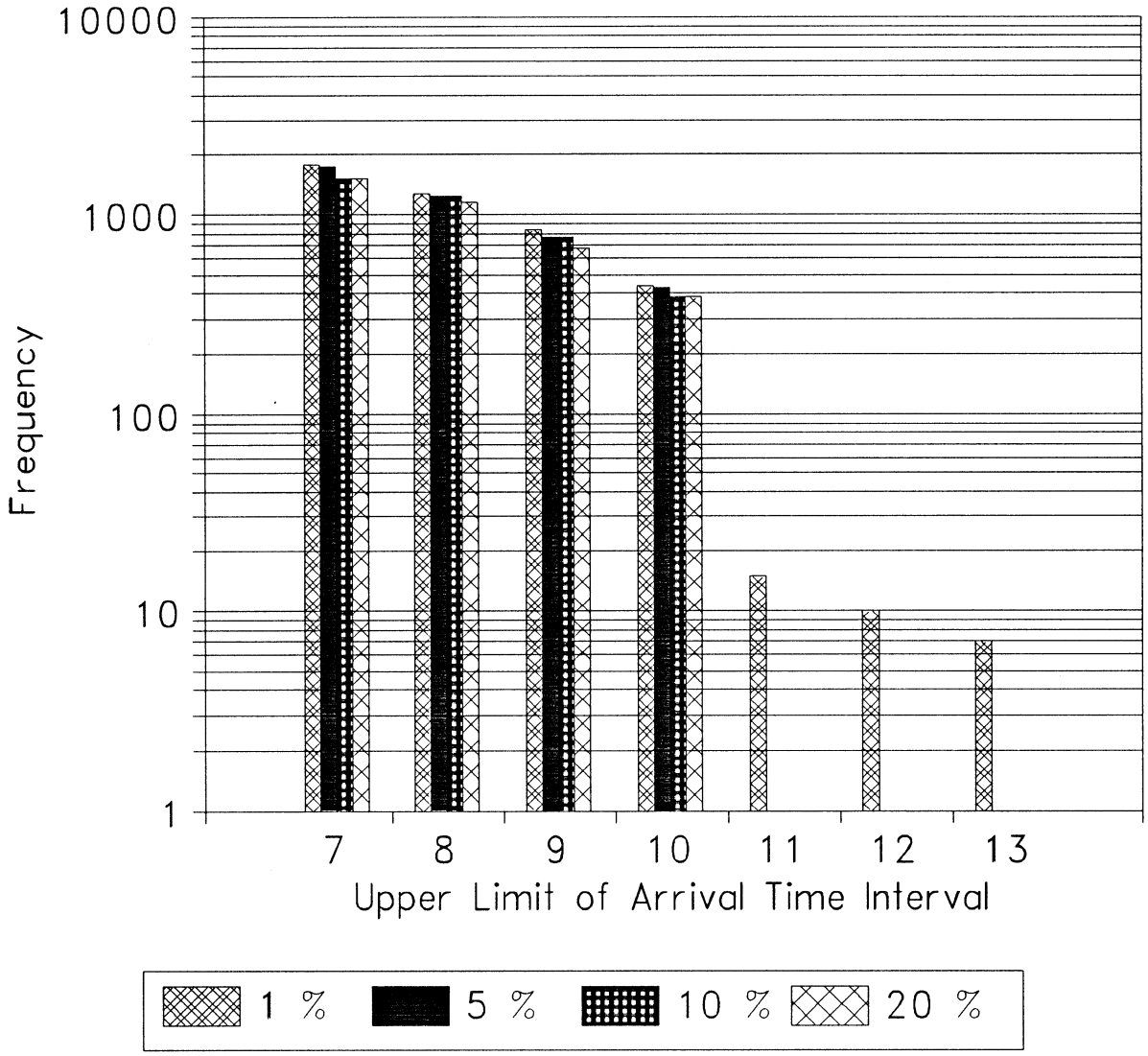

Figure 13. Effect of the Minimum Required Number of Peaks per Time Interval.

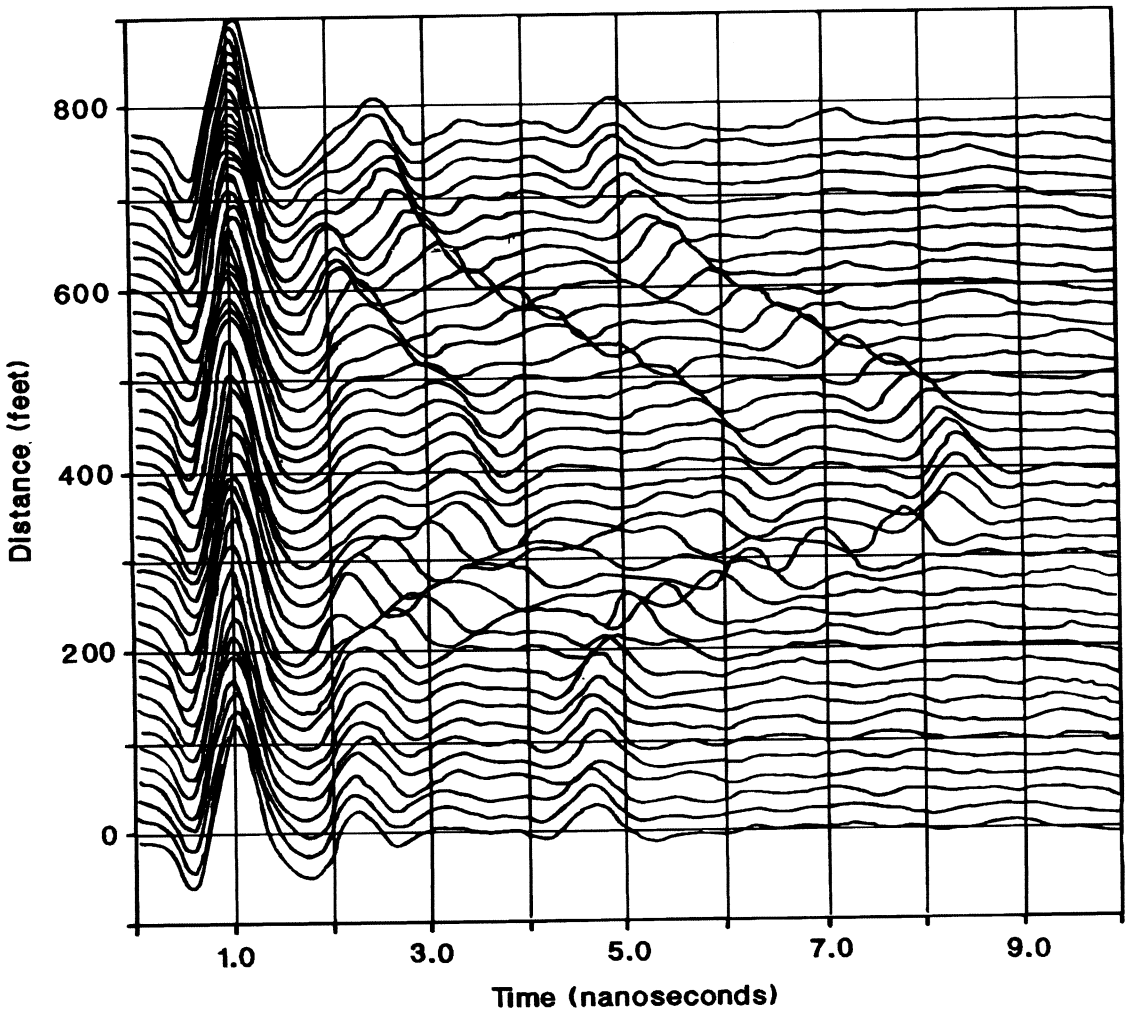

Figure 14. Localized Thickening Observed in Radar Data From In-Service Pavement.

VERIFICATION OF PEAK TRACKING

To further evaluate the procedure developed to detect layer interfaces, researchers applied the method to GPR data with gaps or discontinuities to check if mistracking will occur at locations where these features are present. GPR data from Florida pavements were used in testing the procedure. The findings from the tests conducted are presented in this section.

Figure 15 shows a portion of radar data taken along US 1 in Martin County. Data were collected using FDOT's radar vehicle along the inner wheelpath of the traffic lane going south from the Highway A1A junction to the Palm Beach County line. Visual examination of

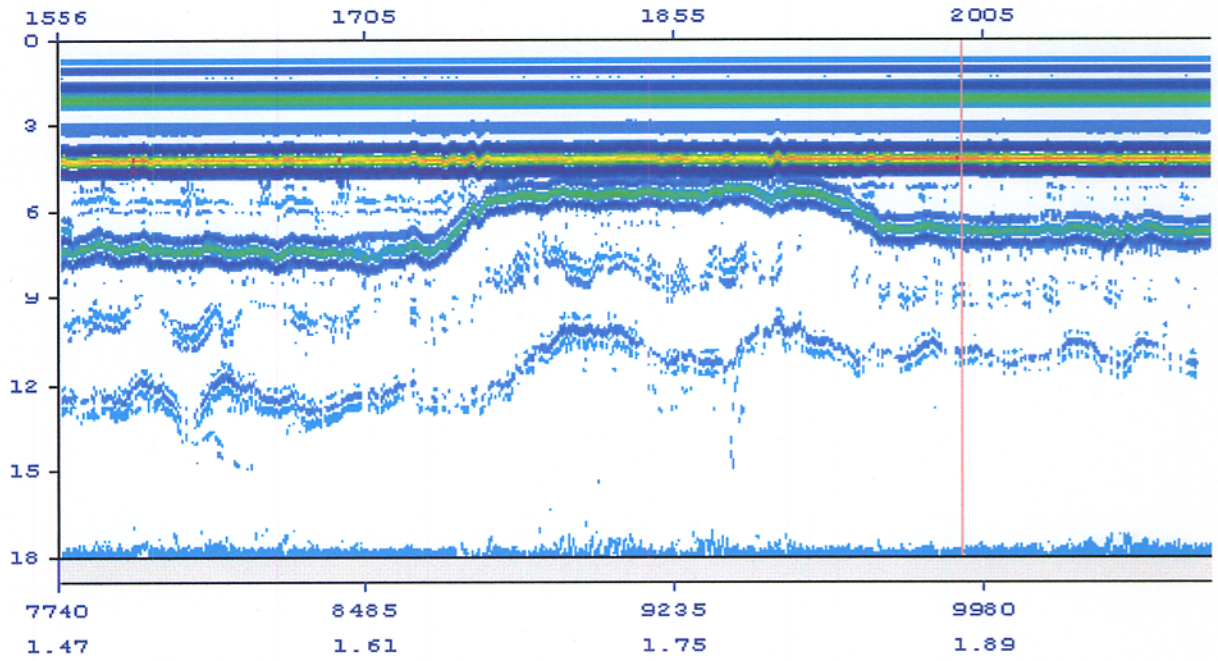

Figure 15. Radar Data Showing a Thinning of the Surface Layer.

the data revealed various changes in pavement section along the route. One such change is the thinning of the surface layer shown in Figure 15 as a rise in the reflections from the bottom of the layer beginning at about 8500 feet from the start of the survey. Then, at about 9600 feet, the surface again thickens as indicated by the increase in the arrival times of the reflections. The peak detection algorithm was tested using the data shown to see if the reflections from the bottom of the surface will be tracked correctly. For this test, the following decision criteria were used:

1. Minimum peak amplitude: 5 percent;
2. Minimum time interval between peaks: 0.9 ns;
3. Minimum amplitude ratio of successive, closely-spaced peaks that are opposite in sign: 1.0; and
4. Minimum required number of detected peaks in a given time interval: 10 percent of the number of traces in the segment analyzed.

Figure 16 illustrates the reflections tracked by the procedure. The reflections identified are colored red in the figure. As may be observed, the reflections from the top and bottom of the surface were detected. Figure 16 shows that the automated procedure for peak detection was

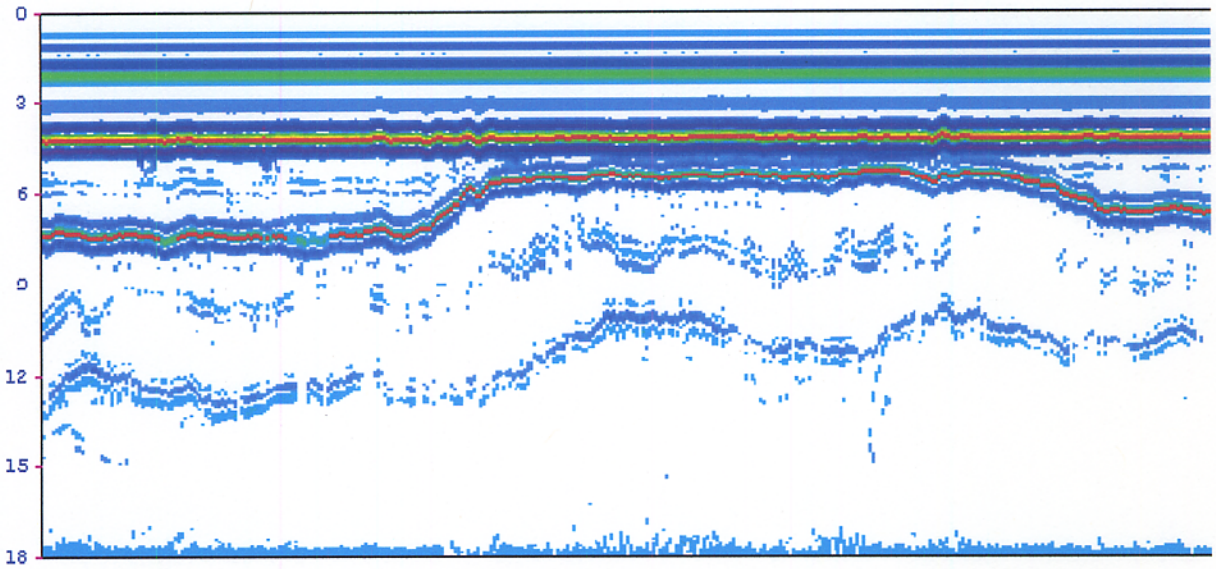

Figure 16. Reflections Tracked Using Data From US 1 in Martin County.

able to recognize the thinning of the surface layer. In particular, the reflections from the bottom of the layer were correctly tracked.

Researchers conducted another test using the data shown in Figure 17. Unlike the previous data which shows a gradual transition in the change of surface thickness, Figure 17 shows an abrupt change in thickness at about 37,100 feet from the start of the survey. The figure shows a portion of the data collected from a radar survey of I-75 in Marion County, from the SR 326 junction to the Sumter County line. Using the same decision criteria from the previous test, the results shown in Figure 18 were obtained. Again, the reflections detected by the method are colored red in the figure. Similar to the previous test, it is observed that the procedure recognized the abrupt change in the arrival times of the reflections from the bottom of the surface. No mistracking of the interface reflections occurred at the location of this abrupt change.

Two other tests were done using the data illustrated in Figure 19 where two features of interest may be observed. The first is an abrupt thickening of the surface layer, from about 10,500 feet to about 11,300 feet from the start of the survey. The other is a gap in the reflections from the bottom of the surface, starting at about 13,600 and ending at about 13,900 feet. This gap appears to be due to a bridge found along the route surveyed. The data shown were taken from radar measurements along SR 528 in Orange County, beginning at 0.8 miles east of SR 15 to 0.4 miles east of the Turnpike Toll Plaza.

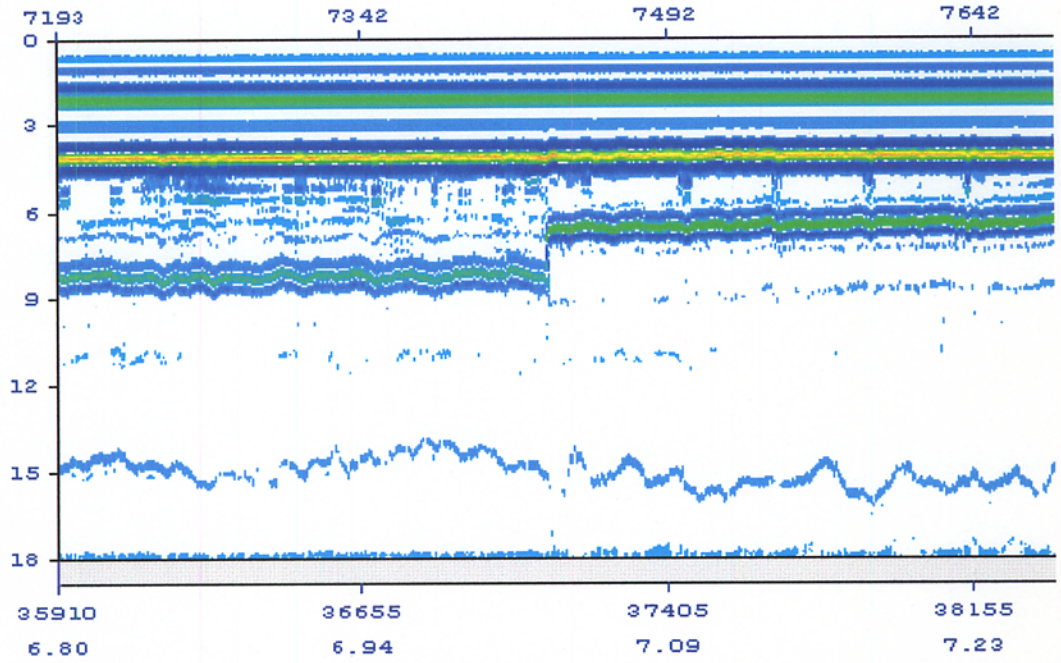

Figure 17. Radar Data Showing Abrupt Change in Surface Thickness.

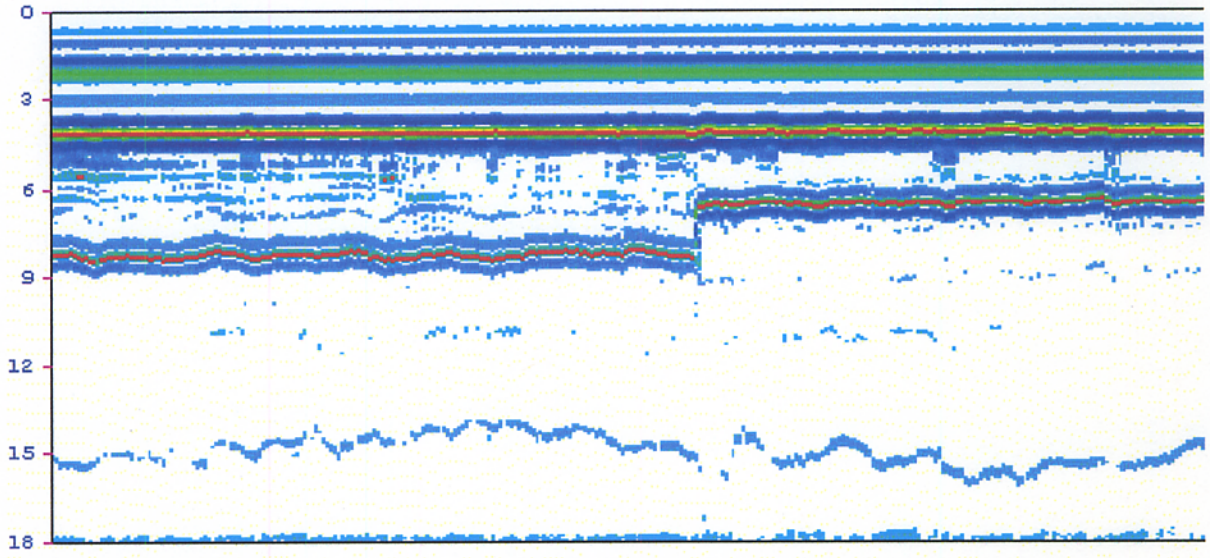

Figure 18. Reflections Tracked Using Data From I-75 in Marion County.

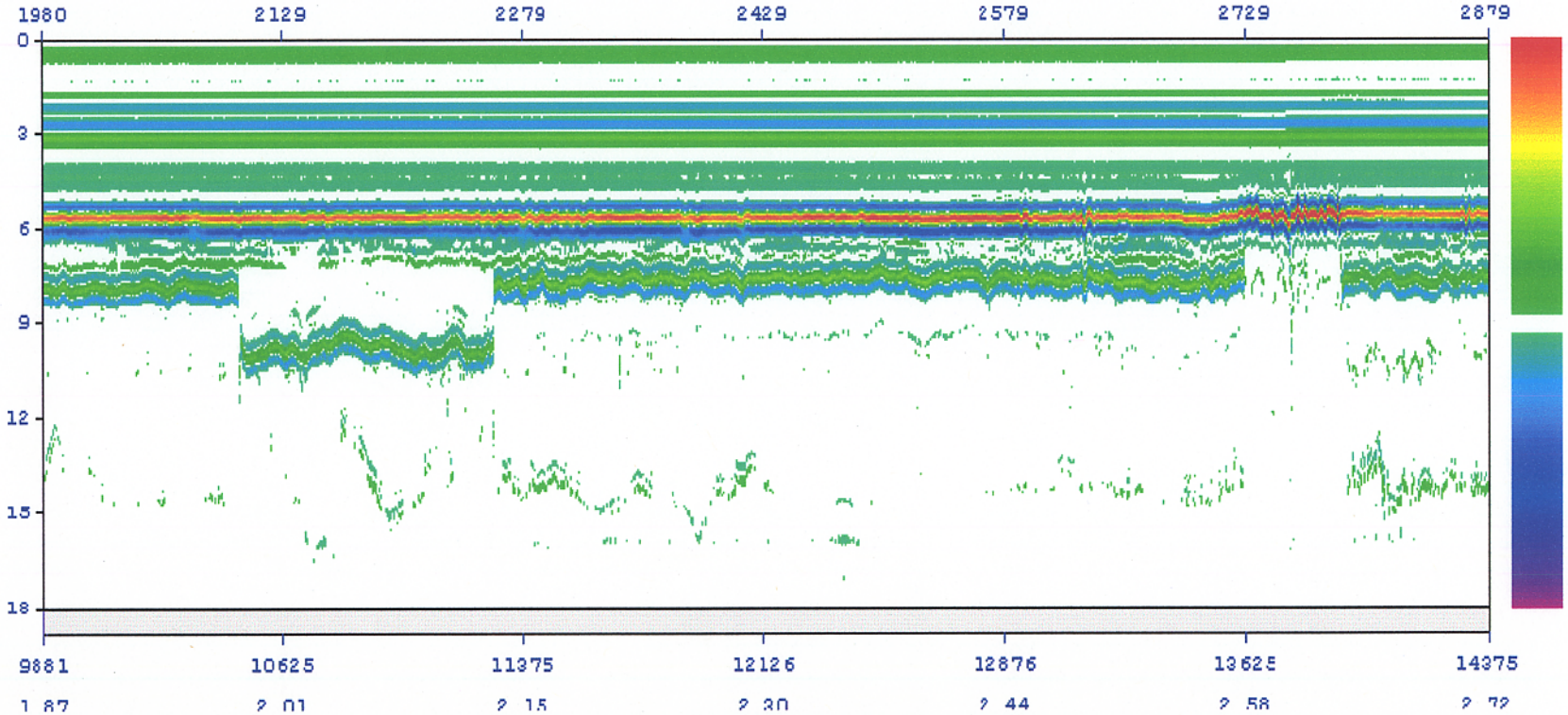

Figure 19. Radar Data From SR 528 in Orange County.

Researchers tested the peak detection algorithm using the radar data within the interval of the abrupt thickening shown in Figure 19. The results of this test are presented in Figure 20. It is observed that the procedure correctly tracked the reflections below the surface layer. The procedure did not mistrack at the first change where a sudden thickening is observed, nor at the second change where the thickness abruptly diminishes.

Figure 21 shows the results from the other test using the data within the vicinity of the gap observed in Figure 19. It is observed from Figure 21 that the peak detection algorithm was able to re-track the reflections from the bottom of the surface after the gap in the data. All test results therefore demonstrate that the automated procedure for layer interface detection is stable and can handle gradual or sudden changes in the patterns of the interface reflections, as well as gaps in the data. The findings verify that the decision criteria incorporated into the procedure provide a reasonable simulation of the process a person goes through when manually identifying the relevant peaks in the radar data. It also does not require much computer time to run based on the test experience.

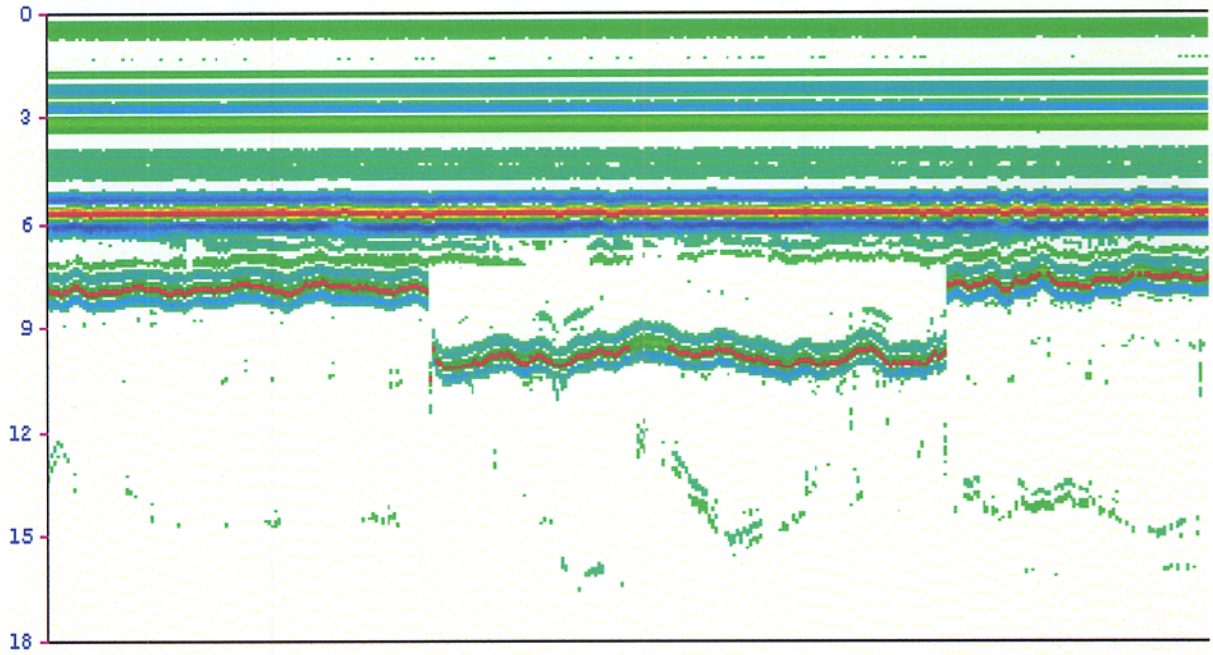

Figure 20. Test Results Using Data From SR 528 Where an Abrupt Thickening is Found.

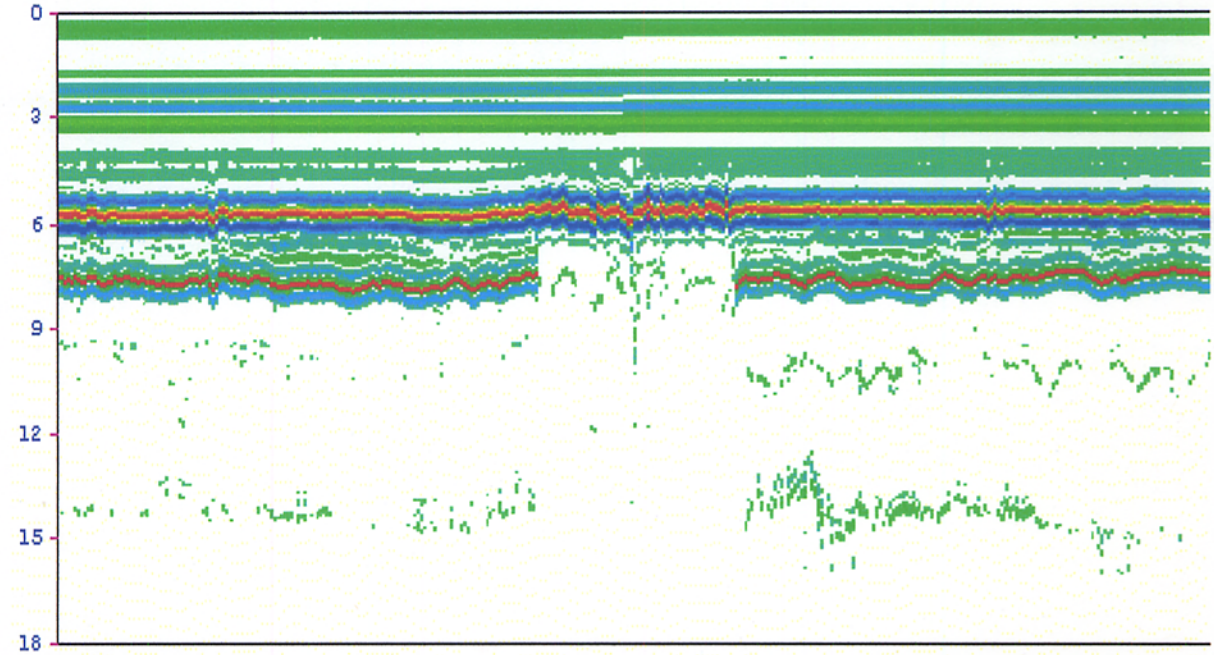

Figure 21. Test Results Using Data From SR 528 Where a Gap in the Reflections From the Button of the Surface is Observed.

CHAPTER IV.
VERIFICATION OF PREDICTED LAYER THICKNESSES FROM THE TERRA PROGRAM

INTRODUCTION

With the development and verification of the peak detection algorithm, researchers came up with a computer program for GPR data analysis by coupling a thickness prediction procedure to the methodology presented in Chapter III. In this computer program, layer thicknesses are computed from the amplitudes and arrival times of the interface reflections using a general *n*-layered pavement model. In addition, the predicted thicknesses are sorted into surface and base layers using decision rules that are tied to the expected values of layer thicknesses and dielectric constants for surface and base materials found in Florida. These rules are based on prior experience with analyzing GPR data collected on Florida pavements. In the following, the TERRA program is verified by comparing layer thicknesses predicted from GPR data with measured thicknesses taken from cores.

VERIFICATION OF TERRA

To verify the TERRA program, researchers used available radar data taken on Florida pavements as part of a study to evaluate the application of the Falling Weight Deflectometer (FWD) to predict pavement deterioration. Table 3 shows the sites included in the evaluation of the TERRA program. The radar data corresponding to each FWD site were first established. Table 3 shows that, in most cases, the radar data and FWD file names are the same. However, there are a few FWD files for which the identification of the corresponding radar data files was not as straightforward. These are the FWD data from SR 134 in Duval county and SR 91 in Lake county. There are four files of FWD data taken on SR 134. Based on the header information input by the operator during data collection, it was determined that the files, SR134_A.DAT and SR134_A2.DAT, contain radar data taken on the eastbound direction. In particular, the header information for SR134_A2.DAT indicate that the radar data were taken on the east passing lane and from the second radar run made in that direction. Based on the beginning and ending milepost limits given in Table 3, the files SR134EB and

Table 3. Routes Where FWD, Radar, and Core Measurements Were Made.

FWD File Name	Section Number	County	Begin Milepost	Ending Milepost	Length of FWD Section (miles)	Radar Data File	Length of Radar Survey (miles)
SR134EB	72220	Duval	0.050	2.550	2.500	SR134_A.DAT	2.086
SR134EBC	72220	Duval	2.600	5.458	2.858	SR134_A2.DAT	2.091
SR134WBC	72220	Duval	2.600	7.777	5.177	Not sure	
SR134WB	72220	Duval	0.072	2.553	2.481	Not sure	
SR13SBC	72160	Duval	0.100	3.115	3.015	SR13SBC.DAT	3.013
SR200NBC	26060	Alachua	6.138	9.400	3.262	SR200NBC.DAT	3.749
SR222WBC	26005	Alachua	0.400	7.952	7.552	SR222WBC.DAT	7.361
SR222EBC	26005	Alachua	4.845	7.194	2.349	SR222EBC.DAT	2.337
SR329NBC	26020	Alachua	1.907	2.233	0.326	SR329NBC.DAT	0.592
SR25NBC	26010	Alachua	2.502	3.234	0.732	SSR25NBC.DAT	3.227
SR9SBC1	70225	Brevard	13.813	22.509	8.696	None available	
SR9SBC21	70220	Brevard	14.335	21.453	7.118	None available	
SR5NBC	70020	Brevard	24.238	27.932	3.694	None available	
SR434NBC	75037	Orange	0.000	2.679	2.679	SR434NBC.DAT	2.777
SR500NBC	75020	Orange	3.405	7.200	3.795	SR500NBC.DAT	4.268
SR500SBC	75020	Orange	10.714	12.280	1.566	SR500SBC.DAT	1.548
SR482WBC	75002	Orange	0.000	2.200	2.200	SR482WBC.DAT	2.320
SR46WBC	77030	Seminole	3.810	4.537	0.727	None available	
SR46EBC	77030	Seminole	8.000	8.448	0.448	None available	
SR19NB	11100	Lake	3.800	4.906	1.106	SR19NB.DAT	1.104
SR91SBC	11470	Lake	7.651	10.954	3.303	SR91SBP1.DAT	3.333
SR91SBC	11470	Lake	22.891	23.793	0.902	SR91SBP.DAT	0.814
SR25NB1	11200	Lake	0.000	3.174	3.174	SR25NB.DAT	14.760
SR25NB2	11200	Lake	3.174	7.350	4.176	SR25NB.DAT	14.760

SR134EBC appear to have been collected from FWD surveys made on two adjacent sections, with SR134EB coming before SR134EBC in the eastbound direction. Since the header information for SR134_A2.DAT indicate that the file was created on the second run of the radar vehicle in that direction, researchers assumed that this file corresponds to the FWD file, SR134EBC, and that the radar file, SR134_A.DAT corresponds to the FWD file, SR134EB.

The radar data files corresponding to FWD files SR134WBC and SR134WB could not be determined with a reasonable degree of certainty based on the available information. From the header cards, it was determined that the radar files SR134_A3.DAT and SR134_A4.DAT were both taken in the westbound direction but on different lanes. SR134_A3.DAT was collected on the westbound passing lane, while SR134_A4.DAT was collected on the westbound traffic lane. Since there were no information available to the researchers that show the lanes on which the FWD data and cores were taken, the correspondence between the radar data and FWD files could not be determined based on the lane information given in the header cards of the radar files. Based on the beginning and ending milepost limits given in Table 3, it appears that the FWD files SR134WBC and SR134WB were taken on two neighboring sections, with SR134WBC coming before SR134WB in the westbound direction. It appears from the header information and from the file names that SR134_A3.DAT was collected prior to SR134_A4.DAT. In view of this, it would seem that the radar file SR134_A3.DAT corresponds with SR134WBC, and that SR134_A4.DAT corresponds with SR134WB. However, the length of the radar survey from which SR134_A3.DAT was obtained is 2.233 miles which is only 43 percent of the length of SR134WBC. Also, the length of the survey corresponding to radar file SR134_A4.DAT is 2.105 miles. Thus, the survey lengths for both radar files are more comparable with the length of SR134WB. As will be shown later, the average surface layer thicknesses from these two radar files are also more comparable with the average of the core thicknesses from SR134WB. In view of the preceding considerations, researchers were not able to resolve the correspondence between the radar and FWD data files for the westbound direction of SR 134 in Duval county.

With respect to the FWD sections along SR 91 in Lake county, there are two sections identified in the list of test files provided to the researchers by the Florida DOT. These are identified in Table 3 as SR91SBC segments. Based on the header information in the radar data files, researchers determined that the radar file SR91SBP1.DAT corresponds with the

FWD segment between mileposts 7.651 and 10.954, and that file SR91SBP.DAT corresponds with the other FWD segment between mileposts 22.891 and 23.793. In particular, the header information for SR91SBP1.DAT indicates that the data were collected between mile marker 285 and south of bridge #70 which is consistent with the segment information provided in the list of FWD test files. Likewise, the header information for SR91SBP.DAT indicates that the data were collected between a county line (identified as Lake/Sumter in the list of FWD test files) and mile marker 297.

The surface thicknesses measured from the cores are reproduced in Table 4. Once the correspondence between the FWD and radar data files were established, researchers predicted the surface and base layer thicknesses from the radar data using the TERRA program. The surface thickness predictions were then compared with the core thicknesses. It is noted that no base thickness measurements were made during coring so that the predictions of base thicknesses from radar data could not be verified against actual measurements.

Before the runs of the TERRA program were made, researchers reviewed the raw radar data for each FWD section. During this review, the segments observed from the radar data were identified by picking the endpoints of each segment. This process created a "pick" file for each FWD section which was input to the TERRA program. For each of the segments identified in the "pick" file, the program detects the layer interfaces based on the user-prescribed criteria given in Table 5, which were explained in Chapter III. As used with the TERRA program, the procedure of "picking" a radar data file involves only the identification of segment endpoints. This procedure is different from that required in the application of the PAVLAYER software where the interface reflections are also identified by the user for each delineated segment. In the TERRA program, the interface reflections for each segment are automatically detected. Thus, the process of picking requires significantly less time and effort. From the analyses of the radar data files conducted, "picking" the segment endpoints required about the same time as viewing the radar data to be analyzed.

To compare the radar thicknesses with the core thicknesses, the locations of the cores with respect to the radar data had to be initially established. It is noted that the cores were obtained separately from the radar surveys. From what researchers know, the radar surveys were done later. In practice, it would be best to conduct the radar surveys prior to coring so that the data may be used to establish where cores should be taken. To tie the core locations

Table 4. Surface Thicknesses Determined From Cores.

FWD File Name	Core Locations and Thicknesses (inches) (OWP=Outside Wheel Path; IWP=Inside Wheel Path; C=Between Wheel Path)					
SR134EB	Milepost	0.734	0.921	1.149	1.673	1.935
	Thickness	3.25	3.00	3.00	3.00	3.00
	Milepost	1.998				
	Thickness	3.00				
SR134EBC	Milepost	3.191 (OWP)	4.172 (OWP)	5.194 (OWP)		
	Thickness	4.00	4.00	4.00		
SR134WBC	Milepost	7.416 (OWP)	5.896 (OWP)	5.380 (OWP)	4.821 (C)	4.543 (OWP)
	Thickness	5.00	4.50	4.00	4.50	4.25
	Milepost	3.925 (IWP)	2.786 (OWP)			
	Thickness	3.75	4.25			
SR134WB	Milepost	2.342	2.136	1.842	1.498	1.440
	Thickness	3.50	3.25	3.00	3.50	3.50
	Milepost	1.005				
	Thickness	3.50				
SR13SBC	Milepost	2.878 (OWP)	2.258 (C)	1.808 (OWP)	1.175 (C)	0.853 (OWP)
	Thickness	4.00	4.00	4.00	4.00	3.75
SR200 NBC	Milepost	6.176 (OWP)	6.677 (OWP)	7.191 (OWP)	7.764 (OWP)	8.247 (OWP)
	Thickness	3.75	4.00	4.00	4.25	4.00
	Milepost	9.260 (OWP)				
	Thickness	3.50				
SR222WBC	Milepost	7.563 (IWP)	6.920 (IWP)	5.544 (OWP)	5.017 (OWP)	4.172 (OWP)
	Thickness	5.00	4.50	4.50	4.25	5.00
	Milepost	3.758 (OWP)	3.759 (OWP)	2.940 (OWP)	2.143 (OWP)	1.627 (OWP)
	Thickness	4.75	4.75	5.00	5.25	5.00
SR222EBC	Milepost	4.845 (OWP)	5.539 (OWP)	5.958 (OWP)	7.103 (OWP)	
	Thickness	5.00	4.75	5.00	5.00	

Table 4. Surface Thicknesses Determined From Cores (continued).

FWD File Name	Core Locations and Thicknesses (inches) (OWP=Outside Wheel Path; IWP=Inside Wheel Path; C=Between Wheel Path)					
SR329NBC	Milepost	1.92 (OWP)	1.975 (OWP)			
	Thickness	3.25	3.25			
SR25NBC	Milepost	2.731 (OWP)	3.047 (OWP)			
	Thickness	4.25	4.25			
SR9SBC1	Milepost	20.930 (OWP)	19.945 (OWP)	19.142 (OWP)	17.440 (OWP)	16.791 (OWP)
	Thickness	6.25	6.25	7.00	6.75	7.00
	Milepost	16.346 (OWP)	15.878 (OWP)	15.408 (OWP)	14.911 (OWP)	14.474 (OWP)
	Thickness	7.00	7.50	6.75	7.50	6.50
SR9SBC21	Milepost	21.434 (OWP)	21.016 (OWP)	20.521 (OWP)	20.024 (OWP)	19.557 (OWP)
	Thickness	5.00	5.75	5.50	5.87	5.25
	Milepost	19.061 (OWP)	18.491 (OWP)	18.027 (OWP)	17.517 (OWP)	17.061 (OWP)
	Thickness	5.50	6.00	6.00	5.50	5.50
SR5NBC	Milepost	24.289 (OWP)	24.804 (OWP)	25.255 (OWP)	25.720 (OWP)	26.049 (OWP)
	Thickness	4.00	4.50	4.00	5.00	4.50
	Milepost	26.583 (OWP)				
	Thickness	4.50				
SR434NBC	Milepost	0.195 (OWP)	2.440 (OWP)			
	Thickness	4.50	4.00			
SR500NBC	Milepost	3.593 (OWP)	4.077 (OWP)	4.603 (OWP)	5.797 (OWP)	6.445 (OWP)
	Thickness	7.25	6.50	3.25	3.25	4.5
	Milepost	6.965 (OWP)				
	Thickness	5.00				

Table 4. Surface Thicknesses Determined From Cores (continued).

FWD File Name	Core Locations and Thicknesses (inches) (OWP=Outside Wheel Path; IWP=Inside Wheel Path; C=Between Wheel Path)					
SR500SBC	Milepost	11.777 (OWP)	10.896 (OWP)			
	Thickness	4.00	3.00			
SR482WBC	Milepost	2.187 (OWP)	1.788 (OWP)	1.319 (OWP)	0.847 (OWP)	0.333 (OWP)
	Thickness	3.00	3.00	4.00	5.00	4.50
SR46WBC	Milepost	4.495 (OWP)	4.406 (OWP)	4.132 (OWP)		
	Thickness	3.50	3.50	3.50		
SR46EBC	Milepost	8.079 (OWP)				
	Thickness	3.50				
SR19NB	Milepost	4.016 (OWP)	4.834 (OWP)			
	Thickness	4.00	4.00			
SR91SBC	Milepost	10.836 (OWP)	10.217 (OWP)	9.697 (OWP)	9.061 (OWP)	8.566 (OWP)
	Thickness	5.50	5.00	4.75	5.00	5.50
	Milepost	8.036 (OWP)	23.496 (OWP)	23.011 (OWP)		
	Thickness	5.00	4.50	5.00		
SR25NB1	Milepost	1.173 (OWP)	1.809 (OWP)	1.809 (C)	2.304 (OWP)	2.995 (OWP)
	Thickness	3.50	3.00	2.50	2.50	3.75
SR25NB2	Milepost	3.866 (OWP)	4.868 (C)	5.800 (OWP)	6.827 (OWP)	6.827 (C)
	Thickness	2.50	3.00	2.25	2.25	2.25

Table 5. Criteria Used in Detecting Layer Interfaces.

Peak Detection Criterion	Value Specified in Analysis
Minimum required amplitude (percent of metal plate reflection)	2 percent
Minimum time interval between reflections	0.9 ns
Minimum amplitude ratio of closely spaced peaks opposite in sign	1.0
Minimum required percentage of peak occurrences within a segment	10 percent

with the radar data, researchers used the first marker in the radar data as a reference since this marker coincides with the beginning of the FWD section from information given by Jerry Moxley of the Florida DOT. Figures 22 to 37 plot the predicted layer thicknesses and the core thicknesses. In evaluating the accuracy of the predicted thicknesses, the following considerations are noted:

1. Errors in tying the core locations with the radar data will affect the comparisons of the measured versus predicted core thicknesses. For this evaluation, location errors may arise because of:
   a) Discrepancies between the first marker location in the radar data and the beginning of the FWD segment;
   b) Accumulation of DMI errors with distance. In practice, it is advisable to have several markers in the radar data that are tied to known physical locations along the survey route. In this way, each core location may be tied to the closest marker in the radar data to minimize distance errors. For this evaluation, the core locations were tied to the radar data using the first marker which supposedly coincides with the beginning of the FWD site. The ground locations of other markers in the data are not known;
   c) Differences between the instruments used to measure distances when the cores were taken and when the radar surveys were made. It is noted that different DMIs were used for the coring and the radar surveys.

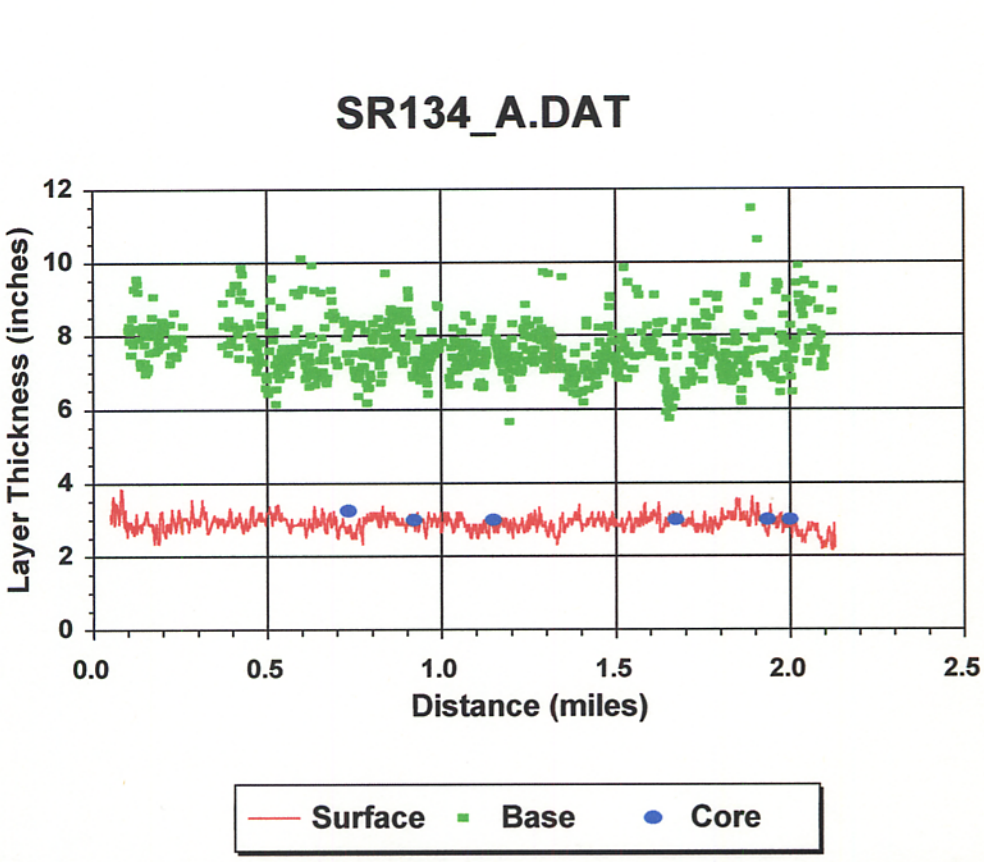

Figure 22. Predicted Layer Thicknesses and Core Thicknesses on FWD Site SR134EB.

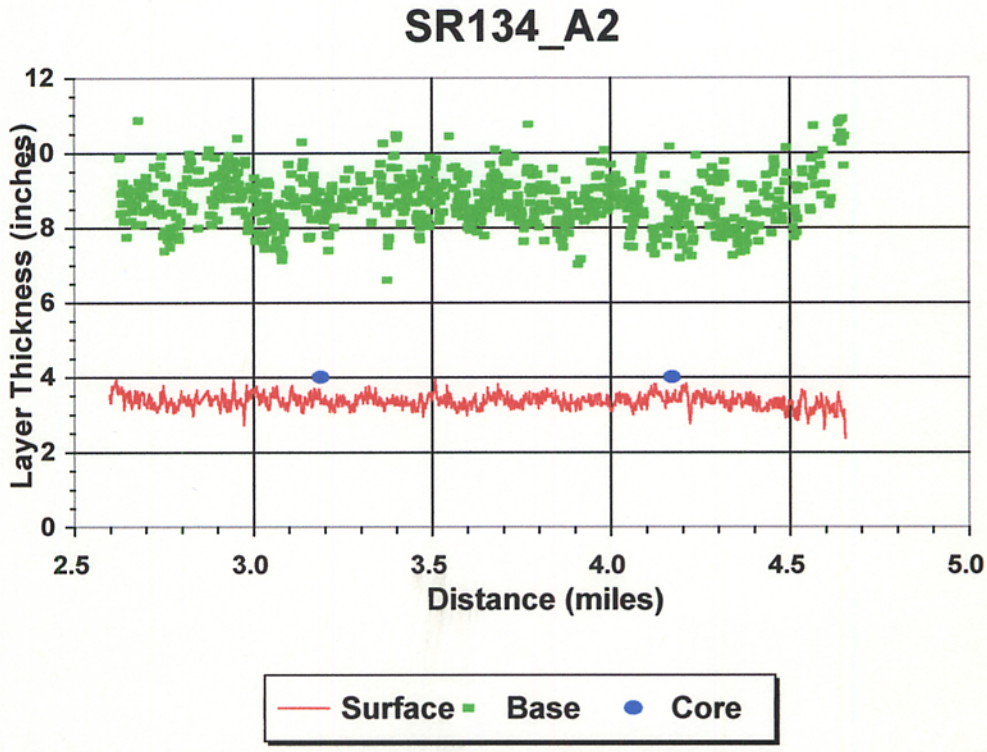

Figure 23. Predicted Layer Thicknesses and Core Thicknesses on FWD Site SR134EBC.

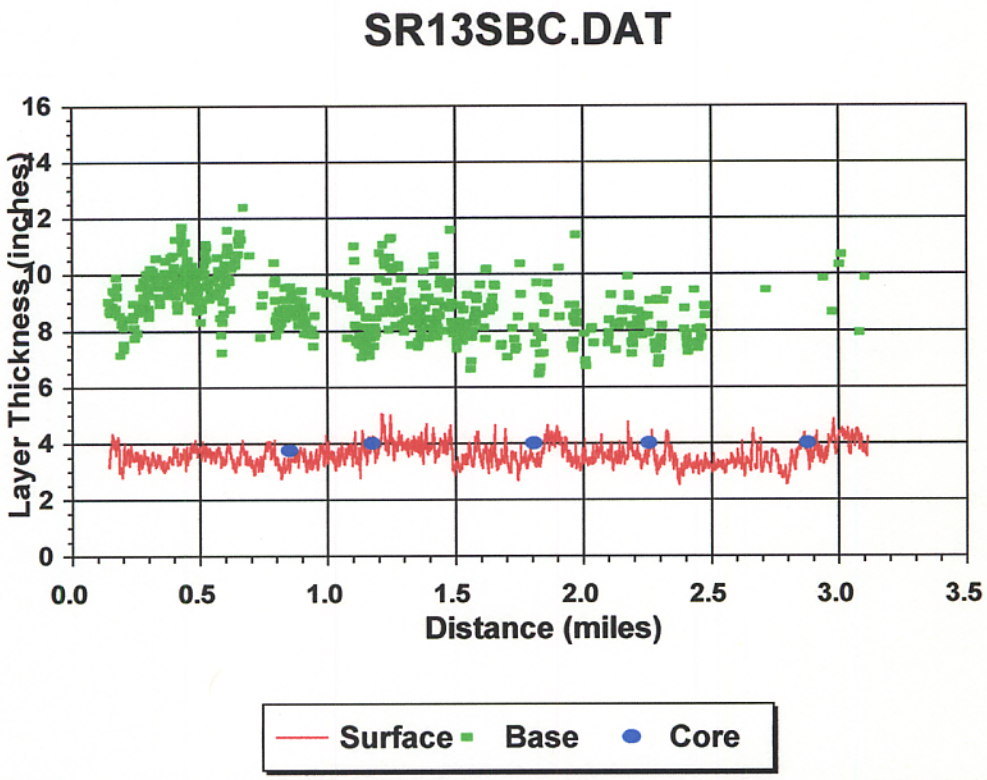

Figure 24. Predicted Layer Thicknesses and Core Thicknesses on FWD Site SR13SBC.

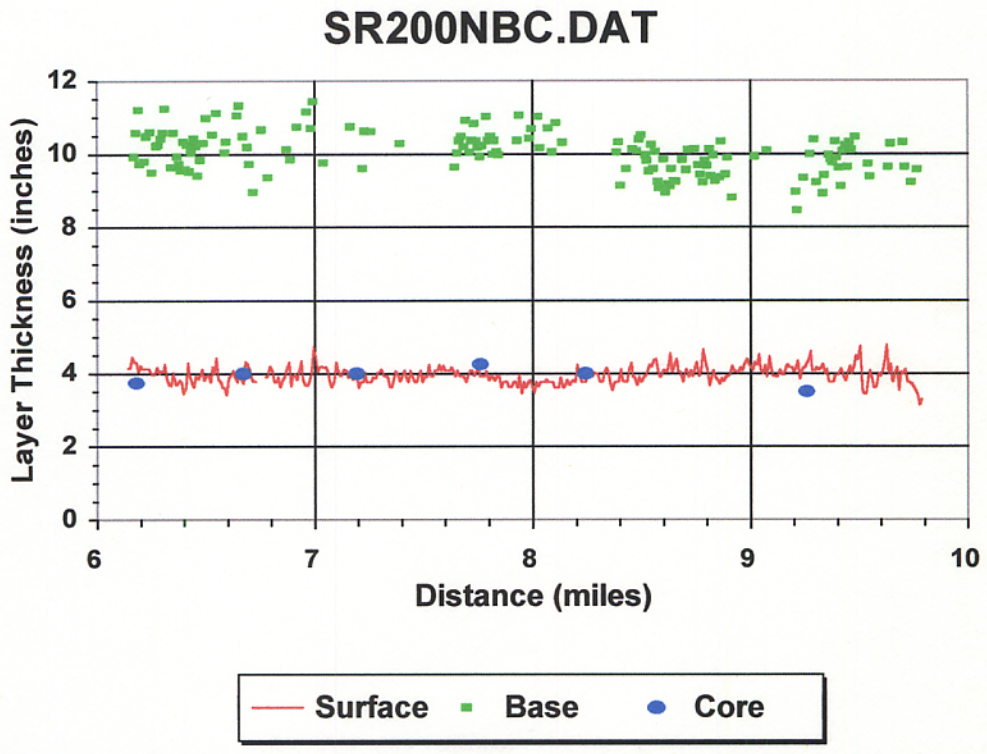

Figure 25. Predicted Layer Thicknesses and Core Thicknesses on FWD Site SR200NBC.

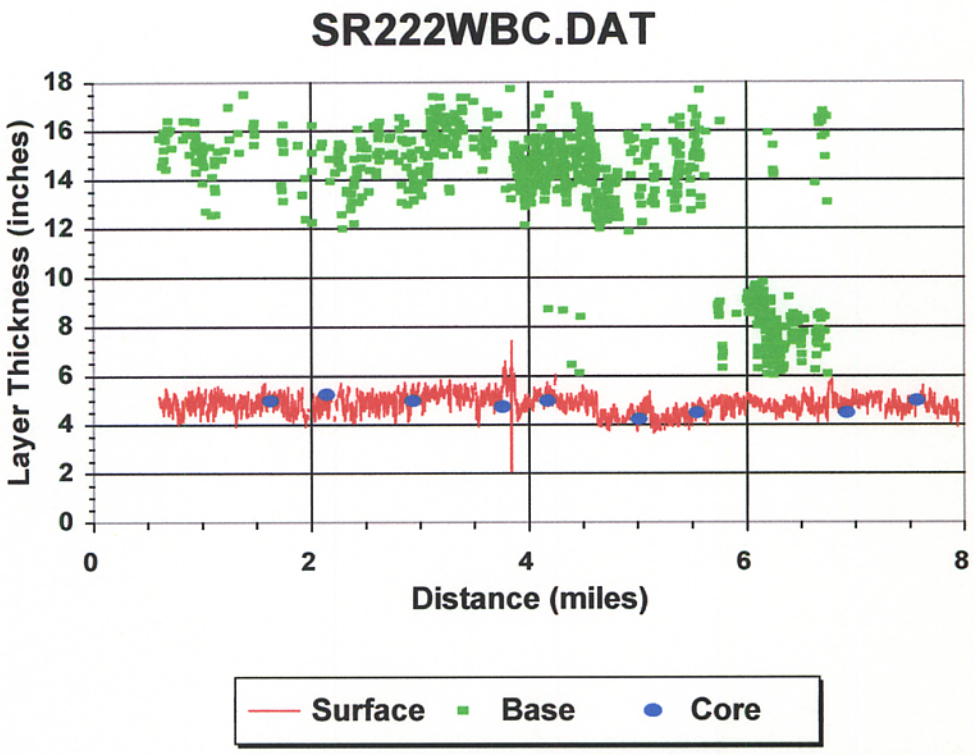

Figure 26. Predicted Layer Thicknesses and Core Thicknesses on FWD Site SR222WBC.

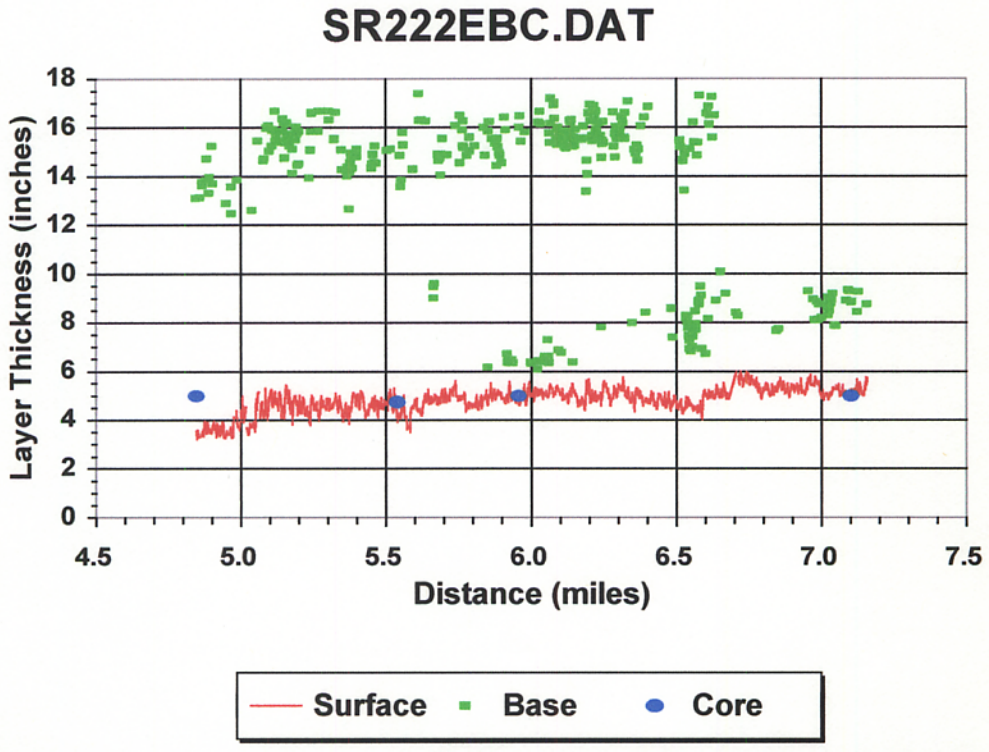

Figure 27. Predicted Layer Thicknesses and Core Thicknesses on FWD Site SR222EBC.

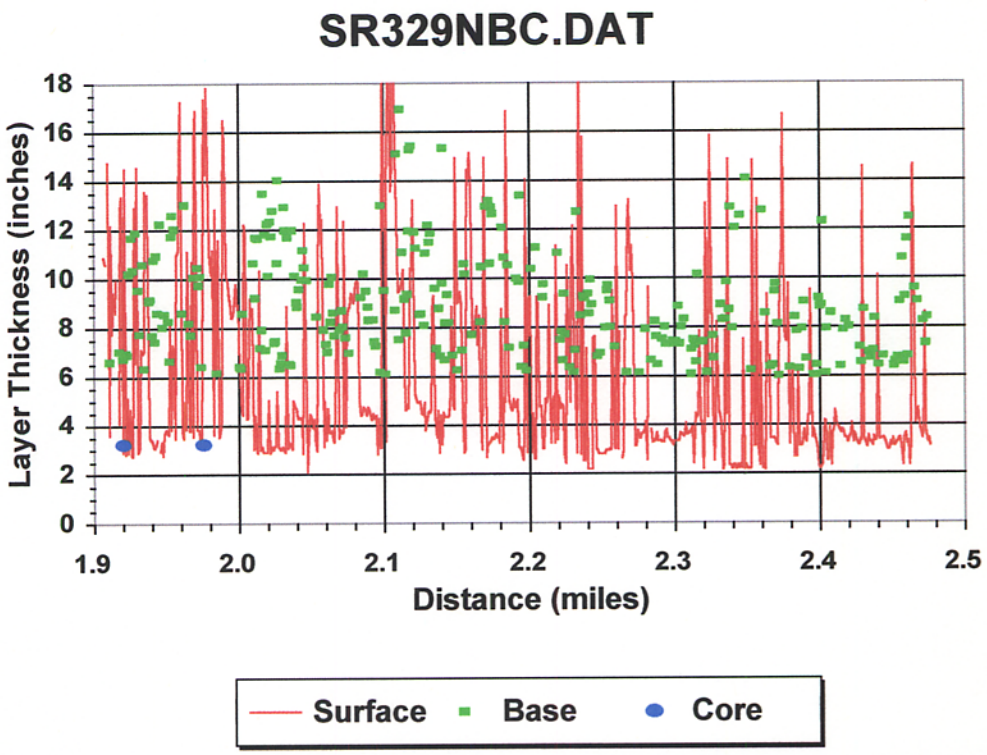

Figure 28. Predicted Layer Thicknesses and Core Thicknesses on FWD Site SR329NBC.

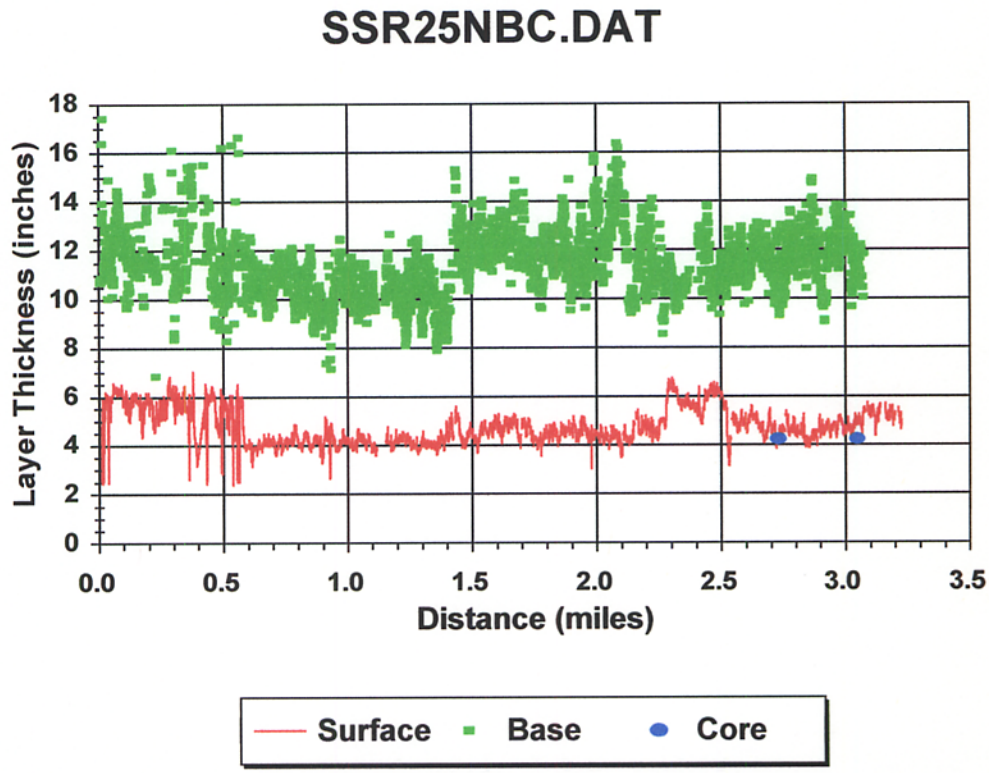

Figure 29. Predicted Layer Thicknesses and Core Thicknesses on FWD Site SR25NBC.

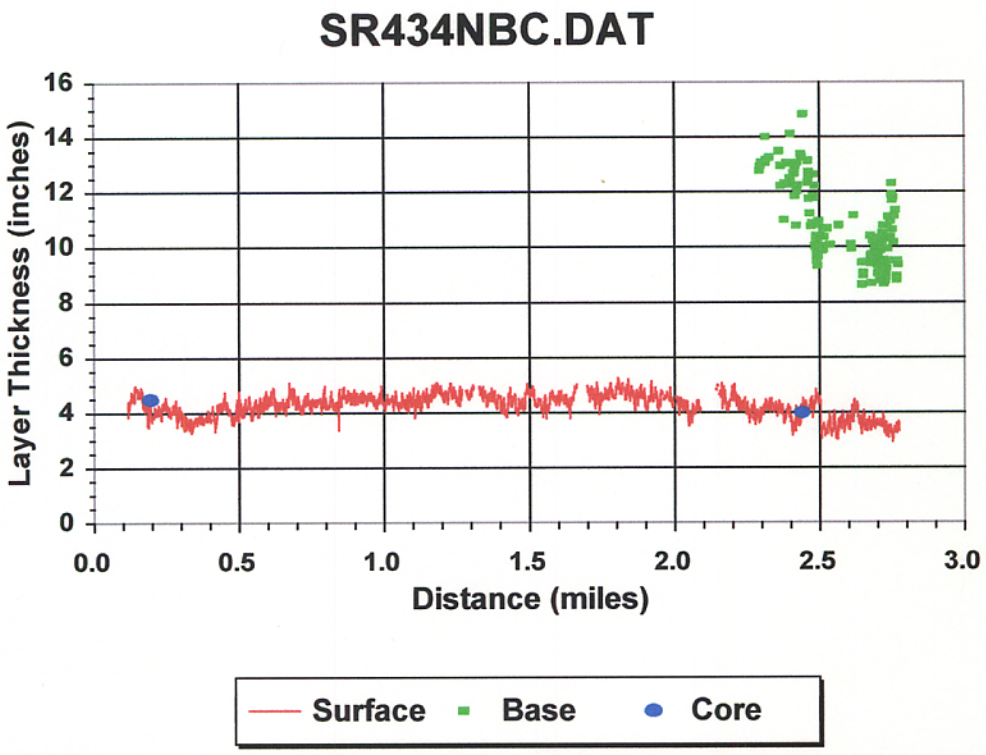

Figure 30. Predicted Layer Thicknesses and Core Thicknesses on FWD Site SR434NBC.

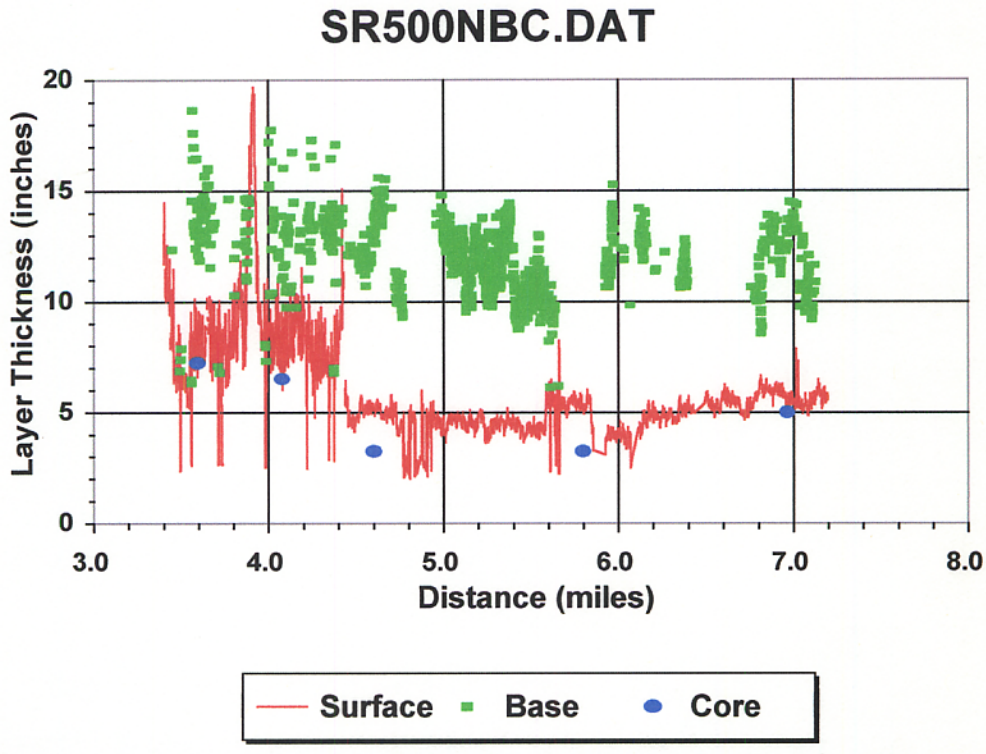

Figure 31. Predicted Layer Thicknesses and Core Thicknesses on FWD Site SR500NBC.

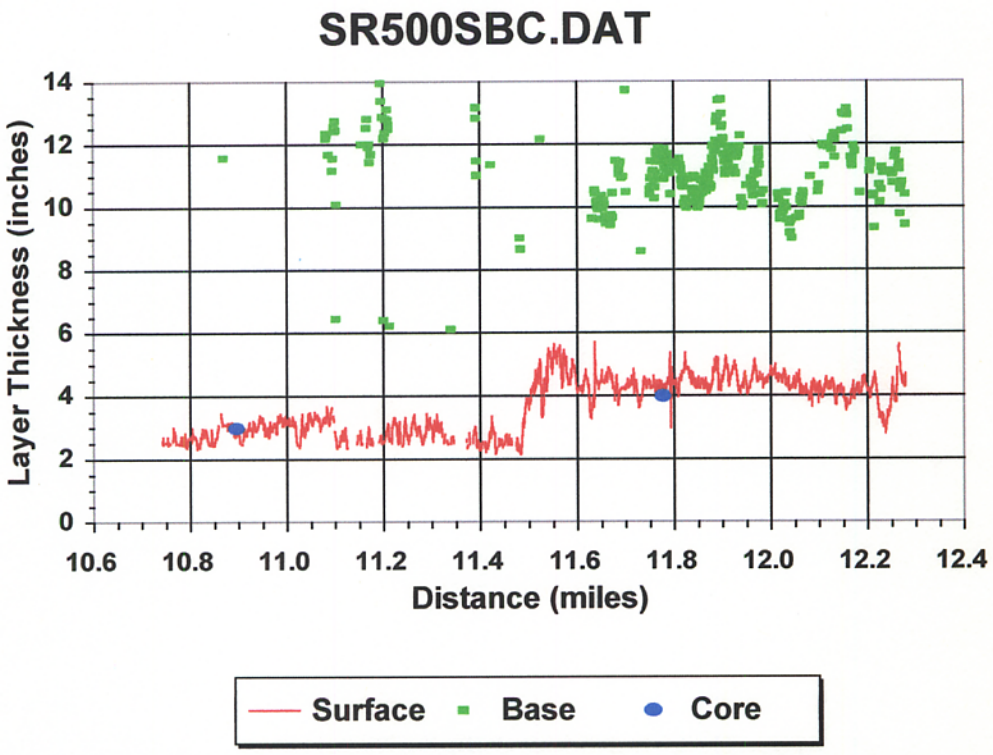

Figure 32. Predicted Layer Thicknesses and Core Thicknesses on FWD Site SR500SBC.

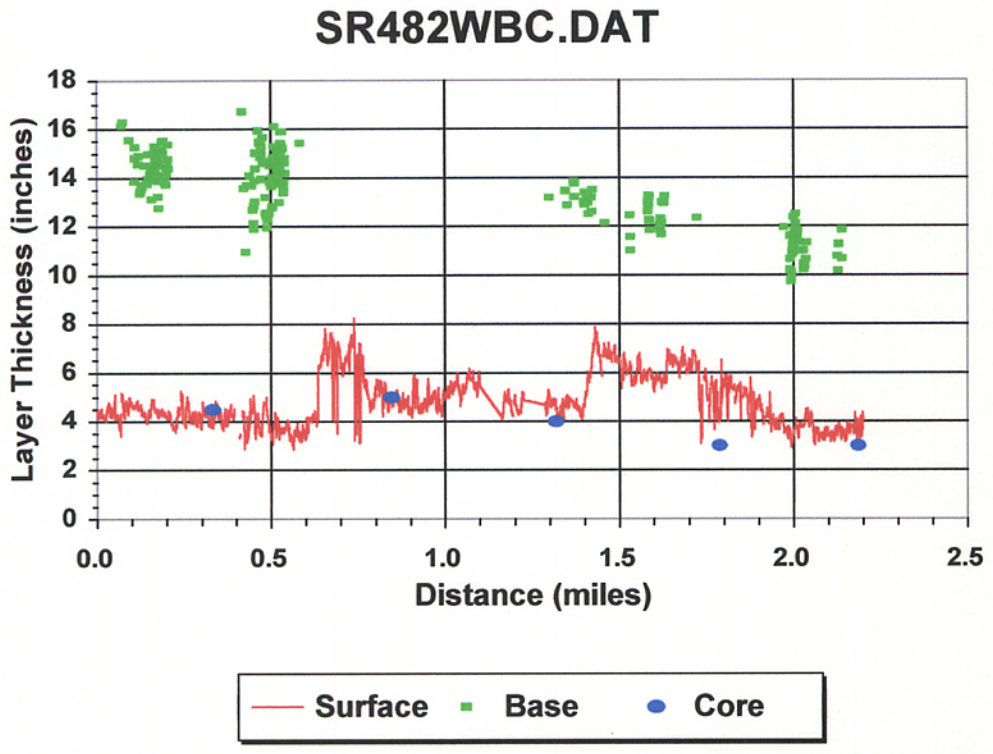

Figure 33. Predicted Layer Thicknesses and Core Thicknesses on FWD Site SR482WBC.

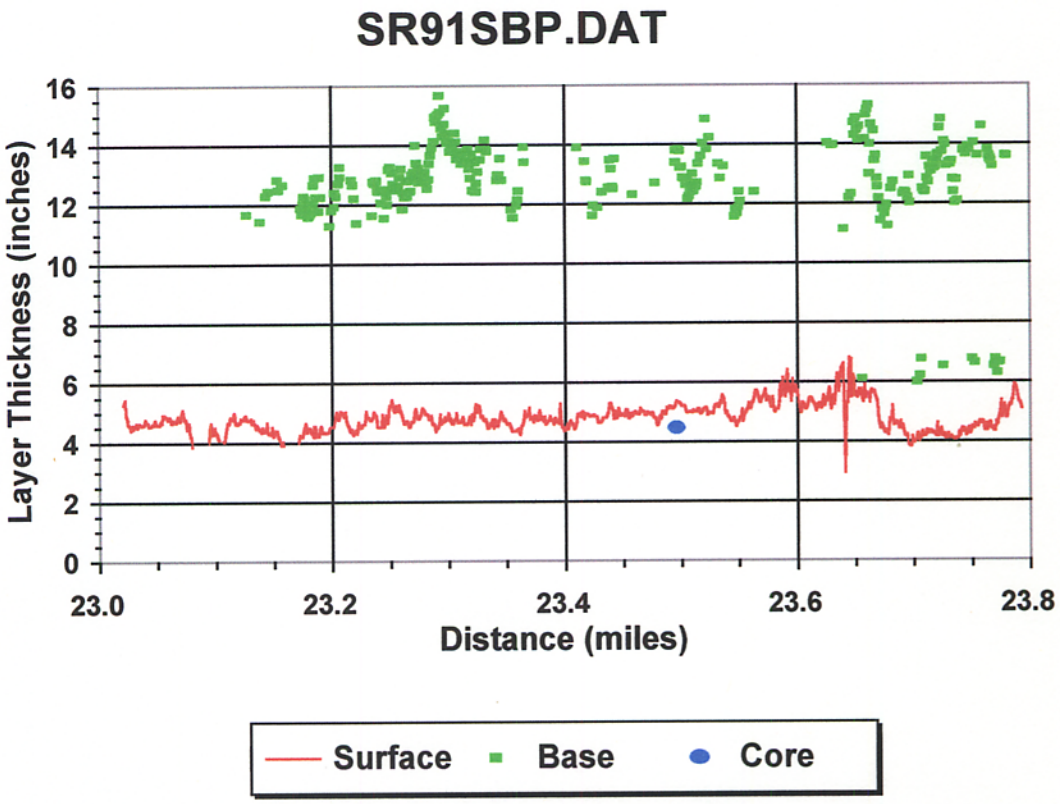

Figure 36. Predicted Layer Thicknesses and Core Thicknesses on FWD Site SR91SBC From Milepost 22.891 to 23.793.

Note: There are two cores for the above FWD segment. However, the radar data collected do not overlap with the other core location at milepost 23.011. Thus, only the core taken at milepost 23.496 is plotted.

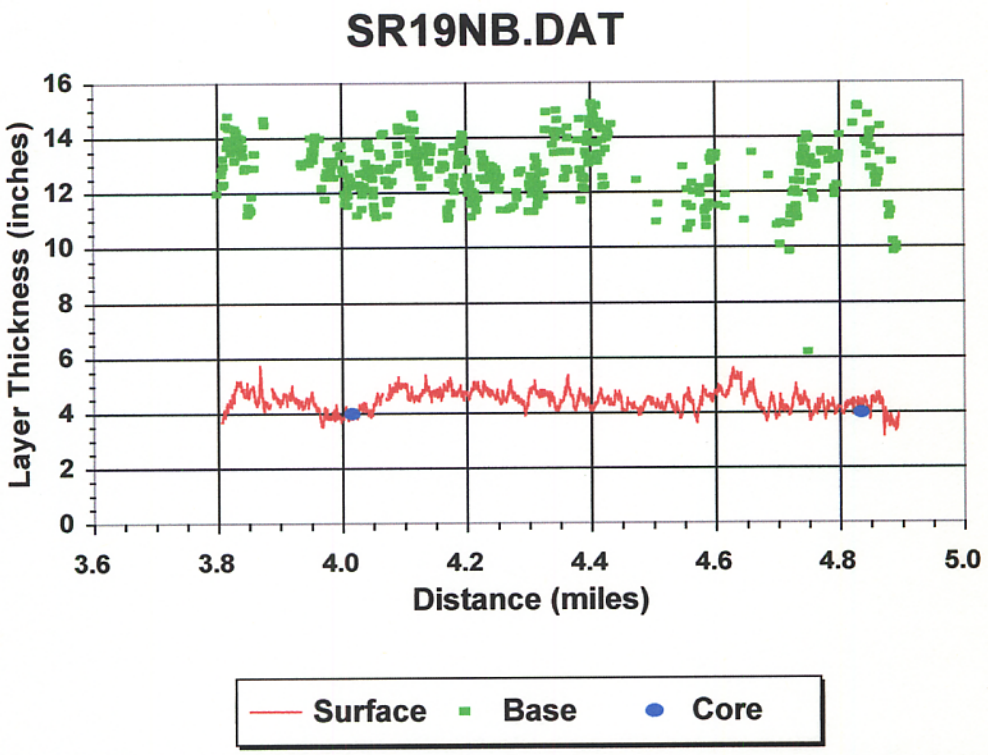

Figure 34. Predicted Layer Thicknesses and Core Thicknesses on FWD Site SR19NB.

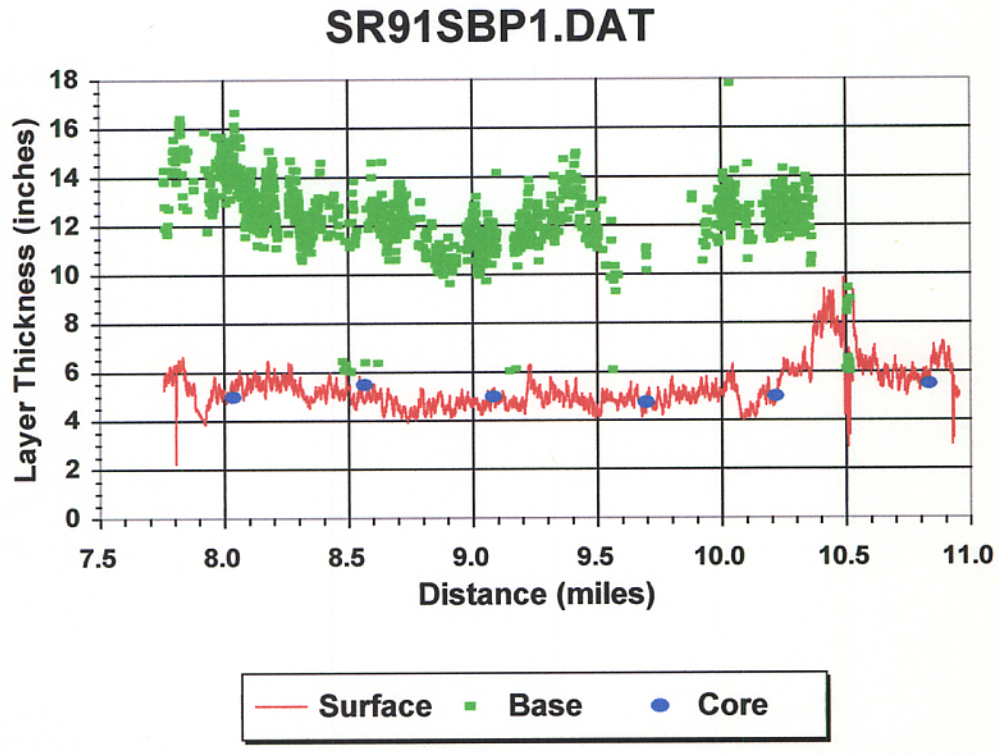

Figure 35. Predicted Layer Thicknesses and Core Thicknesses on FWD Site SR91SBC From Milepost 7.651 to 10.954.

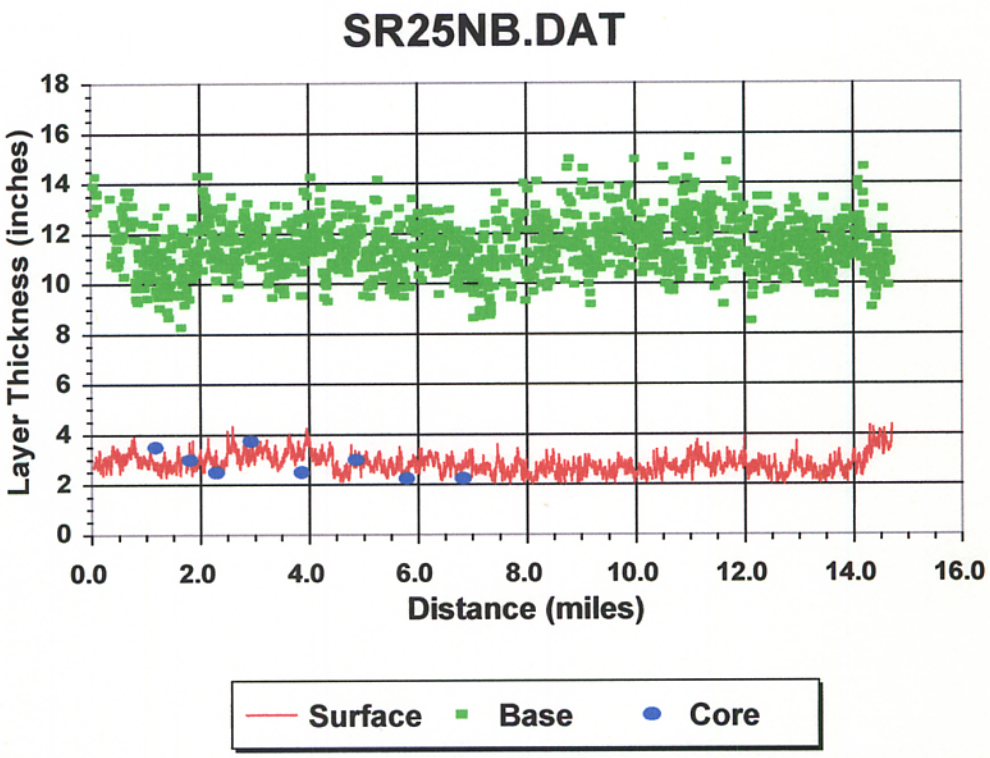

Figure 37. Predicted Layer Thicknesses and Core Thicknesses on FWD Site SR25NB.

Note: In the above chart, the interval from 0.000 to 3.174 corresponds to FWD segment SR25NB1. The interval from 3.174 to 7.350 corresponds to FWD segment SR25NB2.

Table 6. Means (μ) and Standard Deviations (σ) of Layer Thicknesses.

FWD File Name	DMI Interval	Core (surface)		Radar			
				Surface		Base	
		μ (inches)	σ (inches)	μ (inches)	σ (inches)	μ (inches)	σ (inches)
SR134EB	0.050 to 2.550	3.04	0.10	2.92	0.22	7.67	0.76
SR134EBC	2.600 to 5.458	4.00	0.00	3.37	0.19	8.71	0.68
SR134WBC	2.600 to 7.777	4.32	0.40				
SR134WB	0.072 to 2.553	3.38	0.21	3.44[A] 3.50[B]	0.24[A] 0.28[B]	9.27[A] 8.60[B]	0.95[A] 0.97[B]
SR13SBC	0.100 to 3.115	3.95	0.11	3.60	0.41	8.95	1.11
SR200 NBC	6.138 to 9.400	3.92	0.26	3.96	0.24	10.06	0.58
SR222WBC	0.400 to 7.952	4.80	0.31	4.84	0.40	13.23	3.06
SR222EBC	4.845 to 7.194	4.94	0.13	4.81	0.52	13.46	3.47
SR329NBC	1.907 to 2.233	3.25	0.00	5.86[C] (mean) 3.46 (mode)	3.95[C]	8.87[C]	2.19[C]
SR25NBC	2.502 to 3.234	4.25	0.00	4.80	0.43	11.72	0.98
SR9SBC1	13.813 to 22.509	6.85	0.44				
SR9SBC21	14.335 to 21.453	5.59	0.32				
SR5NBC	24.238 to 27.932	4.42	0.38				
SR434NBC	0.000 to 2.679	4.25	0.35	4.26	0.41	10.76[D]	1.49[D]

Table 6. Means (μ) and Standard Deviations (σ) of Layer Thicknesses (continued).

FWD File Name	DMI Interval	Core (surface)		Radar			
				Surface		Base	
		μ (inches)	σ (inches)	μ (inches)	σ (inches)	μ (inches)	σ (inches)
SR500NBC	3.405 to 7.200	4.96	1.65	5.86	2.14	11.97	1.72
SR500SBC	10.714 to 12.280	3.50	0.71	3.70	0.86	10.99[D]	1.12[D]
SR482WBC	0.000 to 2.200	3.90	0.89	4.77	1.06	13.44[D]	1.51[D]
SR46WBC	3.810 to 4.537	3.50	0.00				
SR46EBC	8.000 to 8.448	3.50	N/A				
SR19NB	3.800 to 4.906	4.00	0.00	4.46	0.38	12.85	1.09
SR91SBC	7.651 to 10.954	5.13	0.31	5.33	0.86	12.39	1.49
	22.891 to 23.793	4.75	0.35	4.84	0.46	12.81	1.60
SR25NB1	0.000 to 3.174	3.05	0.57	3.03	0.35	11.41	1.15
SR25NB2	3.174 to 7.350	2.45	0.33	2.91	0.37	11.28	1.02

[A] based on radar data file SR134_A3.DAT taken on westbound passing lane
[B] based on radar data file SR134_A4.DAT taken on westbound traffic lane
[C] very variable reflections; base material is brick from straight line diagram
[D] base thickness predictions are sporadic, i.e., not determined for most of the FWD segment

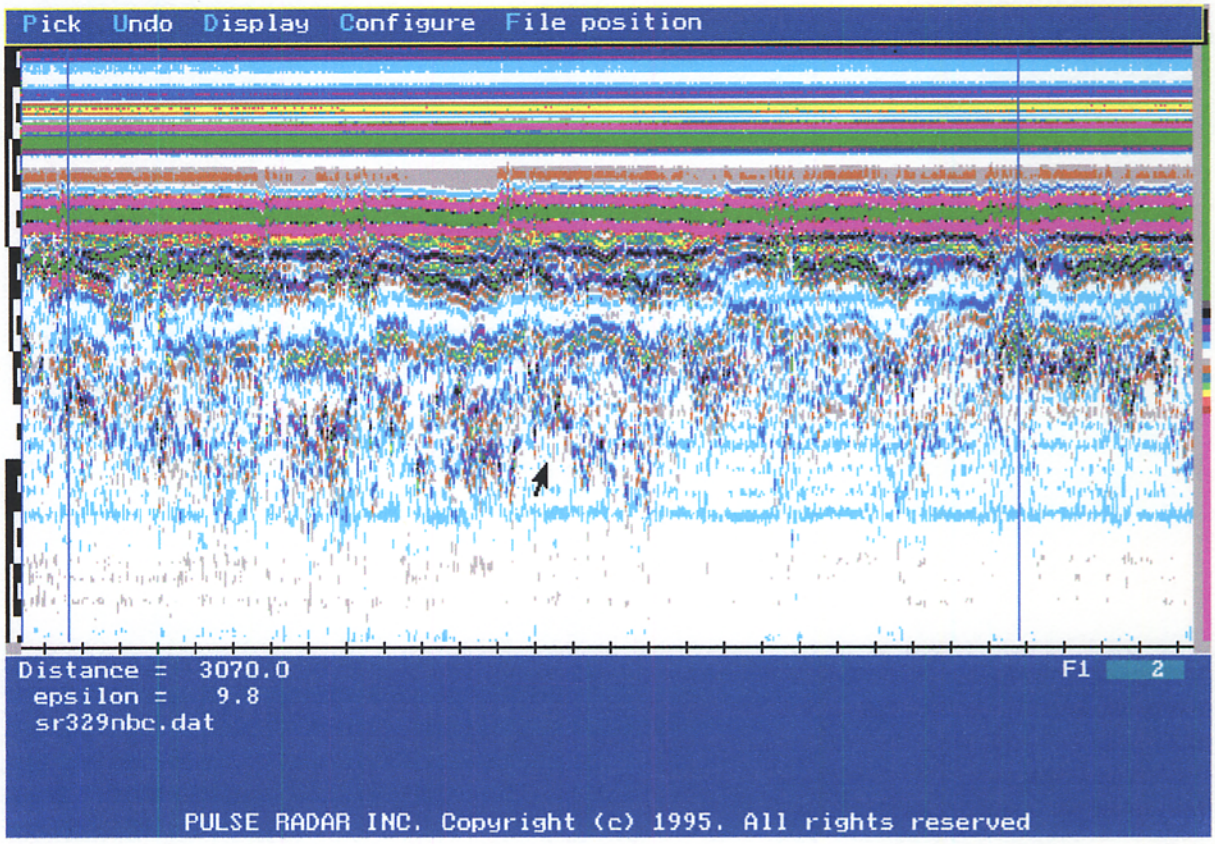

Figure 38. Radar Data on FWD Site SR329NBC Showing Variable Interface Reflections.

of the quality of the radar data. A coefficient of variation in the predicted surface thicknesses greater than 50 percent may be used to flag the need for a closer examination of the radar data to identify reasons for the large variability and to establish the need for cores.

While the average surface thickness from the radar is significantly different from the core average, Figure 28 shows that the baseline predictions compare well with the cores. Consequently, the mode of the surface thickness predictions was also determined. As shown in Table 6, this statistic compares much more favorably with the mean core thickness, indicating that when highly variable reflections are found in the radar data, the mode, and not the mean of the predicted thicknesses, may be more representative of the actual average.

It is noted that actual changes in pavement cross-section may also give rise to a high standard deviation in the predicted layer thicknesses. Figures 31 to 33 show changes in the thickness of the surface layer along FWD sites SR500NBC, SR500SBC, and SR482WBC that were detected by ground penetrating radar. These changes in the surface thickness also result

in high standard deviations as may be observed in Table 6. However, the data for these sites do not show the variability in the reflections that is seen in the radar data for SR329NBC (Figure 38). It is worth noting that the changes in surface thickness detected by radar are confirmed by the cores taken from the sites as evident in Figures 31 to 33.

The absolute differences between the averages of the predicted surface thicknesses and the corresponding averages of the core thicknesses are summarized in Table 7. In view of the variability in the interface reflections observed in the data for SR329NBC, the mode of the predicted surface thicknesses for this site is compared with the mean of the corresponding core thicknesses. It is observed that the average absolute difference is 0.30 inches. This is comparable with the expected accuracy of raw (uncalibrated) surface thickness estimates as established from similar investigations conducted in the previous radar project.

SUMMARY OF FINDINGS

The following findings are noted from the results of the verification presented:

1. Variability in the thickness predictions may indicate the presence of highly variable layer interface reflections in the radar data. This should be confirmed by examination of the data to establish the need for cores along the route surveyed.
2. When the layer interface reflections are highly variable, the mode of the predicted thicknesses may be more representative of the actual average than the mean of the predicted thicknesses.
3. Changes in surface layer thickness were correctly detected by radar as confirmed by the cores taken from sites where such changes were detected.
4. The means of the predicted surface thicknesses were found to compare favorably with the corresponding means of the core thicknesses for the majority of the radar data analyzed. The average of the absolute differences between means is 0.30 inches.

In summary, the results verified the thickness predictions from the TERRA program, indicating that the algorithms used are producing uncalibrated estimates of surface thickness that are of acceptable accuracy. Because of the absence of measured base thicknesses, it was not possible to verify the base predictions on the sites tested. It is recommended that this be done by the Florida DOT at a future date, perhaps as part of its GPR implementation efforts.

Table 7. Absolute Differences Between Means of Core and Radar Thicknesses.

FWD File Name	DMI Interval	Average Surface Thickness (inches)		Absolute Difference (inches)
		Core	Radar	
SR134EB	0.050 to 2.550	3.04	2.92	0.12
SR134EBC	2.600 to 5.458	4.00	3.37	0.63
SR134WBC	2.600 to 7.777	4.32		
SR134WB	0.072 to 2.553	3.38	3.47	0.09
SR13SBC	0.100 to 3.115	3.95	3.60	0.35
SR200 NBC	6.138 to 9.400	3.92	3.96	0.04
SR222WBC	0.400 to 7.952	4.80	4.84	0.04
SR222EBC	4.845 to 7.194	4.94	4.81	0.13
SR329NBC	1.907 to 2.233	3.25	3.46[A]	0.21
SR25NBC	2.502 to 3.234	4.25	4.80	0.55
SR9SBC1	13.813 to 22.509	6.85		
SR9SBC21	14.335 to 21.453	5.59		
SR5NBC	24.238 to 27.932	4.42		
SR434NBC	0.000 to 2.679	4.25	4.26	0.01
SR500NBC	3.405 to 7.200	4.96	5.86	0.90
SR500SBC	10.714 to 12.280	3.50	3.70	0.20
SR482WBC	0.000 to 2.200	3.90	4.77	0.87
SR46WBC	3.810 to 4.537	3.50		
SR46EBC	8.000 to 8.448	3.5		
SR19NB	3.800 to 4.906	4.00	4.46	0.46
SR91SBC	7.651 to 10.954	5.13	5.33	0.20
	22.891 to 23.793	4.75	4.84	0.09
SR25NB1	0.000 to 3.174	3.05	3.03	0.02
SR25NB2	3.174 to 7.350	2.45	2.91	0.46
Average Absolute Difference (inches)				0.30

[A] mode of predicted surface thicknesses

CHAPTER V. SUMMARY AND RECOMMENDATIONS

To address the need for developing a data base of pavement layer thicknesses over the state highway network, this study developed a computer program for analyzing GPR data in a production environment. The computer program developed from the research incorporates decision criteria for automated detection of layer interfaces. Based on the evaluation of the TERRA program presented in this report, the following findings are noted:

1. The sensitivity analysis showed that the peak detection algorithm behaves as expected and produces results that agree with visual examination of the radar data. In particular, the effects of the decision criteria were observed to be logical and consistent with the expected trends in the variation of the detected peaks with changes in the criteria used.
2. Tests conducted to verify the algorithm's capability to track peaks demonstrated the stability of the method. In particular, the results showed that the algorithm is able to handle gradual or sudden changes in the patterns of the interface reflections as well as gaps in the data.
3. Verification of the layer thicknesses predicted from GPR data using the TERRA program revealed the following observations:
    a. Variability in the thickness predictions may indicate the presence of highly variable layer interface reflections.
    b. When the reflections are highly variable, the mode of the predicted thicknesses may be more representative of the actual average than the mean of the predicted thicknesses.
    c. Changes in surface layer thickness were correctly detected by radar as confirmed by cores taken from sites where such changes were detected.
    d. The means of the predicted surface thicknesses were found to compare favorably with the corresponding means of the core thicknesses for the majority of the radar data analyzed. The average of the absolute differences between means is 0.30 inches.

The evaluation results suggest that the TERRA program may be used with confidence to estimate pavement layer thicknesses from GPR data. Implementation of GPR should proceed accordingly within the Florida DOT. It is recommended that initial implementation be directed at the inventory of the layer thicknesses for the Turnpikes. The relatively small size of this highway subsystem provides a manageable starting point for the planned development of a network level data base of pavement layer thicknesses.

Researchers note that GPR is not expected to completely eliminate the need for coring. For many routes, this technology will provide estimates of surface and base layer thicknesses but there will be sections where the layer interface reflections are not visible from the data, or where the reflections are difficult to interpret. Coring will be needed in these instances and GPR can be used to intelligently establish the coring requirements to help interpret GPR data, fill gaps in the thickness predictions, and verify the results. For difficult sections, taking a core is recommended.

It is also advisable to have sections of known thicknesses that may be used to verify the radar system from time to time or as the need arises. FDOT's radar vehicle may be run on these sections to check the thickness predictions with the known values to establish the need for servicing the system.

Finally, other applications of GPR should be investigated. For example, the technology may be used to provide thickness data on a given project that are needed for pavement design or to check the as-built layer thicknesses during construction. GPR may also be used to plan deflection tests along a given route to serve pavement evaluation needs, and to provide the layer thicknesses required for deflection data analysis. Still another application is in forensic studies of premature pavement failures. By investigating and developing other uses of GPR, the Department will be making the most of its investment in this technology.

REFERENCES

1. Fernando, E. G., and K. R. Maser. *Development of a Procedure for the Automated Collection of Flexible Pavement Layer Thicknesses and Materials: Phase I - Demonstration of Existing Ground Penetrating Radar Technology*. Florida DOT State Project 99700-7550, Phase I Final Report, Texas Transportation Institute, Texas A&M University, College Station, Texas, 1992.
2. Fernando, E. G., and K. R. Maser. *Development of a Procedure for the Automated Collection of Flexible Pavement Layer Thicknesses and Materials: Phase IIA - Executive Summary Report*. Florida DOT State Project 99700-7550, Texas Transportation Institute, Texas A&M University, College Station, Texas, 1993.
3. Fernando, E. G., and T. Chua. *Development of a Procedure for Route Segmentation Using Predicted Layer Thicknesses From Radar Measurements.* Florida DOT State Project 99700-7550, Phase IIA Report, Texas Transportation Institute, Texas A&M University, College Station, Texas, 1993.
4. Fernando, E. G., and K. R. Maser. *Development of a Procedure for the Automated Collection of Flexible Pavement Layer Thicknesses and Materials: Phase IIB - Final Report*. Florida DOT State Project 99700-7550, Texas Transportation Institute, Texas A&M University, College Station, Texas, 1997.
5. Fernando, E. G., and T. Chua. *ROADSEG User's Guide: Version 1.0.* Florida DOT State Project 99700-7550, Texas Transportation Institute, Texas A&M University, College Station, Texas, 1997.
6. Fernando, E. G., and W. Liu. *TERRA User's Guide: Version 1.0.* Research Report RF7257-2, Texas Transportation Institute, Texas A&M University, College Station, Texas, 2000.
7. Roddis, W. M. K., K. Maser, and A. J. Gisi. *Radar Pavement Thickness Evaluations for Varying Base Conditions.* Transportation Research Record 1355, Transportation Research Board, Washington, D.C., 1992, pp. 90 - 98.

8. Letto, A. R. *A Computer Program for Function Optimization Using Pattern Search and Gradient Summation Techniques.* M. Eng. Thesis, Department of Industrial Engineering, College of Engineering, Texas A&M University, College Station, Texas, 1968.
9. Box, M. J. *A New Method of Constrained Optimization and a Comparison With Other Methods.* Computer Journal, Vol. 8, No. 1, pp. 42-52, 1965.
10. Rao, S. S. *Optimization: Theory and Application.* 2nd edition, Halsted Press, John Wiley & Sons, Inc., 1984.

APPENDIX

INVESTIGATION OF METHODS TO DELINEATE PAVEMENT SECTIONS IN THE RADAR DATA

INVESTIGATION OF METHODS TO DELINEATE PAVEMENT SECTIONS IN THE RADAR DATA

The original objective of FDOT Project 0510706, "Automating Radar Pre-Processing for Network Level Surveys," was to develop software for subdividing the data into segments and identifying layer interfaces during the pre-processing of radar data. Thus, initial efforts were spent at evaluating procedures for automatically establishing homogeneous segments within the data using either the detected layer interfaces or the raw radar traces. However, since the scope of work was later expanded to cover the development of a complete program for radar data analysis, further evaluation of procedures to subdivide radar data in the pre-processing stage was discontinued. It was established that this work was no longer necessary after development of the procedure for automated detection of pavement layer interfaces that was presented in Chapter 3. The same delineation may be accomplished after estimating layer thicknesses using the ROADSEG program *(5)* developed in the previous radar project. However, for completeness, this appendix is provided to document efforts made during the study to evaluate procedures for automatic segment delineation during the pre-processing stage.

USING DETECTED LAYER INTERFACES TO DELINEATE SEGMENTS

An algorithm based on minimizing the differences in the reflections within a given segment was investigated. This algorithm is based on minimizing the function:

$$\Phi = \sum_{k=1}^{l} \sum_{j=1}^{n_k} \sum_{i=1}^{m_k} \left[\left(V_{ij} - \overline{V}_j \right)^2 + \left(t_{ij} - \overline{t}_j \right)^2 \right]_k \qquad \text{(A1)}$$

where,

V_{ij} = amplitude of reflection, j, in trace, i

t_{ij} = arrival time of reflection, j, in trace, i

m_k = number of traces in segment, k

n_k = maximum number of reflections after the surface echo in segment, k

$\left(\bar{V}_j\right)_k$ = average amplitude of reflection, j, in segment k, and

$\left(\bar{t}_j\right)_k$ = average arrival time of reflection, j, in segment, k.

For a segment with uniform reflections, the value of Φ will be zero if all reflections are perfectly aligned and if all reflections occurring at a given arrival time are of the same magnitudes and directions. The minimization of Φ in Eq. (A1) is accomplished iteratively. Since the number of detected peaks may vary from trace to trace in a given segment, there will be cases where V_{ij} and t_{ij} are non-existent, for a given trace, i, and reflection, j. For these cases, the missing values are set to zeroes in computing the squared differences given in Eq.(A1). The mean amplitude and mean arrival time in Eq. (A1) are computed from all occurrences of the given reflection, j, in a particular segment.

Each segment is constrained to have a length greater than or equal to the prescribed minimum segment length. In addition, the sum of all segment lengths must equal the total length of the route surveyed. There will be at least one segment delineated corresponding to the entire route surveyed. Also, the maximum number of segments that can be generated is limited by the minimum segment length specified by the user.

A number of approaches were used to investigate the proposed algorithm. In one approach, the pattern search technique *(8)* is used to find the lengths of segments that will minimize Φ in Eq. (A1) for a given value of the number of segments, l. In this scheme, different values of l are assumed. For each l, the pattern search algorithm is used to find the length of each of the l segments that will minimize Φ. The solution for the value of l that results in the lowest Φ is selected.

In another approach, a segment of length equal to the minimum specified by the user, is initially established at the start of the roadway to be subdivided. Eq. (A1) is then evaluated for this initial segment. A trace or a range of traces is then added to the segment and Φ is re-calculated. This process is continued until Φ starts to increase with further addition of traces indicating a change in pavement section. The point at which this increase occurs is taken as the endpoint of the initial segment. A new segment of length equal to the minimum specified is established from this point and the process of adding traces and monitoring the change in Φ values is repeated until the endpoint of the new segment is determined as described

previously. Another segment is then established and the entire process is repeated until all traces in the data file have been used.

Both of the above approaches were investigated using radar data taken from a project where the actual segmentation is known. Figure A1 compares the segments determined from the pattern search method with the actual segments. Each vertical line in Figure A1 represents an actual roadway segment of length equal to the distance covered by the line. The horizontal tick marks for each vertical line denote the predicted endpoints of the given segment from the pattern search method. Ideally, the tick marks should be positioned exactly at the endpoints of the vertical line. Deviations represent errors in the delineation of segments from the pattern search.

In using pattern search, several values for the number of segments, l, were assumed, specifically, 2 to 20. For those cases where feasible solutions were found, the lowest value of Φ was obtained when $l = 18$ segments, which corresponds to the actual number of segments. The lengths of the segments determined for this value of l are denoted by the horizontal tickmarks in Figure A1. Table A1 shows the endpoints of the actual segments and the endpoints determined by pattern search. For this method, the average of the absolute errors between actual and predicted starting locations is 59 feet. This is 10.7 percent of the average segment length. The average absolute error for the ending location is 45 feet or 8.2 percent of the average segment length. The absolute deviations between actual and predicted starting locations range from 0 to 130 feet. The corresponding range for the ending location is from 0 to 90 feet.

The second approach, referred to herein as the method of successive trace addition (STA), was also investigated using the same radar data file. It was found that better results are obtained when a range of traces is added at each iteration, in lieu of just a single trace, which tended to accentuate the effects of localized irregularities in the data. Figure A2 compares the actual segmentation with the results from STA when 10 traces are added at each iteration. Again, the vertical lines represent the actual segments while the horizontal tickmarks denote the predicted endpoints from STA. Table A1 shows the endpoints of the actual segments and the endpoints determined by this method. The average of the absolute errors between the actual and predicted starting locations is 93 feet or 16.9 percent of the average segment length. The average absolute error for the ending location is 74 feet or 13.4

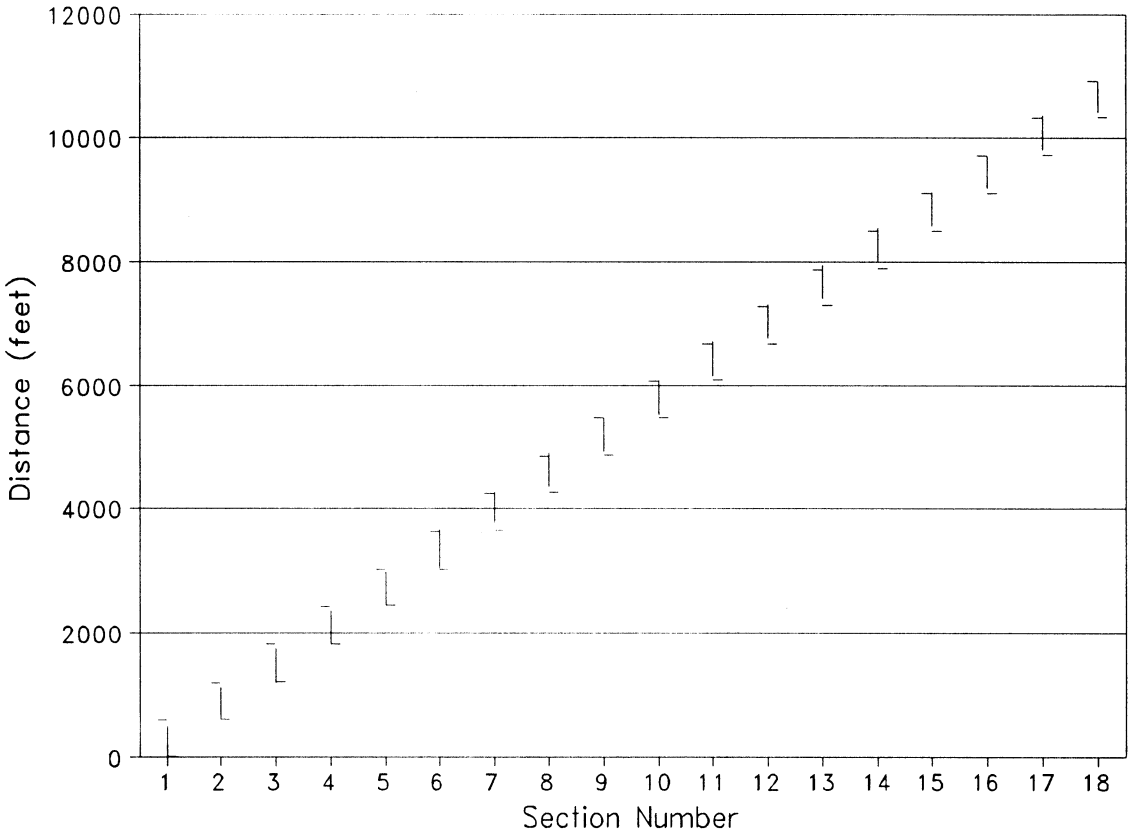

Figure A1. Actual and Predicted Segmentation From Pattern Search.

Table A1. Actual and Predicted Segment Endpoints From Pattern Search and STA.

Section	Actual		Pattern Search		Successive Trace Addition	
	Start (ft)	End (ft)	Start (ft)	End (ft)	Start (ft)	End (ft)
1	3	510	3	600	3	600
2	610	1132	610	1206	610	1206
3	1206	1766	1216	1815	1216	1805
4	1815	2366	1825	2427	1815	2407
5	2437	2990	2437	3029	2417	3009
6	3048	3693	3038	3642	3019	3611
7	3763	4285	3652	4244	3622	4214
8	4347	4910	4255	4849	4224	4818
9	4921	5472	4860	5462	4829	5422
10	5532	6091	5472	6070	5432	6029
11	6143	6739	6080	6669	6039	6631
12	6779	7322	6679	7282	6641	7232
13	7422	7954	7292	7884	7242	7834
14	8013	8566	7894	8497	7844	8438
15	8576	9120	8507	9100	8448	9041
16	9180	9712	9110	9712	9050	9643
17	9801	10370	9722	10319	9653	10248
18	10411	10926	10329	10926	10258	10926

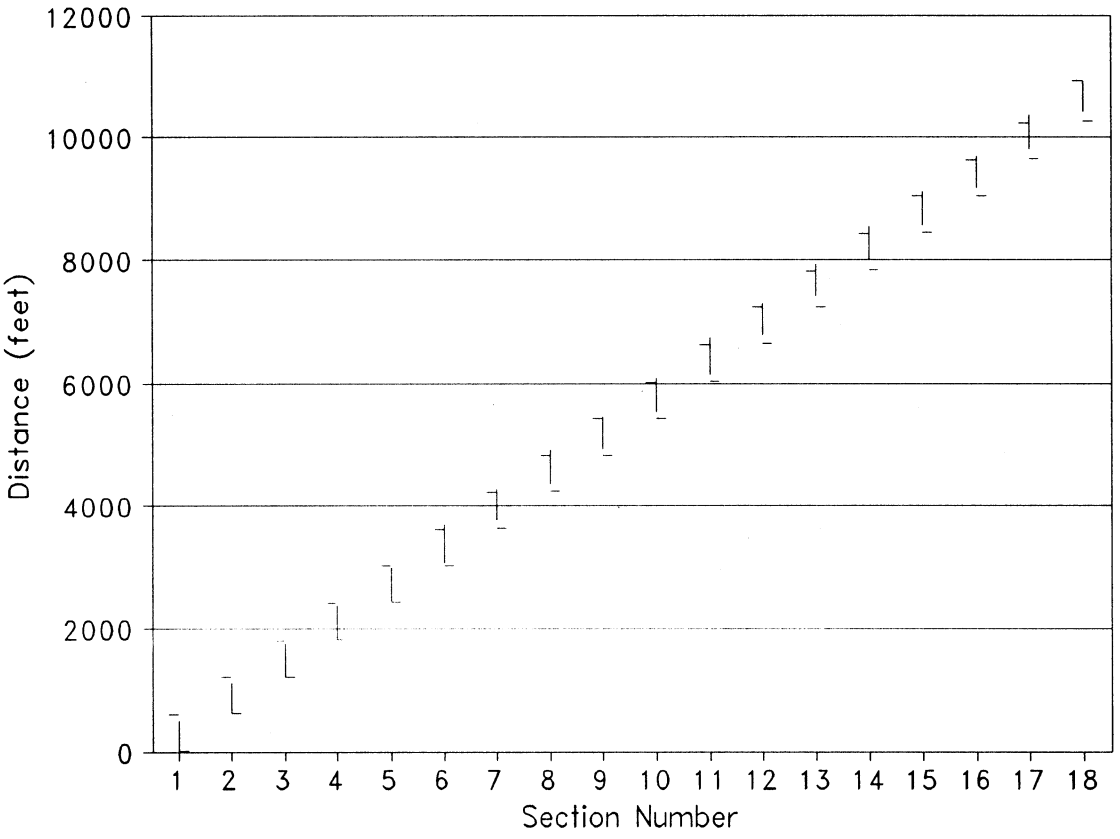

Figure A2. Actual and Predicted Segmentation From the STA Method.

percent of the average segment length. The absolute deviations between actual and predicted starting locations range from 0 to 180 feet. The corresponding range for the ending location is from 0 to 128 feet. Judging from these statistics, the pattern search method did a better job of delineating the segments than the STA method.

Further efforts were spent to improve the accuracy of the segmentation from the algorithm given by Eq. (A1). Based on the initial results, two modifications were made to the objective function that led to the use of absolute differences in lieu of the squared differences to minimize the effect of localized irregularities in the data. The other change is the

application of a scaling factor, F, to the time differences so that the magnitudes of these differences will be more comparable with the amplitude differences. In this way, the time and amplitude differences will be weighed comparably in the solution. The modified objective function is given by:

$$Minimize\ \Phi = \sum_{k=1}^{l} \sum_{j=1}^{n_k} \sum_{i=1}^{m_k} \left[\left| V_{ij} - \bar{V}_j \right| + \frac{\left| t_{ij} - \bar{t}_j \right|}{F} \right]_k \qquad \text{(A2)}$$

where the variables are as described before. The problem is to find the vector $\{\mathbf{X}\}=\{x_1, x_2, x_3,....,x_n\}$ of segment endpoints that satisfies Eq. (A2) above. A procedure known as the Complex method was evaluated as to its applicability for delineating homogeneous segments based on the formulation given by Eq. (A2). This is a relatively simple procedure that does not require the use of derivatives. In this method, a complex of feasible trial solutions is initially generated using random numbers. For each trial solution, the objective function is evaluated and a search is conducted to find a new feasible solution with a lower objective function value. This is accomplished through a process of reflection where a new point in the solution space is determined by moving a current feasible solution a certain distance toward the centroid of the remaining feasible solutions. Convergence is assumed when the distance between each pair of alternative feasible solutions is within a given tolerance, and when the objective function values of the different solutions are within a prescribed limit. Given a sufficient number of initial feasible solutions, the method should converge on a global minimum since the initial solutions are randomly scattered within the feasible region. More detailed information about the Complex method may be found in *(9,10)*. Researchers evaluated this method using the same radar data on which the pattern search and STA methods were tested.

Table A2 presents the results from evaluation of the Complex method. Using this method, the average absolute deviation between the predicted and actual starting locations is 35 feet or 6.4 percent of the actual average segment length. The corresponding statistics for the ending location is 20 feet or 3.6 percent of the average segment length. These results represent an improvement over those obtained using the pattern search and STA methods. Table A3 summarizes the accuracies from all three methods investigated.

Table A2. Actual and Predicted Segment Endpoints From Complex Method.

Section	Actual		Complex Method		Absolute Difference	
	Start (ft)	End (ft)	Start (ft)	End (ft)	Start (ft)	End (ft)
1	3	510	3	510	0	0
2	610	1132	520	1174	90	42
3	1206	1766	1184	1785	22	19
4	1815	2366	1795	2437	20	71
5	2437	2990	2447	3009	10	19
6	3048	3693	3019	3713	29	20
7	3763	4285	3723	4306	40	21
8	4347	4910	4316	4910	31	0
9	4921	5472	4921	5422	0	50
10	5532	6091	5432	6122	100	31
11	6143	6739	6133	6749	10	10
12	6779	7322	6759	7322	20	0
13	7422	7954	7332	7954	100	0
14	8013	8566	7964	8556	49	10
15	8576	9120	8566	9160	10	40
16	9180	9712	9170	9732	10	20
17	9801	10370	9742	10370	59	0
18	10411	10926	10380	10926	31	0
Average Absolute Difference					35	20

Table A3. Accuracy of Methods Investigated to Delineate Segments.

Solution Method	Absolute Difference					
	Starting Location			Ending Location		
	Average (feet)	Percent[1]	Range (feet)	Average (feet)	Percent[1]	Range (feet)
Pattern Search	59	10.7	0 - 130	45	8.2	0 - 90
STA	93	16.9	0 - 180	74	13.4	0 - 128
Complex	35	6.4	0 - 100	20	3.6	0 - 71

[1] As a percentage of the actual average segment length.

USING RAW RADAR DATA TO DELINEATE SEGMENTS

Another approach studied to delineate segments is based on using the raw radar traces in lieu of the interface reflections. For this purpose, researchers modified the objective function so that point-to-point differences in amplitudes are minimized. Specifically, the objective function was modified as follows:

$$Minimize\ \Phi = \sum_{k=1}^{l} \sum_{j=1}^{n_k} \sum_{i=1}^{m_k} \left| V_{ij} - \overline{V}_j \right|_k \qquad \text{(A3)}$$

where,

V_{ij} = amplitude at point, j, for trace, i, in segment, k

$\overline{V}_j$ = average amplitude at point, j, for traces in segment, k

m_k = number of traces in segment, k

n_k = number of points after the surface echo in segment, k

l = number of segments

Thus, the difference between a trace and the average of the traces for a given segment is evaluated and the sum of these differences are minimized in the revised method. All traces are initially aligned with respect to the surface reflection prior to the solution of the objective

function. In addition, only the surface reflection and points thereafter are included in the computations. The Complex method was used to evaluate the approach based on Eq. (A3) using the same data from the previous tests. Table A4 shows the segmentation based on this approach. Using the raw radar data with the Complex method, the average absolute deviation between the predicted and actual starting location is 33 feet or 6.0 percent of the actual average segment length. The corresponding statistics for the ending location is 40 feet or 7.3 percent of the average segment length. By comparing these results with the corresponding data given in Table A3, one sees that the Complex method gave a slightly better correspondence with the actual segmentation when the layer interface reflections were used. Researchers surmise that this is due to the filtering that takes place when the radar data are first processed to identify the interface reflections. This would tend to minimize the effect of localized or isolated irregularities in the radar data which may affect the accuracy of the predicted end point locations. However, from a practical point of view and in the opinion of researchers, either set of results from the Complex method are quite acceptable, particularly if one is concerned with network level applications.

The Complex method was also evaluated using radar data collected along US 1 in Martin County. Data were collected using FDOT's radar vehicle along the inner wheelpath of the traffic lane going south from the Highway A1A junction to the Palm Beach County line. Visual examination of the data revealed various changes in pavement section along this route. From information provided by the Gainesville office, the route surveyed comprised a number of test sections established for the Strategic Highway Research Program (SHRP). Because of this, the site was selected to evaluate the Complex method. Table A5 compares the observed segmentation with the predicted segmentation from the computer program. The observed segmentation was established from visual examination of the radar data to locate where section changes occur. These section changes are illustrated in Figures A3 to A15 which also show markers representing the predicted end points. It is noted that the figures zoom in on the first nine nanoseconds of the radar data to show details more clearly. Vertical lines in the figures denote markers inserted in the data during the radar survey. For example, Figure A3 shows the first four markers in the data file. Counting from the left, the third and fourth markers actually represent the beginning and ending points of a bridge crossed during the survey. To keep the bridge distinct, the segmentation was accomplished in two parts. In the

Table A4. Segmentation Using Complex Method With Raw Radar Data.

Section	Actual		Complex Method		Absolute Difference	
	Start (ft)	End (ft)	Start (ft)	End (ft)	Start (ft)	End (ft)
1	3	510	3	570	0	60
2	610	1132	580	1121	30	11
3	1206	1766	1132	1776	74	10
4	1815	2366	1785	2509	30	143
5	2437	2990	2519	3078	82	88
6	3048	3693	3087	3713	39	20
7	3763	4285	3723	4326	40	41
8	4347	4910	4336	4910	11	0
9	4921	5472	4921	5412	0	60
10	5532	6091	5422	6153	110	62
11	6143	6739	6163	6759	20	20
12	6779	7322	6769	7362	10	40
13	7422	7954	7372	7954	50	0
14	8013	8566	7964	8576	49	10
15	8576	9120	8586	9190	10	70
16	9180	9712	9200	9781	20	69
17	9801	10370	9791	10390	10	20
18	10411	10926	10400	10926	11	0
Average Absolute Difference (ft)					33	40

Table A5. Segmentation Using Complex Method With Raw Radar Data on Florida Highway[1].

Section	Start Location (ft)		Length (ft)	End Location (ft)		Absolute difference (ft)	
	Observed	Predicted		Observed	Predicted	Start	End
1	0	0	1465	1465	1465	0	0
2	1700	1700	1845	3480	3545	0	65
3	3485	3550	500	4020	4050	65	30
4	4026	4056	755	4801	4811	30	10
5	4806	4815	1240	6010	6055	9	45
6	6016	6061	845	6910	6906	45	4
7	6915	6910	650	7775	7560	5	215
8	7780	7566	1104	8666	8670	214	4
9	8670	8675	1040	9731	9715	5	16
10	9735	9721	999	10,650	10,720	14	70
11	10,655	10,726	2000	12,566	12,726	71	160
12	12,570	12,730	630	13,405	13,360	160	45
13	13,410	13,365	2665	16,005	16,030	45	25
14	16,011	16,036	13,854	29,890	29,890	25	0
Average						49	49

[1] Remarks:

a. A bridge exists from 1465 to 1696 ft. The segmentation was conducted outside these limits.

b. In addition to the observed end points above, two other endpoints were observed at 14,220 and 16,920 ft which were not identified from the segmentation analysis.

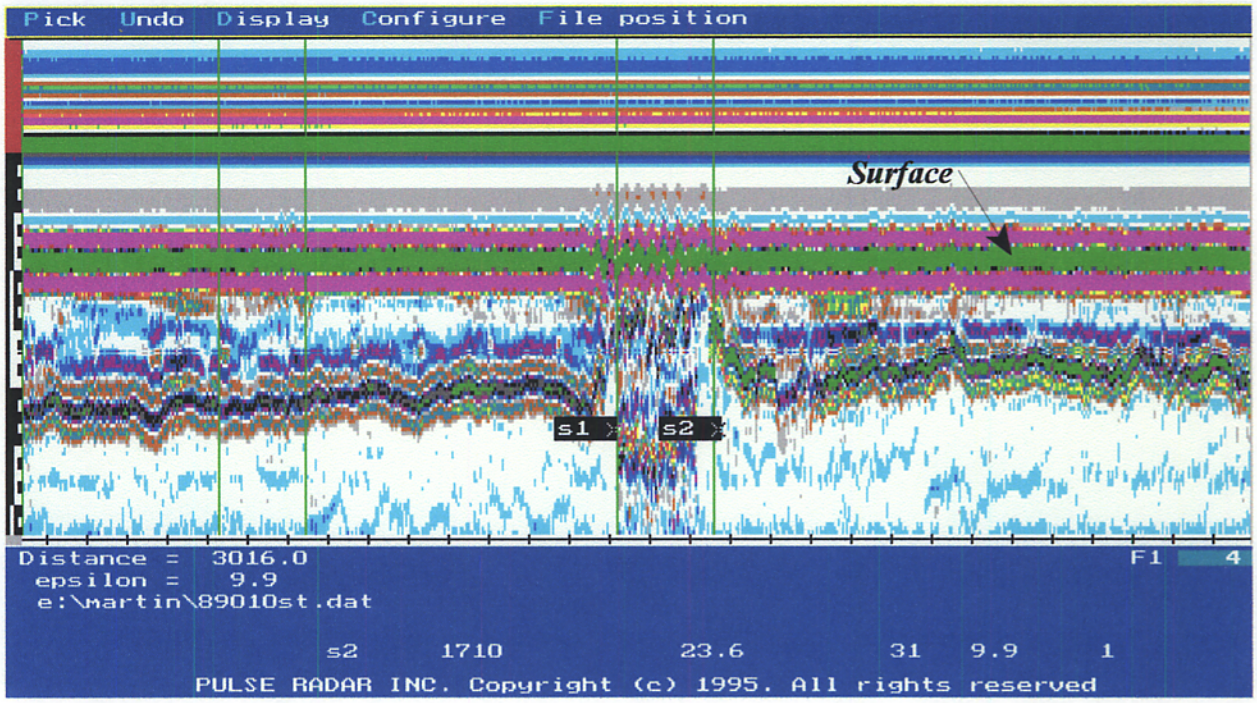

Figure A3. Radar Data on Section 1 (From Start to S1) and Part of Section 2 (Beginning at S2).

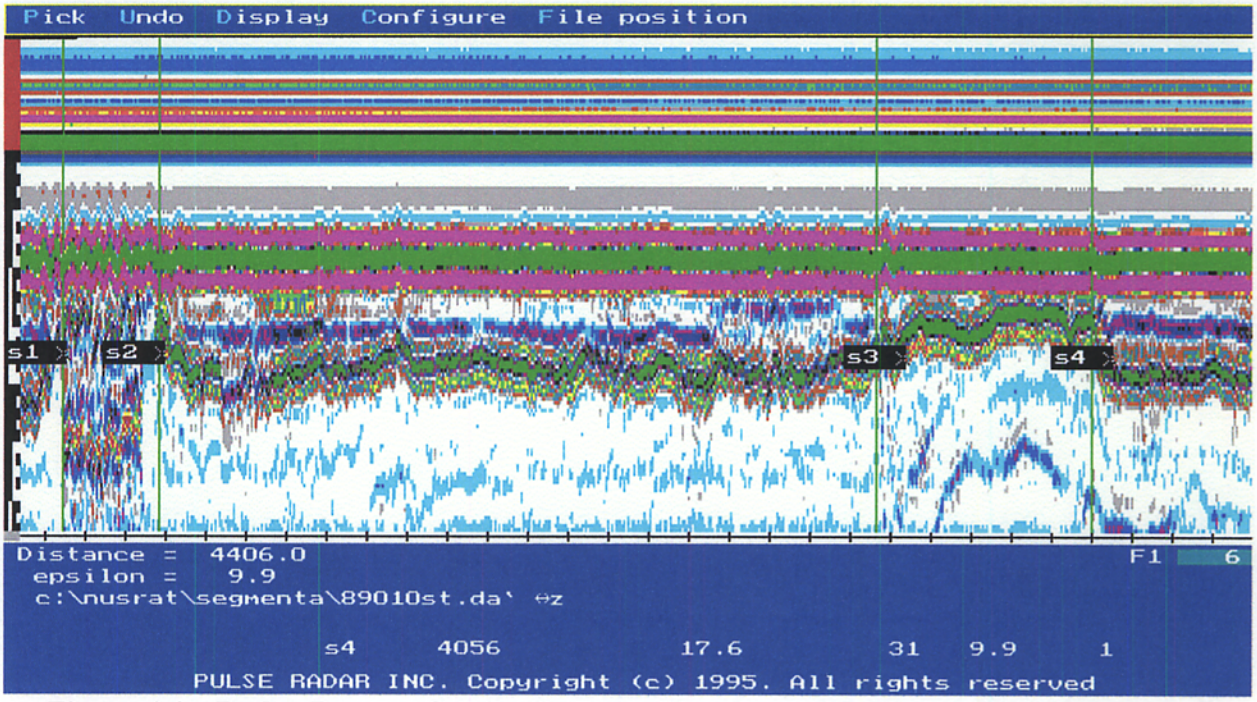

Figure A4. Radar Data on Section 2 (From S2 at End of Bridge to S3) and Section 3 (S3 to S4).

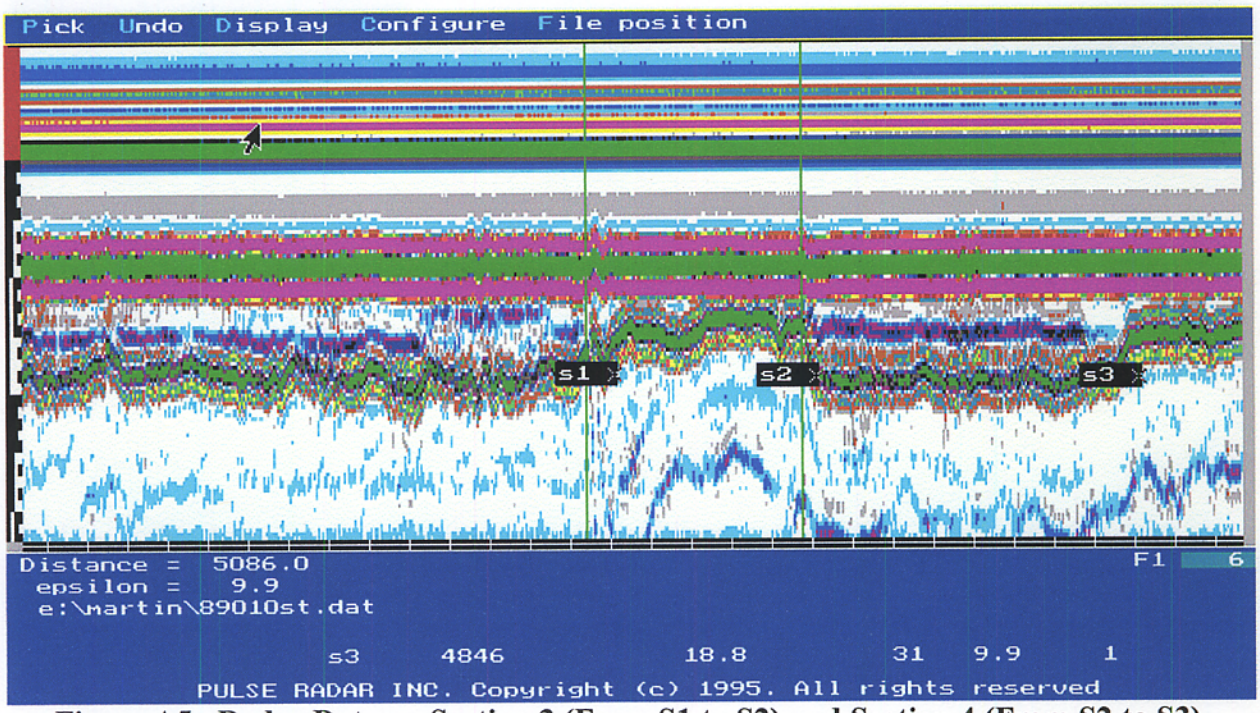

Figure A5. Radar Data on Section 3 (From S1 to S2) and Section 4 (From S2 to S3).

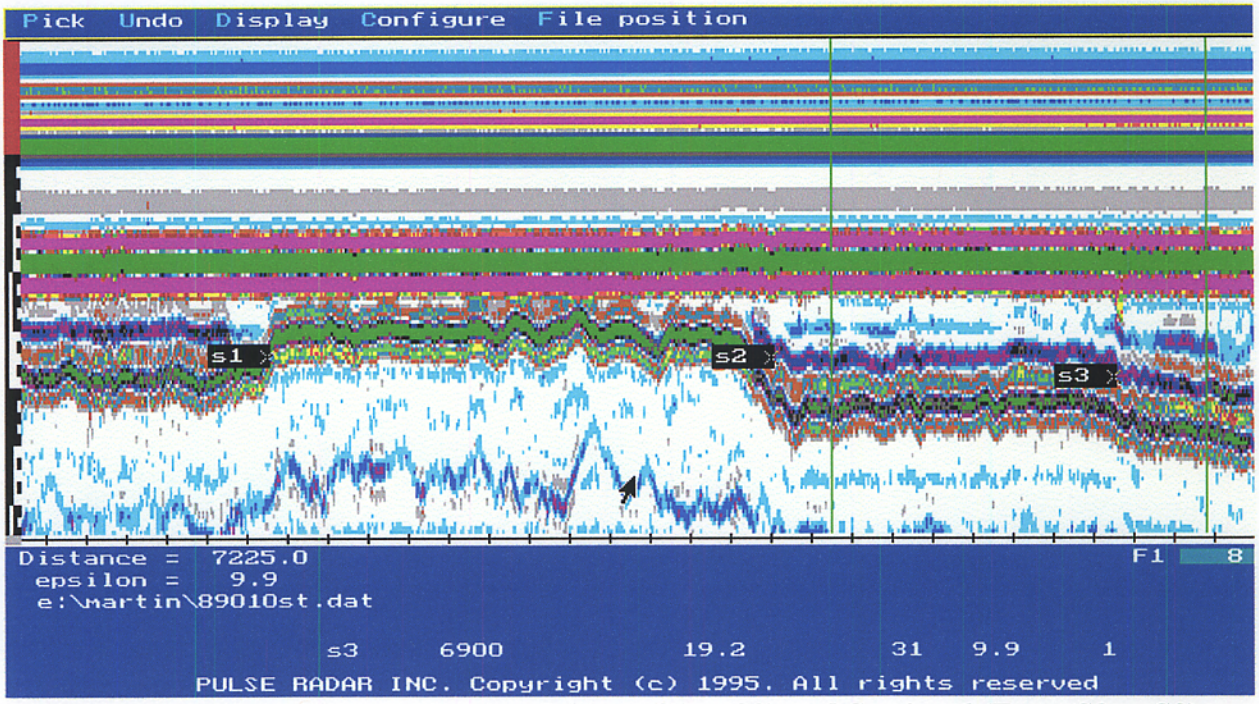

Figure A6. Radar Data on Section 5 (From S1 to S2) and Section 6 (From S2 to S3).

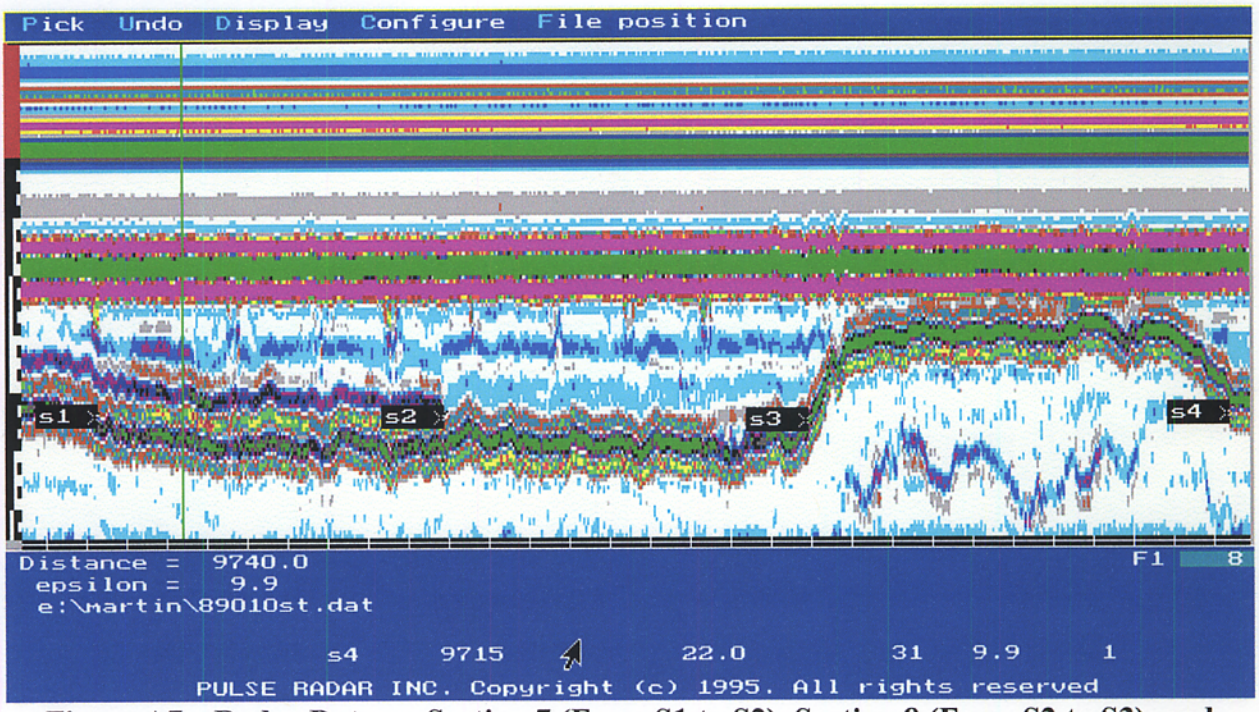

Figure A7. Radar Data on Section 7 (From S1 to S2), Section 8 (From S2 to S3), and Section 9 (From S3 to S4).

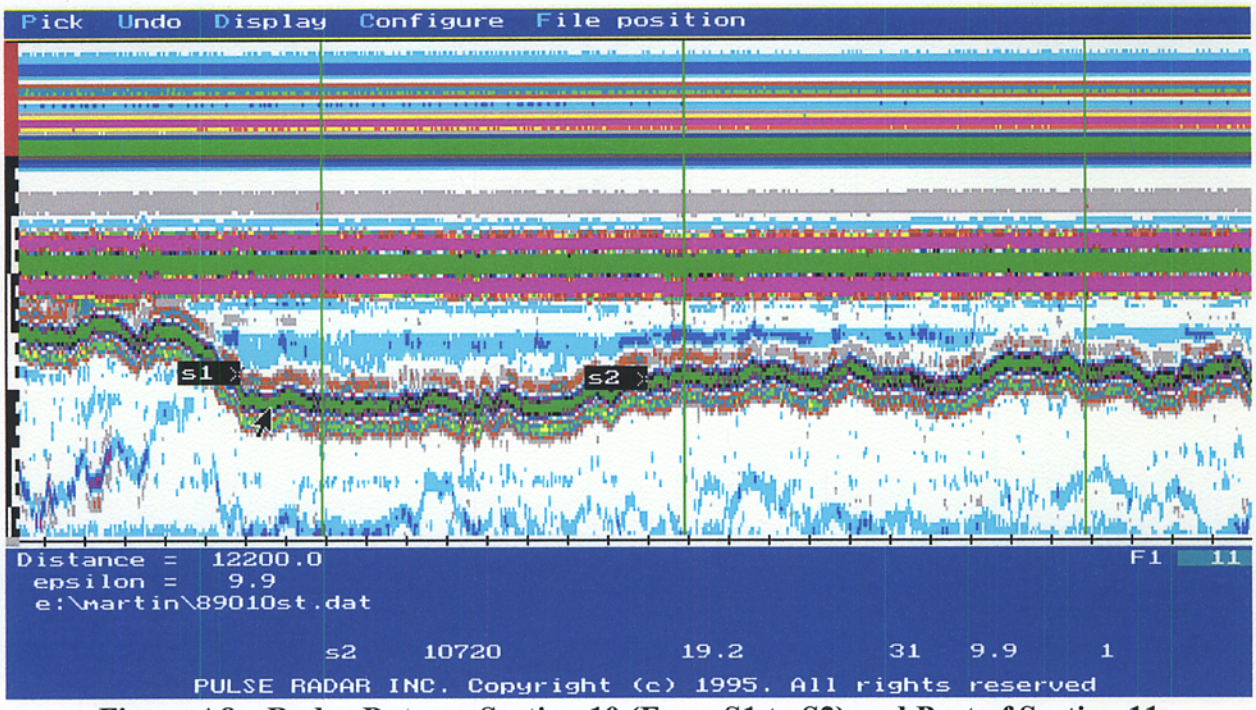

Figure A8. Radar Data on Section 10 (From S1 to S2) and Part of Section 11 (Starting at S2).

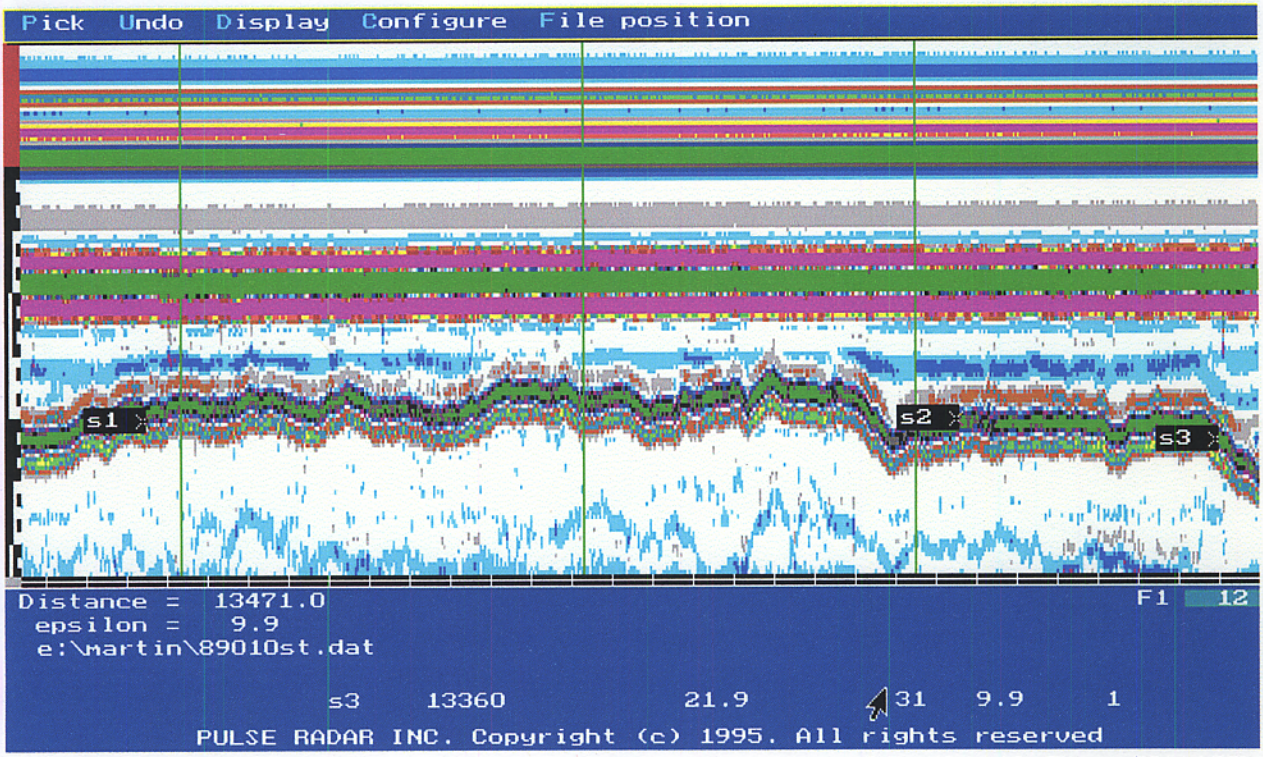

Figure A9. Radar Data on Section 11 (From S1 to S2) and Section 12 (From S2 to S3).

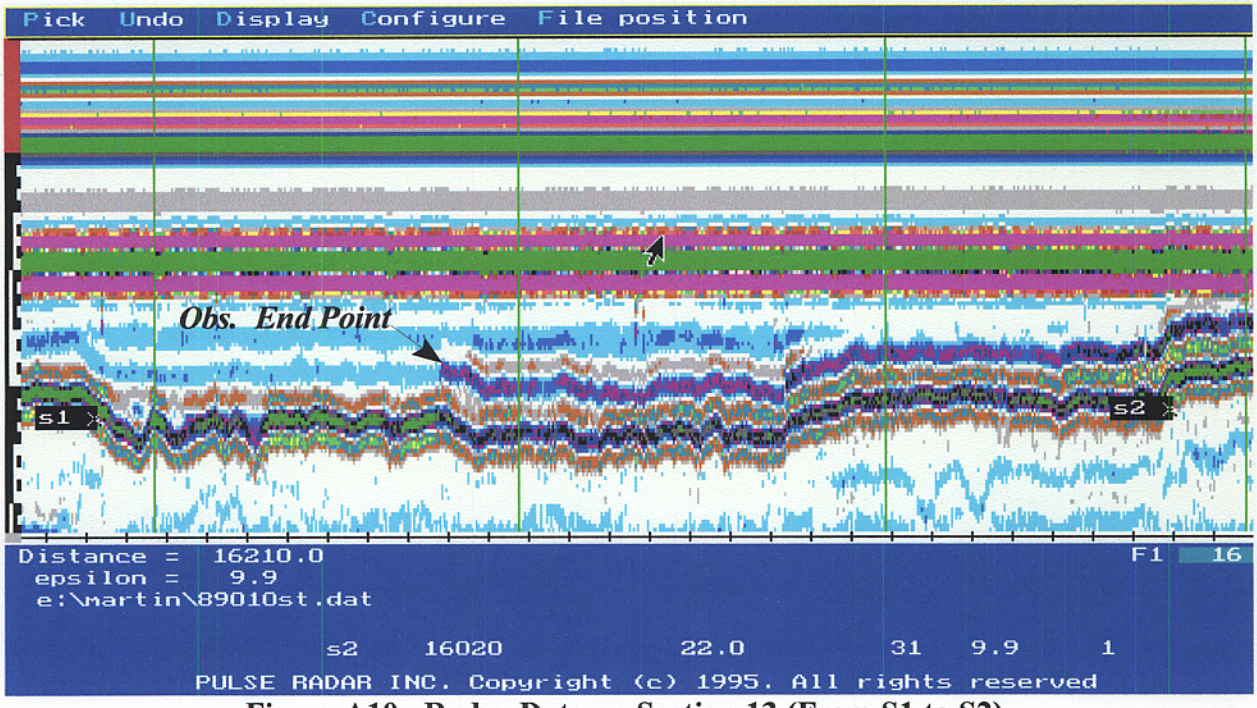

Figure A10. Radar Data on Section 13 (From S1 to S2).

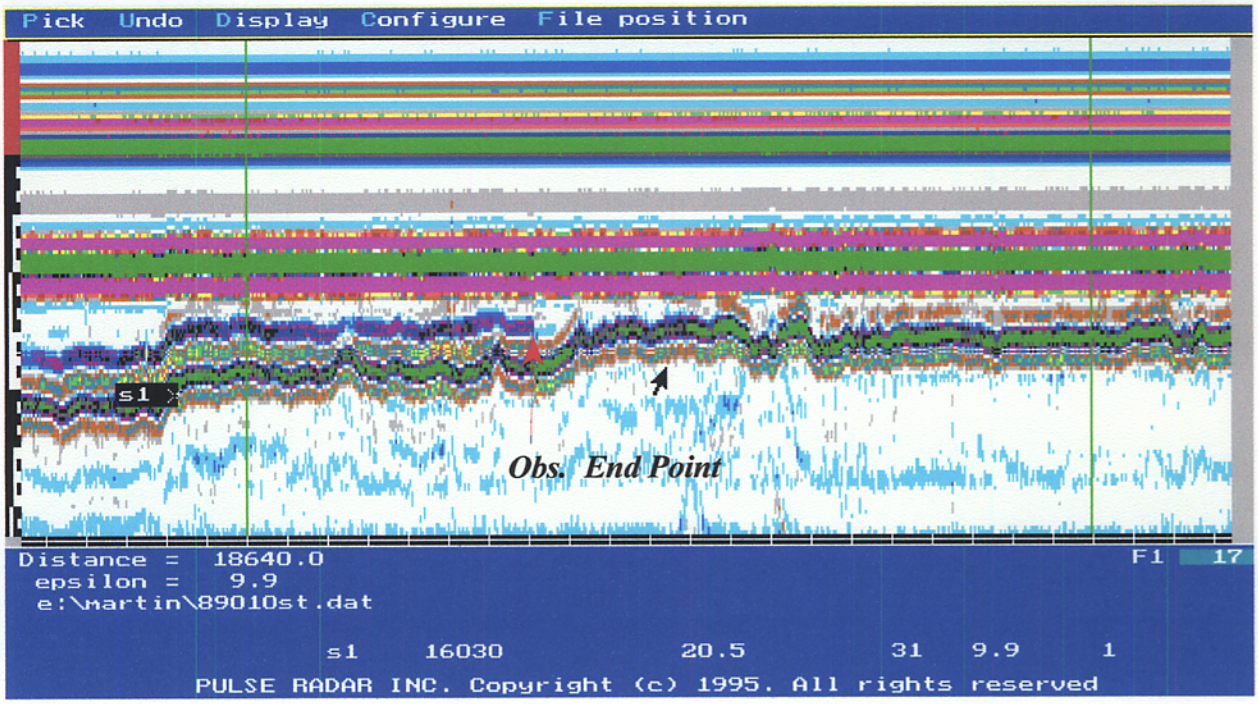

Figure A11. Radar Data on Section 14 (Starting at S1).

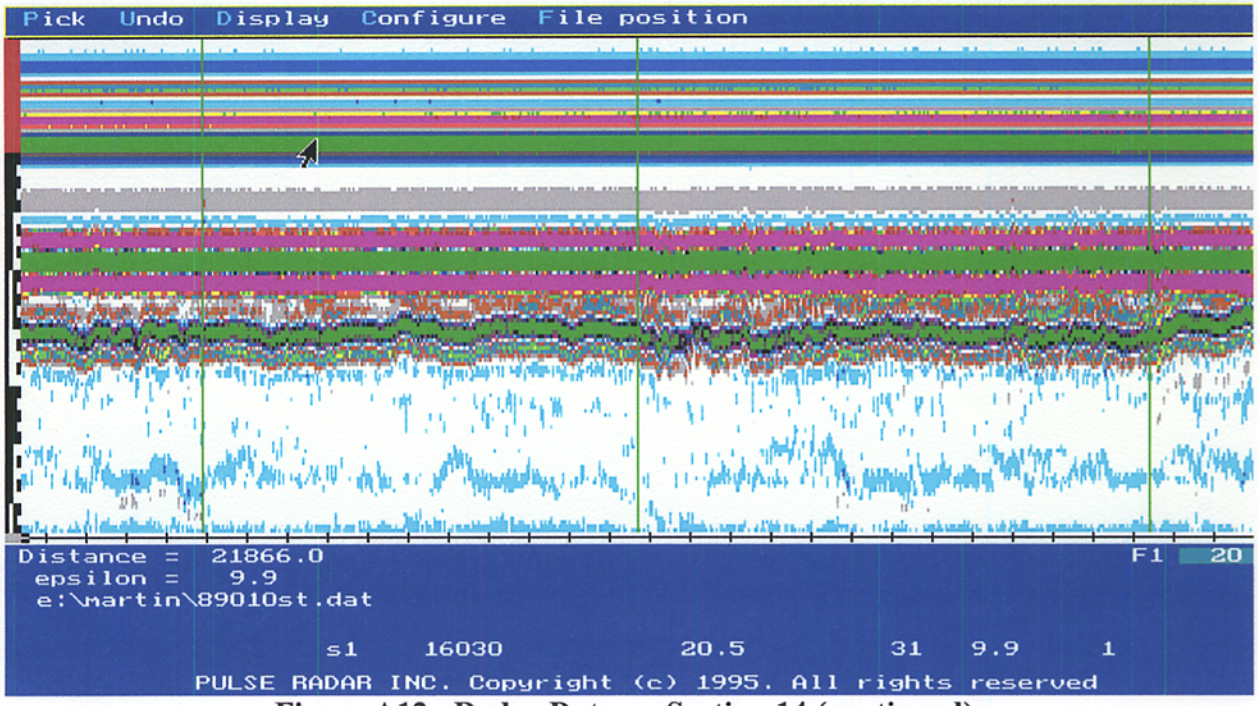

Figure A12. Radar Data on Section 14 (continued).

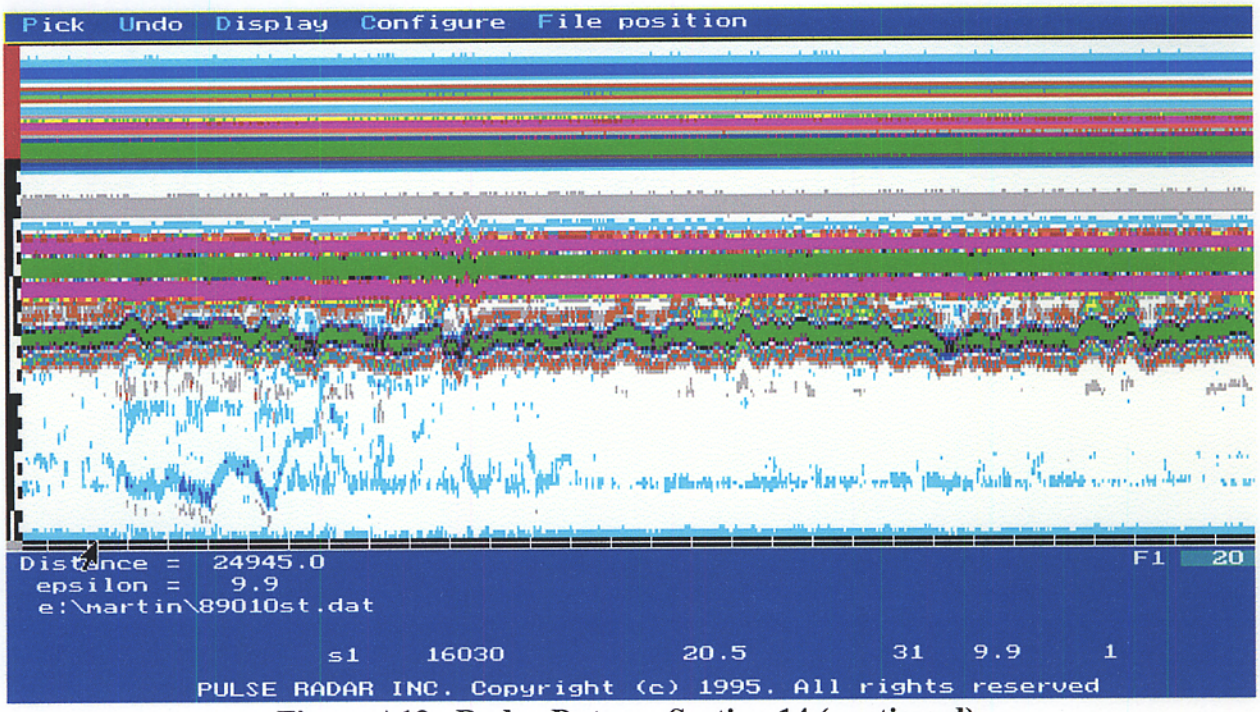

Figure A13. Radar Data on Section 14 (continued).

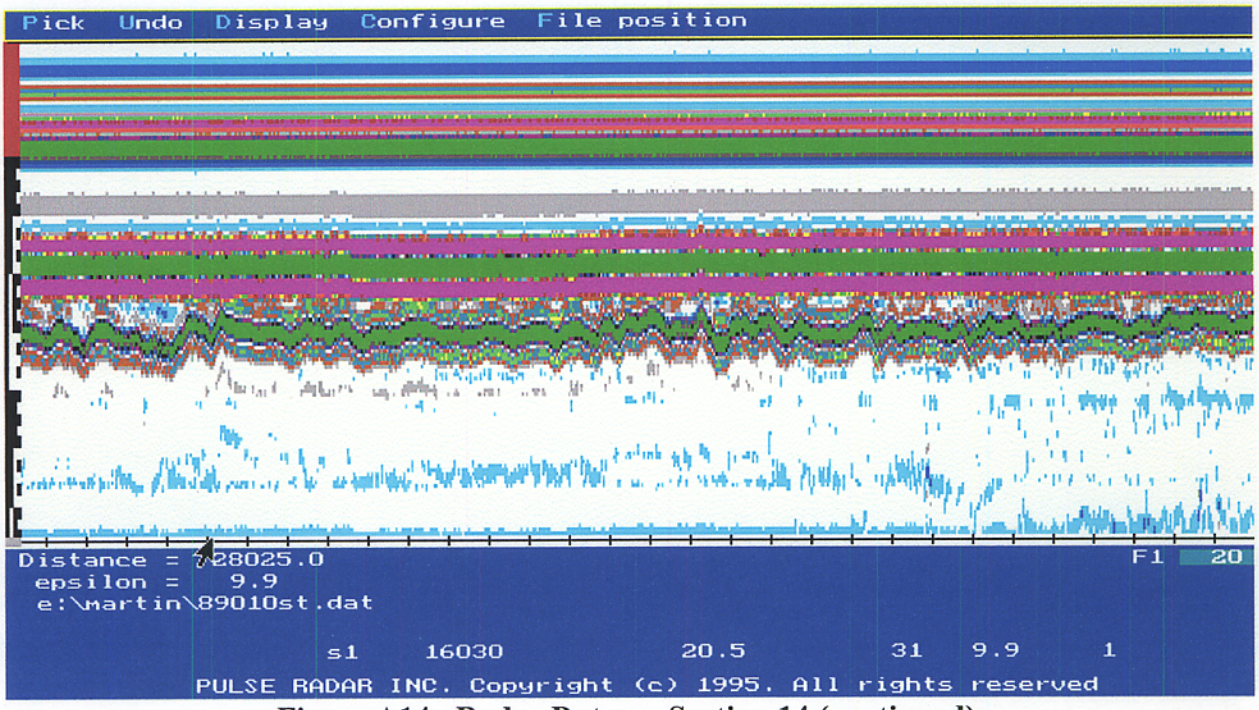

Figure A14. Radar Data on Section 14 (continued).

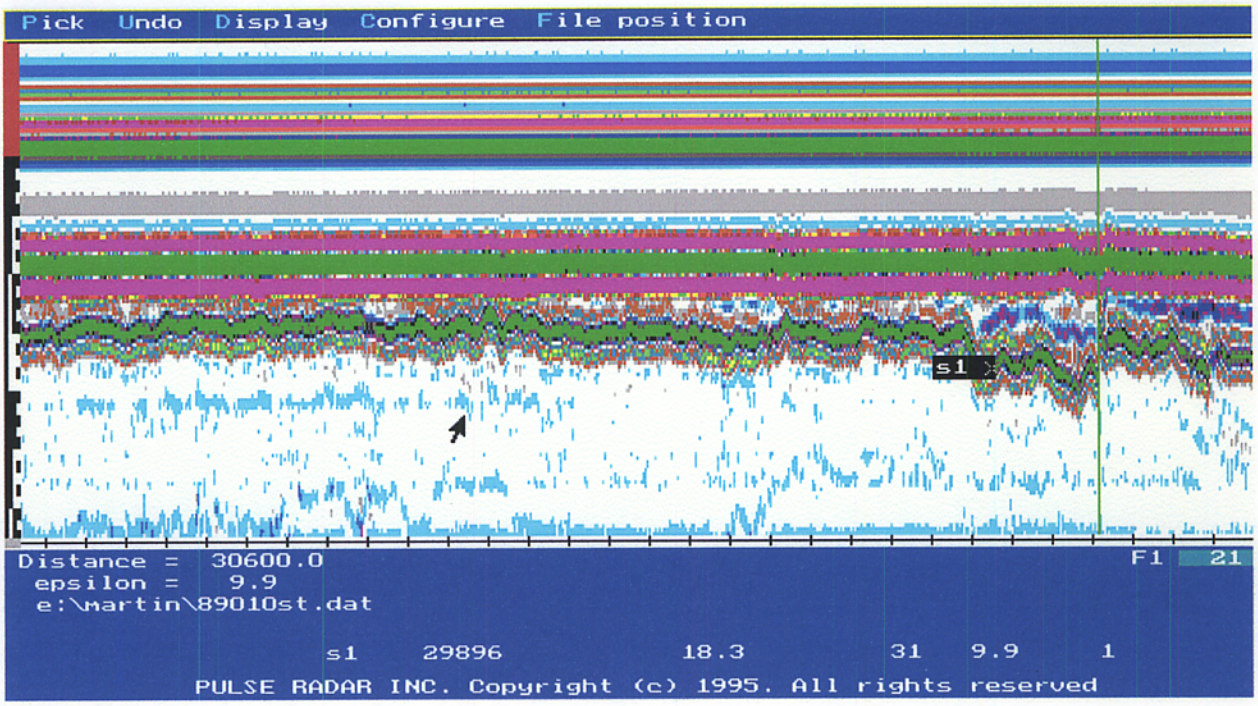

Figure A15. Radar Data on Section 14 (End at S1).

first part, the Complex method was applied to segment the interval between the start of the survey and the beginning of the bridge. In the second part, the segmentation was done on the interval between the end of the bridge and the end of the survey. In this way, the bridge was prevented from being part of a highway segment. It is realized that this approach requires the bridge locations to be known *a priori*. A simple way by which this may be accomplished is to insert markers during the survey that denote distinctly any bridge end points. For example, two successive markers may, by convention, be assigned to designate a bridge end point. This will not require any change in the existing radar data acquisition program but only a very minor change in the current data collection protocol which already includes the practice of marking bridge end points during the radar survey. The segmentation program can then be modified to recognize a pair of successive markers as a bridge end point so that segmentations are done only for the highway intervals between bridges.

The results presented in Table A5 and in Figures A3 to A15 were obtained using a minimum segment length of 500 feet. Thus, the first segment shown in Figure A1, from the start of the route to the beginning of the bridge (Marker 3), could have been divided into two segments. However, the segmentation program detected this as a uniform interval so that it was not

subdivided. This result agrees with the visual interpretation of the data which is quite uniform for the given interval (see Figure A1). The two-character labels, *s#*, in the figures (where the # denotes a number) represent the approximate locations of the predicted segment end points.

The figures generally show very good agreement between the results from the Complex method and the segmentation established by visual examination. The results are encouraging in two respects:

1. Most of the segments identified by visual examination were delineated by the segmentation algorithm.
2. The specified minimum segment length of 500 ft produced acceptable results for the wide range of segment lengths established from the radar data. Note that the minimum predicted segment length is 500 ft (0.09 mi) while the maximum is 13,854 ft (2.62 mi).

However, as noted below Table A5, there were two observed endpoints that were not identified from the segmentation analysis. These endpoints are shown in Figures A10 and A11 as the limits of an interval where the radar data show weak reflections identified by the purplish color band in the figures appearing after the surface echo. Since the amplitudes of these reflections are small, the results suggest that they did not significantly influence the objective function given by Eq. (A3).